Wayne State University Dissertations

1-1-2014

Biofuels Production Via Catalytic Hydrocracking Of Ddgs Corn Oil And Hydrothermal Decarboxylation Of Oleic Acid Over Transition Metal Carbides Supported On Al-Sba-15

Basem A. Al Alwan
Wayne State University,

Follow this and additional works at: http://digitalcommons.wayne.edu/oa_dissertations

Part of the Chemical Engineering Commons

Recommended Citation

BIOFUELS PRODUCTION VIA CATALYTIC HYDROCRACKING OF DDGS CORN OIL AND HYDROTHERMAL DECARBOXYLATION OF OLEIC ACID OVER TRANSITION METAL CARBIDES SUPPORTED ON Al-SBA-15

by

BASEM AL ALWAN

DISSERTATION

Submitted to the Graduate School

of Wayne State University,

Detroit, Michigan

in partial fulfillment of the requirements

for the degree of

DOCTOR OF PHILOSOPHY

2014

MAJOR: CHEMICAL ENGINEERING

Approved by:

_____
Advisor   Date

_____

_____

_____

ACKNOWLEDGEMENTS

TABLE OF CONTENTS

LIST OF TABLES

LIST OF FIGURES

CHAPTER 1

INTRODUCTION

1.1 Overview

New sources of energy, especially inexpensive renewable sources, has received a great deal of research emphasis in the twentieth century to obtain the cheapest source of energy[1]. According to the International Energy Agency (IEA), the world energy demand is expected to increase by more than 55% between 2005 and 2030.[2] The total energy consumption in the United States of America for residential, commercial, industrial, and transportation in 2012 was 95 quadrillion Btu which is more than the domestic energy production (79 quadrillion Btu).[3] About 82% of the energy was derived from fossil fuels.[4] However, only 9% of the energy was produced from renewable sources.

Recently, many researches focus on finding sources of energy that are sustainable and renewable to replace the fossil-derived petroleum products. Triglycerides from plant oils and animal fats may be a suitable source for production of liquid biofuels and useful chemicals.[5] Many processes for producing liquid biofuels from renewable sources (triglycerides) have been discovered; however, the transesterification process has been considered one of the most successful processes to produce liquid biofuels (biodiesel). Although biodiesel shows potential for partially replacing petroleum fuels, it displays some disadvantages that would make it an undesirable product compared to petroleum fuels, such as low oxidation stability and poor cold flow properties.[6] Catalytic hydrocracking processes have been studied for converting triglycerides into biofuels (green diesel) that overcomes the disadvantages of biodiesel.[7] Biofuels that are produced from hydrocracking of triglycerides are quite similar to petroleum fuels;[8] therefore, no

modifications are required to existing infrastructures.[8] During the catalytic hydrocracking process, the triglycerides can be converted to green diesel as a result of hydrogenation, hydrodecarboxylation, hydrodecarbonylation, hydrodeoxygenation, hydroisomerization, and hydrocracking reactions.[9,10]

The hydrocracking process requires a dual function catalyst that is composed of metallic sites and acidic sites. The metallic sites are for hydrogenation and oxygen removal reactions (hydrodecarboxylation, hydrodecarbonylation, and hydrodeoxygenation), while acidic sites are for hydroisomerization, and hydrocracking activities. Supported noble metal catalysts[11] and metal sulfide catalysts[12,13] have been investigated for the hydrocracking of vegetable oils to produce green diesel. The noble metal catalysts are not viable for large-scale processes because of their limited availability, high cost, and sensitivity to contaminants (such as oxygenated compounds) in the feedstock.[14] Although metal sulfide catalysts overcome the issues with noble metal catalysts, the addition of sulfur-containing compounds such as H_2S is required to maintain the catalysts in the active form.[15] Recently, supported metal carbide and nitride catalysts have been receiving considerable attention as catalysts for the hydrocracking of vegetable oils.[16] The existence of carbon atoms or nitrogen atoms in the lattice of transition metals extends the lattice parameter, which leads to increases in the d-band electron density of the metals.[17,18] Bimetallic carbide and nitride catalysts have shown higher activities and stabilities than the monometallic ones.[19] It has been claimed that the carbide form of the NiMo/ZSM-5 catalyst produced a lower amount of CO and CO_2 from soybean oil feedstock than the nitride form; therefore, more hydrodeoxygenation took place on the carbide catalyst compared to the nitride catalyst.[20] A few studies evaluated

the effect of the support on the catalyst performance for the hydrocracking reaction. The support plays a significant role in the cracking and isomerization activity.[21] Wang et al.[22] investigated the effect of several supports on the activity of NiMo carbide catalyst for the hydrocracking of soybean oil. The conversion of soybean oil reached 100% and the selectivity to green diesel was 97% for the NiMo carbide catalyst over Al-SBA-15 during 7 days of reaction at 400 $^{\circ}$C and 650 psi (4.48 MPa).

1.2 Significance of this study

First, the environmental concerns that are associated with using fossil-based fuels, such as Green House Gases (GHG) emissions, would make fossil fuels undesirable from the ecological and sustainability points of view. These emissions are the main reason for global warming and climate change. Therefore, using friendlier fuels (biofuel produced in this study) could help to maintain the carbon balance on the earth and reduce the GHG emissions. One study shows that using the jet fuel produced from camelina seeds could reduce the carbon emissions by 84% compared to the conventional petroleum jet fuel.[23]

Second, expanding and diversifying the energy production from sources other than petroleum oils, especially from renewable sources, is desirable. The biofuels feedstock used in this study is renewable biomass (plant oil). The U.S. Strategic Petroleum Reserve has been used under the event of an energy emergency three times, most recently in June 2011 when the President directed a sale of 30 million barrels of crude oil to offset disruptions in supply due to Middle East unrest.[24] Therefore, biomass derived fuels could help to avoid using the Strategic Petroleum Reserve.

Finally, there is a need to fill in the gaps in the literature by investigating inexpensive catalysts that have great potential for the hydrocracking of triglycerides and lowering the

cost of the process. Bimetallic carbide catalysts (relatively inexpensive catalysts) can exhibit high activity similar to the noble metal catalysts (expensive catalysts). Waste vegetable oils will be used as feedstocks and milder operating conditions will be applied in order to minimize the process cost.

1.3 Objectives of this study

The primary objective of this study is to develop catalysts for converting triglycerides and fatty acids to biofuels (particularly, green diesel) with high conversion of triglyceride, high selectivity to diesel, and long lifetime. There are three specific objectives that should be followed in order to achieve the main objective as follow:

1. To understand the effect of Ni-W ratio and preparation method on the activity and selectivity of the bimetallic carbide catalysts supported on Al-SBA-15 for the hydrocracking of distiller dried grains with solubles (DDGS) corn oil. The Ni-W ratios are 1:9, 1:1, 2:1, and 9:1. The preparation methods are co-impregnation method and dendrimer-encapsulated nanoparticle (DENP) method.

2. To investigate the effect of the fractional sums of the electronegativities of the transition metal carbide catalysts on the activity and selectivity for the hydrocracking of DDGS corn oil. Also, to test a hypothesis that the closer the fractional sum of the transition metal electronegativities is to the electronegativity range of the noble catalysts (2.0–2.2), the better the catalyst performance will be. The catalysts are nickel-based carbide catalysts combined with four different metals (Mo, Nb, W, and Zr) and supported on Al-SBA-15.

3. To study the efficiency of the transition metal carbide catalysts for producing biofuels from the hydrothermal decarboxylation of oleic acid and soybean oil in

the absence of hydrogen. The effect of super-critical water and glycerol on the catalyst activity and selectivity will be studied.

CHAPTER 2

LITERATURE REVIEW

2.1 Introduction to feedstock

In general, biomass feedstock is the main renewable source for producing biofuels. There are three basic categories of biomass feedstock: lignocellulosics, amorphous sugars, and triglycerides as it is shown in Figure 1.[4] Amorphous sugar feedstocks such as starches and simple sugars are an undesired one because of the arguments of food versus fuel debate. First generation biofuels were produced from food crops and the loss of crops to fuel productions can inflate the food price.[25] Lignocellulose which is a composite material of rigid cellulose fibers, lignin, and hemicelluloses is a less desired feedstock since it is considered as a low-energy-density feedstock.[4] Corn stover, forage grasses, paper mill residue, wood chips, and switchgrass are examples of lignocellulosic biomass. However, triglycerides, a glycerol group attached to three fatty acids as shown in Figure 2,[4] seem to be the most ideal candidate for biofuel production because of the higher energy density content and uncompromising of valuable food when non-edible sources are used. Triglycerides are commonly found in vegetable oils, animal fat, and waste oils. The three fatty acids in a triglyceride molecule can be all the same, or vary in their carbon chain length and the number of double bonds. Table 1 shows the most common structures of the fatty acids, and indicates that vegetable oils mainly consist of palmitic, oleic, linoleic, and linolenic fatty acids.[26] Selecting a feedstock for the biofuel productions depends on financial manageability and local availability of the feedstock. For instance, rapeseed and sunflower oils are used in the European Union, palm oil is used in Asian countries, and soybean oil is used in the United States.[27,28] On the other hand, using fresh

oils as feedstock will compromise food, land, and water resources. Therefore, using the

second or third generation feedstock such as Jatropha and algal oils is highly desirable.
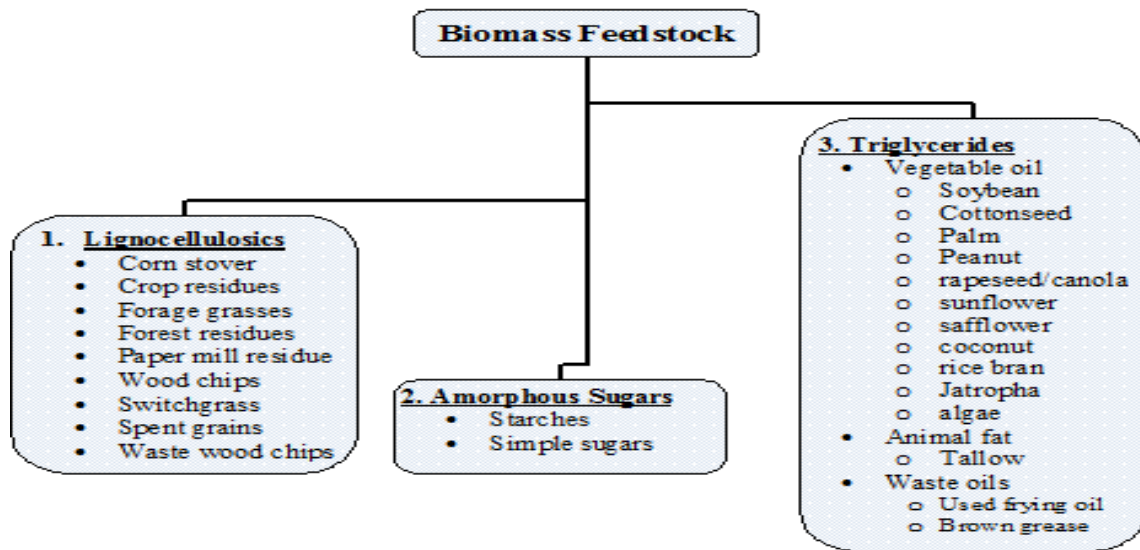
Figure 1. Biomass feedstock classification for biofuel production.[4]

Jatropha is a non-edible source and an easily grown crop. Jatropha is mainly grown in

Mexico and Central America; however, tropical and subtropical areas such as India,

Africa, and North America are also suitable for planting Jatropha. Jatropha seeds

normally contain of 27-40% oil, which can be used for biofuel production. Algal oils are

extracted from algae and considered to be a third generation feedstock. Algae can double

their weight several times a day, and some species contain up to 80% oil based on dry

weight. It is believed that algae would need only 3% of the crop land in the United States

to supply the domestic fuels needs, while 61% of the land would be required in the case

of using the first generation feedstock.[29] Algal oils are long-chain polyunsaturated fatty

acids and differ from those of animal and vegetable sources. There are some modest attempts that use algal oils to produce biofuel and commercialize it. For example, AlgaeLink and KLM claim that they will be able to develop the next generation alternative jet fuel to be used in the Air France/KLM aircraft.[30] However, there are some challenges against implementing this process such as infrastructure requirements, which makes the process very costly. The first attempt to commercialize the process of converting algal oils to biofuels was in 1985 and it was unsuccessful.[31] Animal fats such as tallow, lard, and fish oils have been used as feedstock to produce biodiesel.[32] Tyson Food Inc. produces about 300 million gallons of animal fat, which could be the main feedstock to produce biofuel.[33] Nevertheless, using animal fats as feedstock to produce biofuel has some disadvantages such as high cloud point of the biofuel produced from animal fats. Therefore, the biofuel would not be appropriate to be used in cold weather.[33] Waste oils such as used frying oils and brown grease would be one of the most promising resources to be used as feedstock because of low cost.[34] However, the variations in free fatty acid (FFA) composition, triglycerides, water content, and impurities would make the treatment of waste oils hard to be accomplished. Therefore, the conversion methods have to be adaptable for each case or pretreatment stages have to be added to the process, which increases the operation cost.
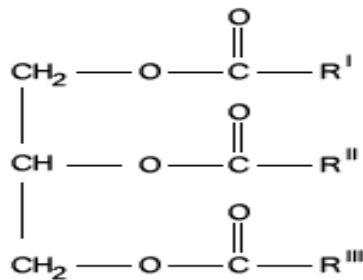
Figure 2. Structure of a triglyceride molecule.[4]

The main reason of holding back biofuels to replace petroleum-based fuels is the relatively high cost of the triglycerides feedstock. Choice of the feedstock as a source of biofuel production is an important consideration since the 70-85% of the total production expense is related to the feedstock cost.[6]

Table 1. The most common structures of the fatty acids.[26]

Structure	Nomenclature	Common name	Natural source
OOH	C10:1 n-1	Capreol	Ruminants milk
OOH	C12:1 n-3	Lauroleic	Cow milk
OOH	C16:0	Palmitic	All fats
OOH	C16:1 n-7	Palmitoleic	Nut and fish oil
OOH	C 18:1 n-9	Oleic	Vegetable oil
OOH	C18:1 n-7	Vaccenic	Ruminant fat
OOH	C18:2 n-6	Linoleic	Vegetable oils (sunflower, corn, soy)
OOH	C18:2 n-3	Linolenic	Soy and other vegetable oils
OOH	C20:0	Arachidiq	Peanut oil
OOH	C20:1 n-11	Gadola	Fish oil

*C10:1 n-1 means a molecule with 10 carbon atoms and 1 unsaturated bond that is located at the first carbon atom.

2.2 Mechanism of hydrocracking of triglycerides

Although the overall reaction of the hydrocracking of vegetable oils was carried out as early as the 1980s, the process mechanism and kinetics are still under investigations because of its complexity.[7,8] Since most vegetable oils usually contain 80-90% of triglyceride, the reaction mechanism focuses on the hydrocracking of triglyceride molecules only. During the hydrocracking process, the richness of hydrogen in the reactor saturates the side chains of the triglycerides, so double bonds will be converted to single bonds. This is then followed by scission of C-O bonds to produce free fatty acids. The free fatty acids will be subjected to three main reactions: hydrodeoxygenation,

decarbonylation and decarboxylation in order to remove oxygen as shown in Figure 3.[35] Oxygen must be removed to obtain a liquid fuel with a high-energy content and high thermal stability similar to fossil fuels.

Hydrogenation

CH_2-O-CO-$C_{17}H_{33}$
|
CH-O-CO-$C_{17}H_{33}$ $\xrightleftharpoons{+3 H_2}$
|
CH_2-O-CO-$C_{17}H_{33}$

CH_2-O-CO-$C_{17}H_{35}$
|
CH-O-CO-$C_{17}H_{35}$ $\xrightarrow[-C_3H_8]{+3 H_2}$ $C_{17}H_{35}COOH$
|
CH_2-O-CO-$C_{17}H_{35}$

a. **Decarboxylation:**

$C_{17}H_{35}COOH \longrightarrow C_{17}H_{36} + CO_2$

b. **Decarbonylation:**

$C_{17}H_{35}COOH + H_2 \longrightarrow C_{17}H_{36} + H_2O + CO$ (Catalytic reaction)

$C_{17}H_{35}COOH \longrightarrow C_{15}H_{31}CH{=}CH_2 + H_2O + CO$ (Thermal reaction)

c. **Reduction (hydrodeoxygenation):**

$C_{17}H_{35}COOH + 3H_2 \longrightarrow C_{18}H_{38} + 2H_2O$
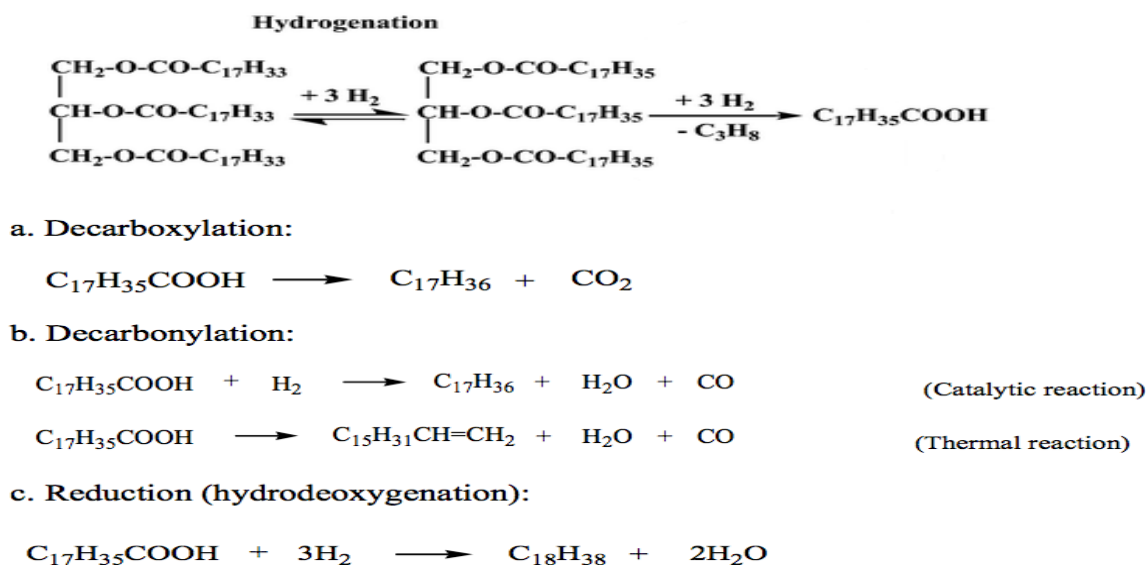
Figure 3. Mechanism of hydrocracking reaction of triglyceride. [35]

The produced straight chain alkanes will undergo isomerization and cracking reactions as shown in Figure 4.[35] The isomerization reaction is responsible for converting straight chain alkanes to branched chains to enhance the energy content and prevent engine knocking. The cracking reactions will convert long chain hydrocarbons to shorter chains in order to improve the selectivity to diesel, jet fuel, and gasoline.

a. Hydroisomerization

n-RH $\xrightarrow[\text{Catalyst}]{H_2}$ iso-RH

b. Hydrocracking

iso-RH $\xrightarrow[\text{Catalyst}]{H_2}$ iso-R_1H + iso-R_2H
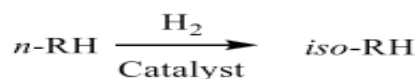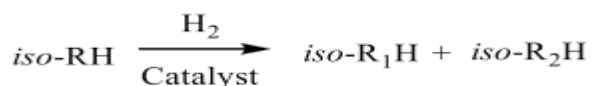
Figure 4. Hydroisomerization and hydrocracking reactions of produced alkanes.[35]

Donnis et al.[36] describe how the three carboxylic acids are stepwise liberated and hydrogenated into linear alkanes. The reaction pathways were studied both in model compound tests and in real feed tests with mixtures of straight-run gas oil and rapeseed oil. Studying the hydroprocessing of methyl laurate into n-dodecane describes the detailed pathway of the HDO route. It shows that the aldehyde formed is enolized before further hydrogenation. Another important study investigated the mechanism of the hydroprocessing of triglyceride, as shown in Figure 5, using a liquid phase batch reactor at atmospheric pressure with the presence of hydrogen over NiMo/zeolite catalyst.[37] The study claimed that the diameter and chain length of the triglyceride molecule are (5.3-7.4 Å) and (30-45 Å), respectively. Therefore, the triglyceride molecule was able to penetrate the pores of zeolite catalyst (pore diameter is about 5.6 Å). The triglyceride molecule was cracked first, and then the metallic sites of the catalyst saturated the double bonds in the nonene to form nonane.

2.3 Hydrocracking process (catalysts & process parameters)

Theories and fundamental phenomena established for catalytic processes in the more-studied petroleum industry can be used as a starting point for catalysis in vegetable oils conversion since the catalysts and processes used are quite similar. In general, the catalysts that are used in the hydrocracking of vegetable oils should consist of two sites: metallic sites and acidic sites. The metallic sites are required for hydrogenation, decarboxylation, decarbonylation, and hydrodeoxygenation reactions. On the other hand, the acidic sites are required for isomerization and cracking reactions. Therefore, balancing between metal and acid is very important factor in catalyst design in order to modify selectivity, activity, and durability of the catalysts.[38-40]
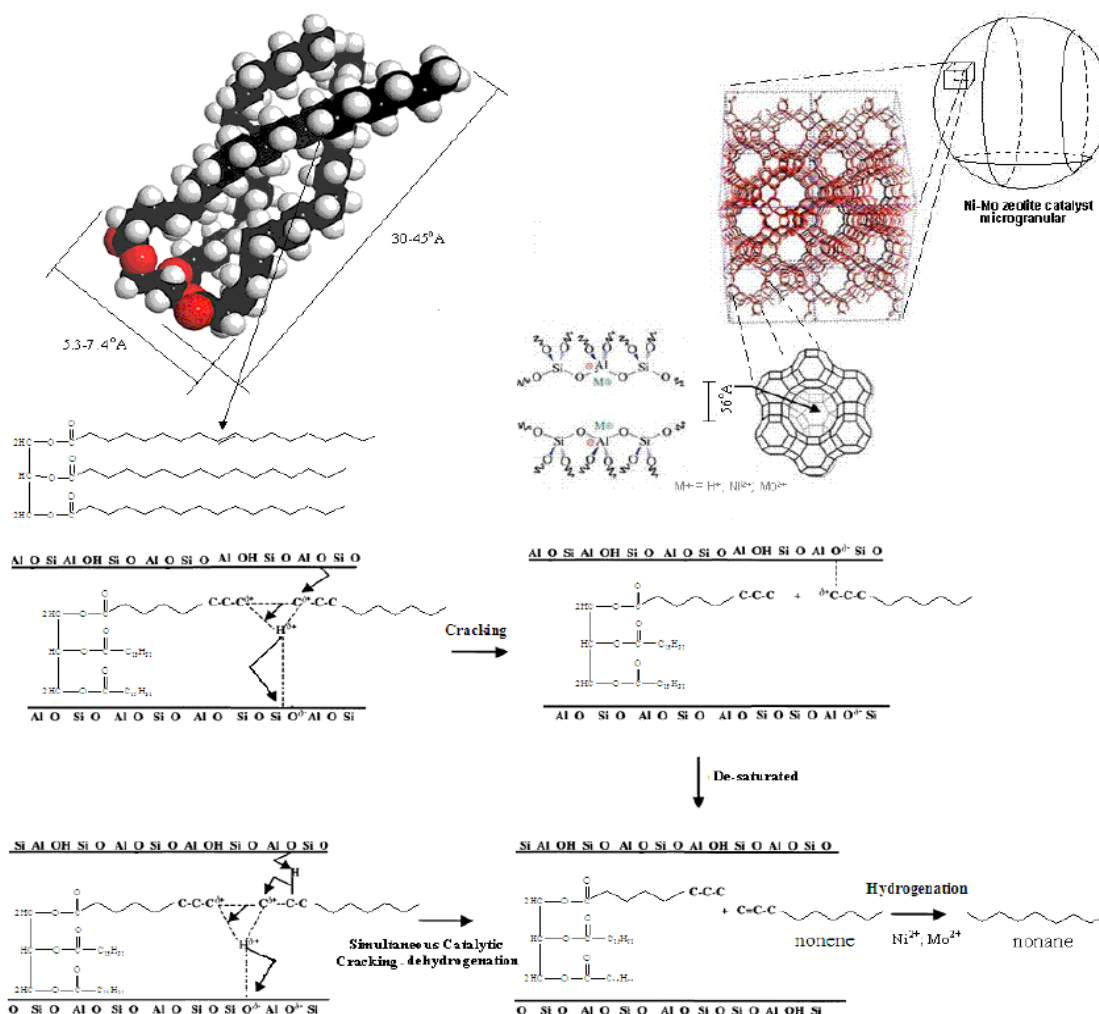
Figure 5. Proposed mechanism of hydroprocessing of triglyceride.[37]

A batch reactor has been used earlier to carry out the hydrocracking of soybean and palm oil over NiMo/γ-Al$_2$O$_3$ at temperature of 350-400 $^{\circ}$C and hydrogen partial pressure of 10-200 bar.[8] The results showed that soybean and palm oil were completely converted to n-alkanes, cycloalkanes, aromatics, and carboxylic acids due to decarboxylation, decarbonylation, and reduction reactions. The influences of the reactions, temperature, and pressure on the product compositions were studied and it was concluded that the higher hydrogen pressure used, the less aromatic compounds obtained.[41] Also, a study

investigated alumina and mesoporous (MCM-41) catalysts for the hydrocracking of palm oil by using a batch reactor and showed that the yield was 43 vol.% of gasoline.[42] Fuel obtained from rapeseed oil has been studied at various reaction conditions in the presence of Ni-Mo/alumina.[43] A fixed bed reactor was used in this experiment in addition to a salt bath heating system. The reactor had dimensions of 900 mm length and 40 mm inner diameter. The reactor was loaded with 100 g of Ni-Mo/alumina catalyst and the flow rates of feedstock and hydrogen were 100 g hr^{-1} and 0.1 Nm^3 hr^{-1}, respectively. Two different temperatures, 310 and 360 $^{\circ}$C, and two different pressures, 7 and 15 MPa, were investigated to obtain fuels from rapeseed oil. The conversion of the rapeseed oil reached 100% at 360 $^{\circ}$C while it was 99% at 310 $^{\circ}$C. The product contains water, gaseous hydrocarbons and organic liquid product (OLP) with yields of 11 wt%, 6 wt% and 83 wt%, respectively.[43] The n-haptadecane and n-octadecane dominated the composition of OLP by almost 75 wt%. Also, no oxygenated compounds were detected at 360 $^{\circ}$C. The range of boiling point of the OLP was calculated and it was found that the narrow range of the boiling point was due to the narrow range of the carbon atom numbers of the OLP.[43] Most of the compositions of the OLP fall into the boiling point range of diesel fuel, which is about 300-310 $^{\circ}$C. The properties of the OLP such as density, kinematic viscosity, and cetane index show similar values to diesel fuel; however, the OLP shows poor low-temperature properties such as cloud point. Although the density of the OLP is a little lower than the density of diesel fuel, blending the OLP with a suitable heavier fraction would help to overcome this issue.

Although several types of continuous reactors have been tested for the hydrocracking process, fixed bed reactors have been used the most due to their simplicity on controlling the operation conditions and placing the catalyst bed. On the other hand, it is necessary to consider the effect of pressure drop across the reactor and the effectiveness of heat and mass transfer. Diluting the bed by using quartz sand can eliminate the effect of pressure drop and enhance the transfer of heat and mass. Saskatchewan Research Council (SRC), Natural Resources Canada, and Agriculture and Agri-Food Canada studied the conversion of vegetable oil to diesel fuel by using conventional refinery technology. The results, as reported in the U.S. Patent No. 4992605, which compares the conversion of a wide range of vegetable oils such as canola and sunflower to diesel fuel. The diesel yield was about 80% of feedstock by applying medium severity conditions of temperature and pressure, and using conventional hydrotreating catalysts.[44] The characterization of the product showed that the product properties resemble diesel fuel properties. In addition, the cetane number of the product is between 55 and 90 compared 40 for diesel fuel.[44]

The U.S. Patent No. 4992605 described a process that converts different types of vegetable oils to liquid hydrocarbons that have the boiling range of the diesel fuel by using a 30 mL fixed bed reactor. Various grades of canola oil, rapeseed oils, and sunflower oils have been tested as feedstocks. The temperature was in the range of 350-450 $^{\circ}$C, the pressure was between 4.8 to 15.2 MPa, and the liquid hourly space velocity (LHSV) was from 0.5 to 5.0 hr^{-1}. It has been explored by the patent that hydrotreating of vegetable oil could lead to a significant yield of diesel. Different experiment conditions were applied for each type of feedstock and the yield of the diesel (the fraction of 210-

343 $^{\circ}$C) was about (70-77%). The GC-MS analysis showed that the composition of the product is mainly composed of 15 to 18 carbon atoms.

A conventional hydrotreating catalyst, NiMo/Al$_2$O$_3$, was used in a fixed bed reactor to study the hydrocracking of used cooking oil that was collected from restaurants.[45] The properties of the products show a good agreement to the properties of diesel fuel; however, the deactivation of the catalyst was a crucial parameter that influences the process efficiency. The catalyst deactivation was due to the high content of sulfur, nitrogen, and oxygen in the used cooking oil in comparison to a new vegetable oil.[45]

2.3.1 Metal carbides and nitrides

In the last decade, novel multi-functional catalysts have shown favorable results as hydrocracking catalysts comparison to conventional catalysts. Nevertheless, the cost and limitation of noble metals such as platinum hindered the utility of this type of catalyst for wide use in the hydrocracking processes. Recently, metal carbides and nitrides have been receiving most of the attention and some studies extensively studied the preparation, characterization, chemical and physical properties of this kind of catalysts.[46-48] Figure 6 illustrates the structures of Mo carbides and nitrides in comparison to MoS$_2$. It shows that the structure of Mo nitrides and carbides are body-centered cubic and hexagonal close-packed crystal structure, respectively.[49] Introducing carbon or nitrogen into the Mo metal lattice increases the lattice parameter $a_{o,}$ which leads to an increase in the d-electron density.[50] Therefore, carburization or nitridation of metals could act as efficient as the noble metal catalysts. There are two types of metals as follow

- Interstitial carbides and nitrides (Mo, Nb, Zr, Re, W, Hf and Ta)
- Intermediate carbides and nitrides (Ti, V, Cr, Mn, Fe, Ni and Co)
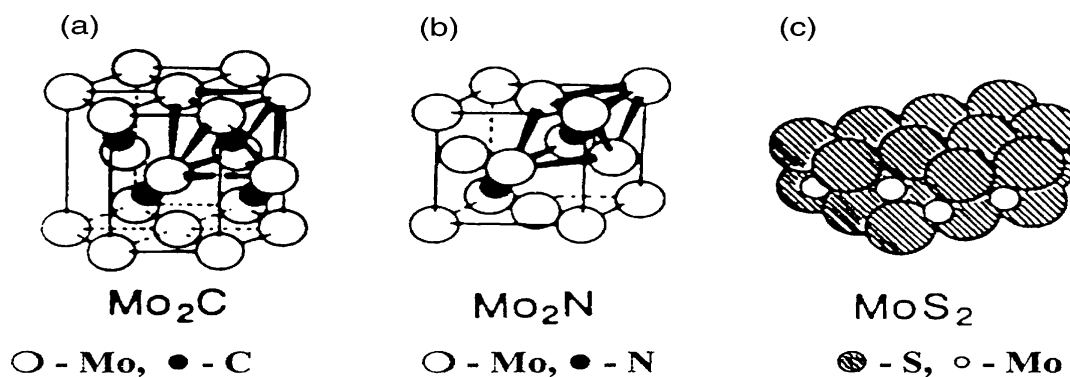
Figure 6. Crystal structures of Mo carbides and nitrides in comparison to MoS$_2$.[49]

The electronegativity of Mo carbides and nitrides are 0.7 and 1.2, respectively. According to that, the bonding is partly covalent and ionic but resembles metals due to the high ratio of Mo/carbon or nitrogen.[51] The similarity of Mo carbides and nitrides to metals increases their electrical conductivity, thermal conductivity, melting point, and hardness. The activity of metal carbides and nitrides catalysts has been investigated extensively.[46-48] It has been found that the surface structure and chemical composition determines the activity of the catalysts. Also, the preparation conditions are important factors in determining the activity. For instance, different categories of Mo carbides such as α-Mo$_2$C, β-Mo$_2$C, and η-Mo$_3$C$_2$ can be prepared by changing the preparation temperature that leads to variations in the density of active sites on the surface.[52] Similarly, changing the nitriding temperature can produce different sorts of Mo nitrides such as γ-Mo$_2$N and β-Mo$_2$N$_{0.78}$.[53] Metals, which are usually in the form of oxides, can be carburized by using H$_2$/methane, H$_2$/ethane and H$_2$/hydrocarbon at temperature between 773 and 1173 K.[54] While metal nitrides can be produced by using either a mixture of NH$_3$/He or pure NH$_3$.[53] Because of the probability of carbon to be deposited on the

surface when using inappropriate temperature and carburization composition, the preparation of metal carbides is more difficult than the preparation of metal nitrides.

As it has been mentioned before, hydrocracking catalysts have to be able to adsorb H_2, activate the adsorbed H_2 and transfer the activated H_2 to the reactants. Therefore, the hydrogen adsorption-activation has a crucial impact on the activity of metal carbides and nitrides. Many studies have focused on this issue in order to obtain the optimal catalyst; however, an additional investigation is needed for metal carbides because most of these studies concentrated on metal nitrides. Many studies claimed that the hydrogen is strongly adsorbed on the surface, and the activity of hydrocracking catalysts is increased as the hydrogen adsorption increased.[55,56] The existence of planes {111} on the catalyst surface can elevate the catalyst activity.[57] For example, adding cobalt to Mo_2N would increase the activity because of the increasing in the concentration of {111} planes.[58] Ni-Mo carbides/alumina catalyst shows higher rate of hydrodesulphurization and hydrogenation than some industrial catalysts such as $NiMo/Al_2O_3$.[59] Several attempts tried to postulate a mechanism of hydrogen adsorption/activation process in order to modify the performance of the catalysts.[60,61]

Wang et al.[20] claimed that the carbide form of NiMo/ZSM-5 catalyst produced an amount of CO and CO_2 from hydrocracking of soybean oil lower than that of the nitride form catalyst. Also, complete conversion of soybean oil and 50 wt% yield of hydrocarbons were obtained over the carbide form of NiMo/ZSM-5 catalyst. Most recently, the effect of several supports on the activity of NiMo carbide catalyst for the hydrotreating of soybean oil has been investigated.[22] The conversion of soybean oil

reached 100% and the selectivity to green diesel was 97% for the NiMo carbide catalyst over Al-SBA-15 during 6 days of reaction at 400 $^{\circ}$C and 650 psi.

2.3.2 NExBTL renewable synthetic diesel

NExBTL, <u>N</u>ext generation <u>B</u>iomass <u>T</u>o <u>L</u>iquid diesel technology, was commercially established by Neste oil in 2005 to produce synthetic diesel from vegetable oils and animal fats as shown in Figure 7.[62] The technology produces a superior green diesel because of its favorable properties such as

- Cetane value close to 100

- Cloud point lower than (-30 $^{\circ}$C)

- Free of aromatics and sulfur

- Compatible with the existing infrastructure

- Good storage stability

- Can be operated by existing vehicles
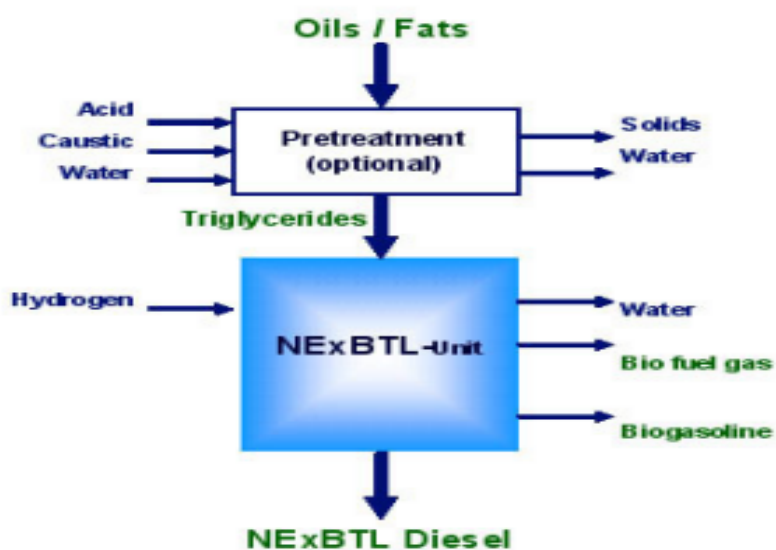
Figure 7. Schematic diagram of NExBTL process.[62]

NExBTL can provide 170,000 metric tons per year, which is sufficient for supplying 100,000 vehicles. The diesel product from NExBTL has been compared to European sulfur-free EN-590 diesel. It shows significant improvements such as reduction in greenhouse emissions, NO_x, particulate matter, and carbon monoxide by over than 60%, 15%, 25%, and 5%, respectively. However, the high moisture content of biomass feedstock can be problematic for processing operations, which requires pretreatment and separation steps.

2.4 Catalytic hydrothermal decarboxylation of fatty acids

The cost of producing green diesel from hydrocracking of triglycerides is largely determined by the cost of the feedstock. Low-cost feedstocks such as waste cooking oils and waste greases are difficult to process in a conventional fuel production facility because of the large amount of free-fatty acids and water impurities. Furthermore, the hydrocracking process requires a large amount of hydrogen that makes the process not likely to be competitive with the petroleum-based diesel process. The large hydrogen demand negatively impacts the process sustainability since hydrogen is primarily derived from fossil fuels.[63,64] A way to reduce the cost of the green diesel production is to use lower cost feedstocks and eliminate the additional hydrogen. Catalytic hydrothermal decarboxylation of fatty acids can provide the potential solution to minimize the economic gap between the production of green diesel and the petroleum-based diesel. The carboxylic acids, fatty acids, can be decarboxylated by suspending the acid in an immiscible and high boiling-point liquid as shown in (Rxn 1).[65]

$$H-O-\underset{\underset{O}{\|}}{C}-R' \xrightarrow{\text{het. cat.}} CO_2 + R'\text{-H} \qquad \text{(Rxn 1)}$$
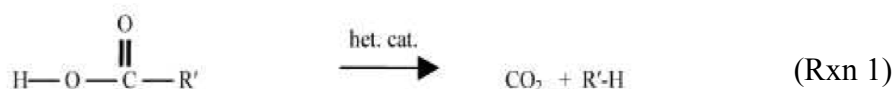
A sequence of elementary reactions for the decarboxylation of fatty acid on Pd/C catalyst has been proposed by Immer as shown in Figure 8.[66]

$$RCOOH + 2* \rightleftharpoons RCOO* + H*$$
$$RCOO* \rightarrow CO_2 + R*$$
$$R* \rightleftharpoons R' + H*$$
$$R* + H* \rightleftharpoons RH + 2*$$
$$H* + H* \rightleftharpoons H_2 + 2*$$
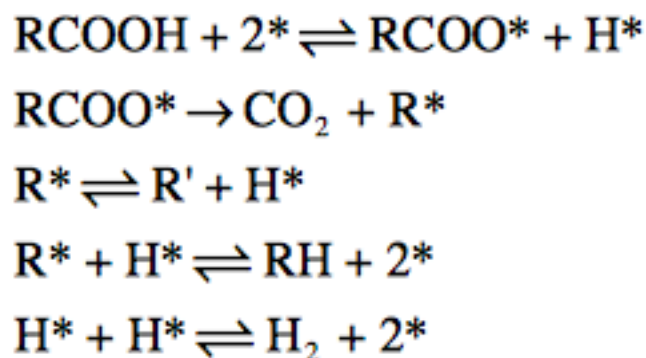
Figure 8. Elementary reactions of decarboxylation of fatty acid, where * is a catalytic site.[66]

There is a modest body of literature on catalytic hydrothermal decarboxylation.[67-70] Water at subcritical condition (200-374 $^{\circ}C$ and 5-20 MPa) becomes a unique reaction medium. Under these conditions, the dielectric constant of water decreases, which makes water similar to non-polar solvents.[70] Therefore, the solubility of lipids in water increases, since most of the lipids are non-polar materials. Watanabe et al.[71] investigated the effect of alkali hydroxide (NaOH and KOH) and metal oxides (CeO_2, Y_2O_3, and ZrO_2) on the decarboxylation of steric acid in supercritical water at 400 $^{\circ}C$ for 30 min. Both of alkali hydroxide and metal oxides enhanced the decarboxylation reaction with the main product of C_{17} alkane and C_{16} alkene, respectively. However, the selectivity to deoxygenated products was low (<15%). The catalytic effect of Pd/C and Pt/C on the hydrothermal decarboxylation of palmitic acid in sub- and super-critical water has been studied.[72] 5% Pt/C is a more active catalyst than 5% Pd/C for the hydrothermal decarboxylation of palmitic acid, with the pentadecane selectivity greater than 90%. Only

a partial hydrogenation reaction was observed when oleic acid was used, with stearic acid being the primary product.[73] A complete conversion of unsaturated fatty acid to fuel hydrocarbons is not achieved, suggesting that hydrogenation step is necessary prior to decarboxylation step. Fu et al.[74] reported that activated carbons (as an inexpensive catalytic material) can convert saturated and unsaturated fatty acids to fuel-range hydrocarbons in sub- and super-critical water. It has been claimed that either water molecules (reactive at sub- and super-critical conditions) or fatty acid molecules served as the hydrogen donor.

Triglycerides, a type of neutral lipids, can be rapidly hydrolyzed in hydrothermal media to produce saturated and unsaturated free fatty acids, as well as glycerol.[75] Some studies examined hydrothermal catalytic reforming of glycerol, commonly referred to as aqueous phase reforming (APR), to generate hydrogen.[76-81] Utilizing glycerol APR for *in situ* hydrogen production can promote the hydrogenation of unsaturated fatty acids. The addition of Re to Pt/C catalyst can motivate the glycerol APR due to the reduction of the affinity for CO,[79,82] A complete deoxygenation of oleic acid was achieved over Pt-Re/C catalyst when a 1:3 glycerol-to-oleic acid molar ratio was applied within 2 h reaction. The catalyst was experienced moderate sintering, suggesting additional work is needed to investigate its hydrothermal stability with time on stream. Figure 9 proposed an integrated catalytic hydrothermal reaction for the conversion of triglycerides to hydrocarbon fuels with *in situ* hydrogen production from glycerol.[75] A continuous hydrogen supply can be obtained by the APR of glycerol released from triglyceride hydrolysis.
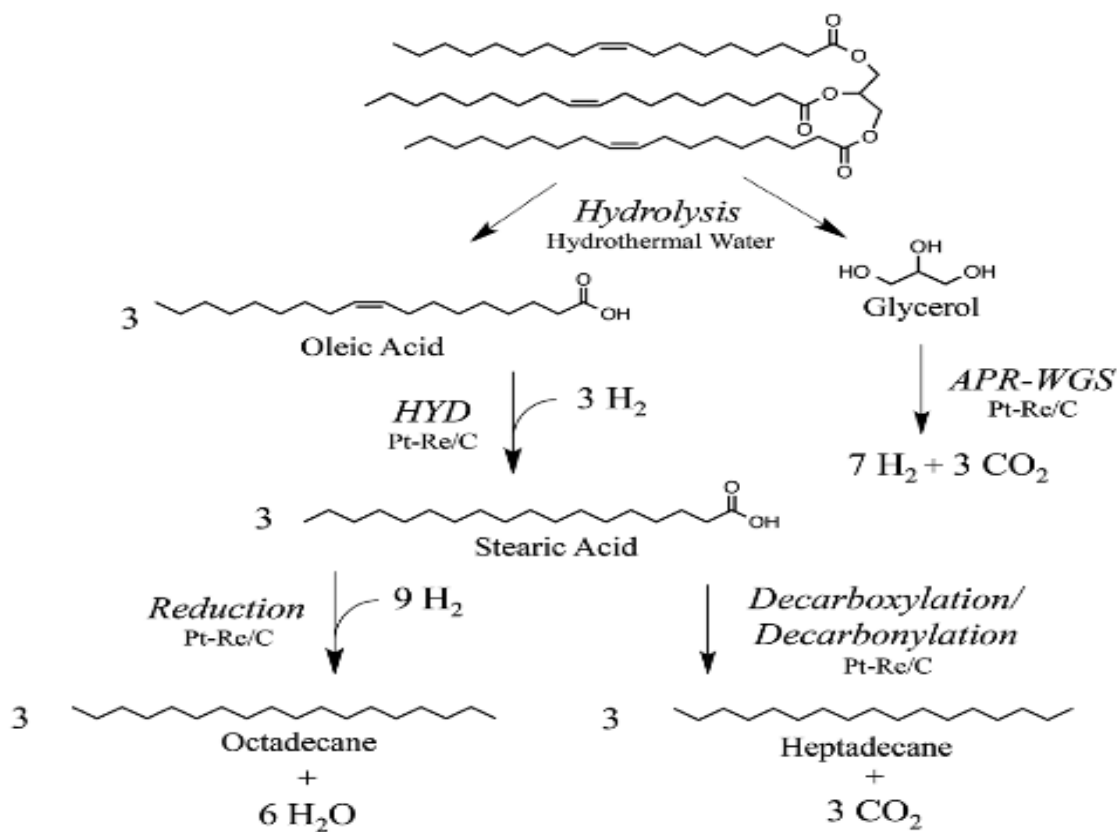
Figure 9. Proposed reaction scheme for catalytic hydrothermal reaction of the triglyceride molecule into hydrocarbons with *in situ* hydrogen production.[75]

CHAPTER 3

Effect of Metal Ratio and Preparation Method on Nickel−Tungsten Carbide Catalyst for Hydrocracking of Distillers Dried Grains with Solubles Corn Oil[*]

3.1 Introduction

Economic, ecological, and environmental issues associated with the energy derived from fossil sources has spurred research into developing alternative sources of energy that are sustainable and renewable.[83,84] Triglycerides from vegetable oils may be a suitable sources for liquid biofuel production (green diesel) via catalytic hydrocracking process. Because of the need to avoid a high-cost process and food competition, low-quality vegetable oils such as distillers dried grains with solubles (DDGS) corn oil could be an appropriate alternative to using fresh vegetable oils as feedstock. Biofuels that are produced from hydrocracking of renewable oils are quite similar to petroleum fuels; therefore, no modifications are required to existing infrastructures.[8]

During catalytic hydrocracking of vegetable oils, the triglycerides can be subjected to several reactions (Figure 10). Several types of catalysts, such as supported noble metal catalysts and sulfided bimetallic catalysts, have been investigated for the hydrocracking of vegetable oils to produce biofuels. Incorporated metal properties along with the catalyst support properties play a significant role for the deoxygenation and cracking activities of the catalysts. The noble metal catalysts are not viable economically because of the limited availability, high cost, and sensitivity to contaminants (such as oxygenated compounds) in the feedstock.[14] Although platinum supported on zeolite (H-ZSM-5 and HY) showed a great resistance to catalyst de- activation, the diesel yield was low (20 and 40 wt %, respectively).[85] Moreover, the support with higher acidity (H-ZSM-5) led to

---

lower diesel yield because of high cracking activity that favors gasoline production. On the other hand, sulfided bimetallic catalysts need to be maintained in the sulfided form in order to be active; therefore, a sulfurization cofeed needs to be added to the feedstock.[20] Koivusalmi et al.[86] reported that sulfided MoNi catalyst supported on γ-Al$_2$O$_3$ showed a high diesel yield ranging between 70 and 80 wt %. However, the low acidity of γ-Al$_2$O$_3$ did not contribute to the production of isoparaffins, which leads to a product with poor cold flow properties. In addition, the catalyst experienced a severe deactivation due to coke formation, which leads to lowering the diesel yield and building up pressure in the reactor.[87]

1. Hydrogenation
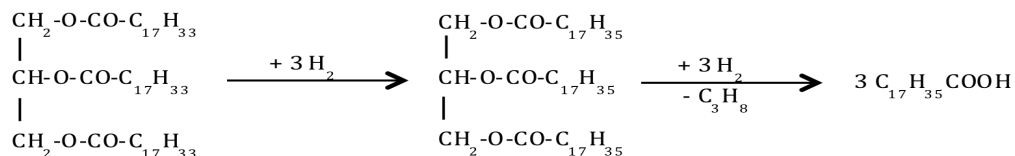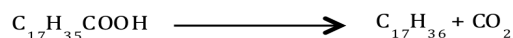
$$\begin{array}{l} CH_2\text{-}O\text{-}CO\text{-}C_{17}H_{33} \\ | \\ CH\text{-}O\text{-}CO\text{-}C_{17}H_{33} \\ | \\ CH_2\text{-}O\text{-}CO\text{-}C_{17}H_{33} \end{array} \xrightarrow{+\,3\,H_2} \begin{array}{l} CH_2\text{-}O\text{-}CO\text{-}C_{17}H_{35} \\ | \\ CH\text{-}O\text{-}CO\text{-}C_{17}H_{35} \\ | \\ CH_2\text{-}O\text{-}CO\text{-}C_{17}H_{35} \end{array} \xrightarrow[-\,C_3H_8]{+\,3\,H_2} 3\ C_{17}H_{35}COOH$$

2. Decarboxylation

$$C_{17}H_{35}COOH \longrightarrow C_{17}H_{36} + CO_2$$

3. Decarbonylation

$$C_{17}H_{35}COOH + H_2 \longrightarrow C_{17}H_{36} + H_2O + CO$$

4. Hydrodeoxygenation

$$C_{17}H_{35}COOH + 3H_2 \longrightarrow C_{18}H_{38} + 2H_2O$$

5. Hydroisomerization

$$n\text{-RH} \xrightarrow[\text{Cat.}]{H_2} iso\text{-RH}$$

6. Hydrocracking

$$iso\text{-RH} \xrightarrow[\text{Cat.}]{H_2} iso\text{-R}_1\text{H} + iso\text{-R}_2\text{H}$$
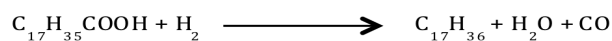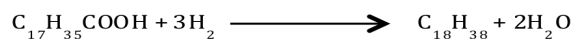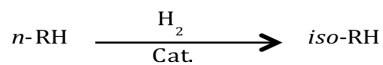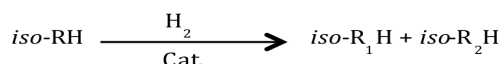
Figure 10. Hydrotreating reactions of triglycerides.

Recently, supported metal carbide and nitride catalysts have been receiving

considerable attention as catalysts for the hydrocracking of vegetable oils.[16] The existence of carbon atoms or nitrogen atoms in the lattice of transition metals extends the lattice parameter, which leads to increases in the d-band electron density of the metals.[17,18] Molybdenum carbide catalysts supported on carbon nanotubes (20% Mo_2C/CNTs) showed a good resistance to leaching; however, only 86% yield of paraffin and 46% selectivity of branched paraffin were obtained from rapeseed oil feedstock.[88] Furthermore, the bimetallic carbides and nitrides catalysts have shown activity and stability higher than that of the monometallic ones.[19] However, it has been claimed that the carbide form of NiMo/ZSM-5 catalyst produced an amount of CO and CO_2 from soybean oil feedstock lower than that of the nitride form catalyst.[20] Therefore, more hydrodeoxygenation took place on the carbide catalyst compared to the nitride catalyst. It has been reported that promoting the catalyst with nickel as a second metal increases the ratio of I{111}/I{200}, which leads to an increase in the hydrogenation activity of pyridine.[18] A few studies evaluated the effect of the support on the catalyst performance for the hydrocracking reaction. The support plays a significant role in the cracking and isomerization activity.[21] Most recently, Wang et al.[22] investigated the effect of several supports on the activity of NiMo carbide catalyst for the hydrotreating of soybean oil. The conversion of soybean oil reached 100% and the selectivity to green diesel was 97% for the NiMo carbide catalyst over Al-SBA- 15 during 7 days of reaction at 400 °C and 650 psi (4.48 MPa).

In the present work, a new NiWC/Al-SBA-15 catalyst was developed for the hydrocracking of DDGS corn oil. The effect of the Ni−W ratio and the catalyst preparation method on activity, selectivity, and durability of the catalyst for green diesel

production was investigated under relatively mild reaction conditions. The metal dispersion on the support and the alloy formation were studied to elucidate their effects on the catalyst performance and provide a better understanding of the hydrocracking process. The experiments were conducted in a plug flow reactor.

3.2 Experimental section

3.2.1 Catalyst Preparation (NiWC/Al-SBA-15) by Impregnation Method

A neutral support, SBA-15 with a 9 nm pore diameter and Brunauer−Emmett−Teller (BET) surface area of 600 m^2 g^{-1}, was purchased from ACS (Advanced Chemicals Supplier) and was modified by aluminum isoprop- oxide (Sigma-Aldrich) to adjust the acidity of the support following the synthesis procedure of Wu et al.[89] SBA-15 (20 g) was dissolved in 150 mL of hexane, and then 0.067 g of aluminum isopropoxide was added with stirring to the aqueous solution for 24 h. The solution was filtered, dried, and calcined at 550 °C for 4 h. Appropriate amounts of $N_2NiO_6 \cdot 6H_2O$ and $H_{42}N_{10}O_{42}W_{12} \cdot H_2O$ (Sigma-Aldrich) solution were used to provide Ni and W, respectively. Four different ratios of Ni−W were prepared (Table 2). For the impregnation, the salts were dissolved in sufficient distilled water equal to the total pore volume of the Al-SBA-15 and immediately added to 20 g of the Al-SBA-15.[20] This solution was then gently agitated to impregnate the entire pore volume of the catalyst with the metals. The resulting solid was dried in a programmable high-temperature oven at 120 °C for 24 h and then calcined at 450 °C for 4 h.

Carburization was conducted using temperature-programmed reduction (TPR), according to the method of Claridge et al.[90] Each metal oxide precursor was placed in a quartz tube, and a flow of 30 cm^3 min^{-1} of a mixture of (20% CH_4/80% H_2) was used at a

heating rate of 10 K min^{-1} to 250 °C and then at 2.0 K min^{-1} to 730 °C. The temperature

was maintained at 730 °C, the optimal temperature for carbide formation, for 30 min to

complete the reaction. After being cooled, the catalyst was passivated by using a mixture

of (1% O$_2$/99% Ar) for 1 h to eliminate the pyrophoric properties[19] and protect the bulk

of the catalyst against deep oxidation.[91]

Table 2. Reaction quantities used for the synthesis of NiWC/Al-SBA-15 using impregnation and DENP methods.

Ni/W Ratio	N$_2$NiO$_6$.6H$_2$O (g)	H$_{42}$N$_{10}$O$_{42}$W$_{12}$.H$_2$O (g)	weight of G4 PAMAM (g)	volume of NaBH$_4$ (mL)
1:9	0.5	1.25	0.362	81.6
1:1	2.46	0.69	0.2	45
2:1	3.32	0.46	0.133	30
9:1	4.5	0.139	0.04	9.0

3.2.2 Catalyst Preparation (NiWC/Al-SBA-15) by Dendrimer-Encapsulated Nanoparticles Method

The protocol for preparing the catalysts by the DENP method was adapted and modified from a previous study.[92] An amine-terminated fourth generation poly(amidoamine) dendrimer (PAMAM G4.0-NH$_2$ 10 wt % in methanol) (Sigma-Aldrich) was used as a template to prepare DENP of W nanoparticles. The W nanoparticles were synthesized by complexing W ions to the interior amine groups of the dendrimer followed by chemical reduction of the ions using sodium borohydride (NaBH$_4$ 12 wt % in 14 M NaOH) (Sigma-Aldrich) to obtain encapsulated zerovalent W particles (Figure 11).[93] According to a previous study,[94] the optimal molar ratio of W to dendrimer

for G4, G5, and G6 are 16, 32, and 64, respectively. These ratios determine the maximum capacity of the dendrimers to coordinate with W ions to the tertiary amine groups of the dendrimers. Table 2 shows the weights of the G4 dendrimer. An aqueous dendrimer solution with a concentration of 10 µM was prepared, then the appropriate weight of W salt was added into the aqueous solution to achieve the desired Ni−W ratio. The solution was stirred for 20 min to ensure that W ions were anchored with the tertiary amine groups of the dendrimer. The W ions were reduced by using excess $NaBH_4$ that is added dropwise to produce encapsulated zerovalent W particles (Table 2). Surface chemisorption is accomplished through the strong interaction of the Al-SBA-15 surface with pendant ($-NH_2$) groups on the peripheral surface of PAMAM.[95] Consequently, the use of dendrimers provides the advantage of decreasing the particle size and enhancing the particle dispersion with minimal postagglomeration. The Ni supported by Al-SBA- 15 was prepared by following the impregnation method as described above using the appropriate weights of Ni salt added to the aqueous solution. The nanoparticles supported by Al-SBA-15 were collected by using a centrifuge, dried at 100 °C for 2 days, and calcined at 500 °C for 3 h. Finally, the carburization and passivation steps were conducted as described above.
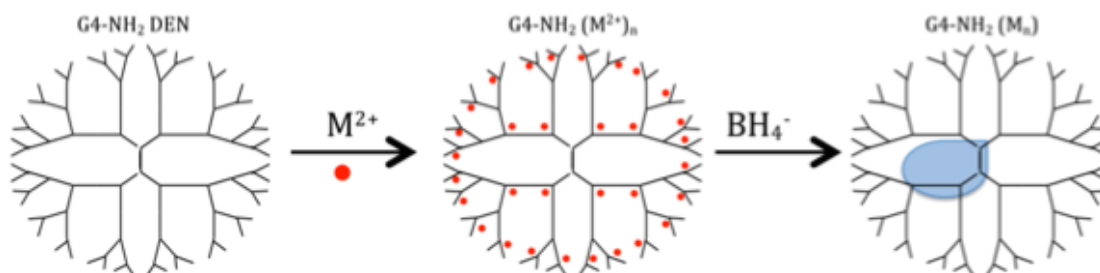
Figure 11. Synthesis of dendrimer-encapsulated nanoparticles.

3.2.3 Catalyst characterization

BET surface area and Barrett−Joyner−Halenda (BJH) pore size and pore volume were determined using a Micromeritics model ASAP 2010 surface area analyzer with 99.9% purity nitrogen gas, and the results were collected on a Tristar 3020 instrument. The degassing conditions were at 400 °C with a heating ramp of 10 °C min^{-1} for 2 h prior to analysis. X-ray diffraction (XRD) patterns were collected on SmartLab Guidance and MDI Jade 8 instrument using a Rigaku RU2000 rotating anode power diffractometer (Rigaku Americas Corporation, TX) at a scan rate of 4° min^{-1}. Scanning electron microscopy (SEM, JSM-6510LV) and X-ray energy-dispersive spectrometry (EDS) were used for elemental spectra and mapping. Transmission electron microscopy (TEM) images were obtained with a JEM 2010 HR TEM instrument, which is equipped with a digital camera system enabling the capture of both high-resolution images and electron diffraction patterns. Inductively coupled plasma (ICP) spectrometry (Optima TM 2100 DV ICP-OES system, PerkinElmer) was used to investigate the catalyst leaching.

3.2.4 Experimental procedure

The hydrocracking reaction of DDGS corn oil was performed in a system (BTRS-Jr, Autoclave Engineers, PA) that consists of a fixed bed reactor with an internal diameter of 1.31 cm and a length of 61 cm, a heater, a pressure regulator, and a condenser (Figure 12). The experimental conditions were similar to those from a previous study,[20] in which biofuels were produced via hydrocracking of soybean oil over transition-metal carbides and nitrides supported on ZSM-5. A 2 g sample of the catalyst prepared by the impregnation method (20−80 nm particle size) or the catalyst prepared by the DENP method (5−20 nm particle size) was mixed with 4.5 g of quartz beads and loaded in the

reactor. The catalyst was reduced by using a hydrogen flow of 30 mL min^{-1} at 450 °C for 3 h. Quartz beads were used to dilute the catalyst bed to prevent plugging and enhance the heat and mass transfer. The reaction was carried out at 400 °C and 650 psi (4.48 MPa). The hydrogen flow was maintained constant at 30 mL min^{-1}, and the DDGS corn oil was fed at liquid hourly space velocity (LHSV) of 1 h^{-1}. The outlet liquid phase was separated from the gas phase via a condenser. The liquid samples were collected and consisted of two phases: organic liquid product (OLP) and aqueous phase. The OLP samples were analyzed qualitatively and quantitatively using gas chromatography−flame ionization detection (GC-FID). The green diesel fraction was identified as (C_{12}−C_{22}) using GC standards. Fourier transform infrared (FTIR) and gas chromatography−mass spectrometry (GC-MS) were employed to qualitatively determine the OLP distribution to identify the unknown compounds.
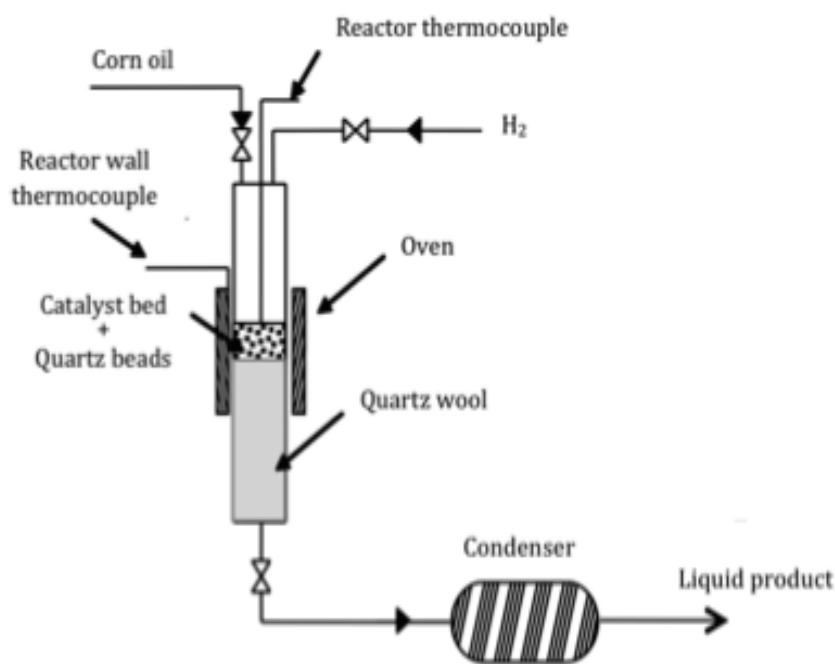
Figure 12. Reactor system set up.

3.3 Results and discussion

3.3.1 Catalyst characterization

Figure 13 presents the XRD patterns of the modified support (Al-SBA-15) and four different catalysts prepared by the impregnation method. The XRD pattern of the support has no distinct peak, indicating that the support is amorphous. Also, the broad peak (between 2θ of 15 and 30°) suggests that the support is mesoporous. The XRD patterns of the catalysts show that there are three main peaks at $2\theta = 44.2°$, $51.9°$, and $76.1°$, corresponding to Ni particles because Ni metal can be reduced easily.[96] The intensities of the peaks increase as Ni content increases. The peak at 2θ of 48.1° corresponds to Ni−W alloys (Ni_4W) with a structure of (211). This peak intensity increases with increasing Ni content for the all catalyst ratios; interestingly, the peak is not observable for the Ni−W ratio of 9:1, indicating that there is little or no alloy formed. The tungsten carbide phase was found in every catalyst except for that with a Ni−W ratio of 9:1, which suggested that the W carbide phase was very well-dispersed on the support.
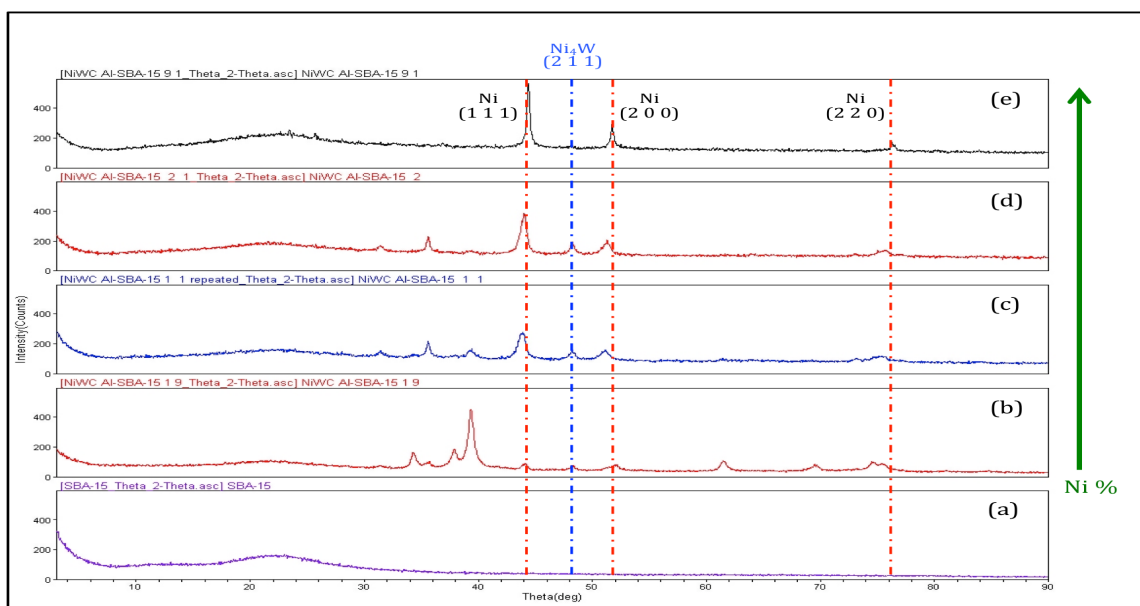
Figure 13. XRD patterns of the support and catalysts prepared by impregnation method: (a) Al-SBA-15, (b) Ni-W=1:9, (c) Ni-W=1:1, (d) Ni-W=2:1, and (e) Ni-W=9:1.

Figure 14 shows the N_2 sorption isotherm of the catalysts prepared by the impregnation method. H1 hysteresis by the IUPAC classification is observed, which is associated with the presence of a mesoporous matrix (SBA-15). The surface area, pore size, and pore volume are summarized in Table 3. The surface area and pore size of the catalysts decreased as compared with those of the Al-SBA-15 (surface area of 600 m^2 g^{-1} and pore size of 9 nm), which could be caused by structural loss and/or pore blockage.[97] No significant differences were seen among the catalysts with different loadings.
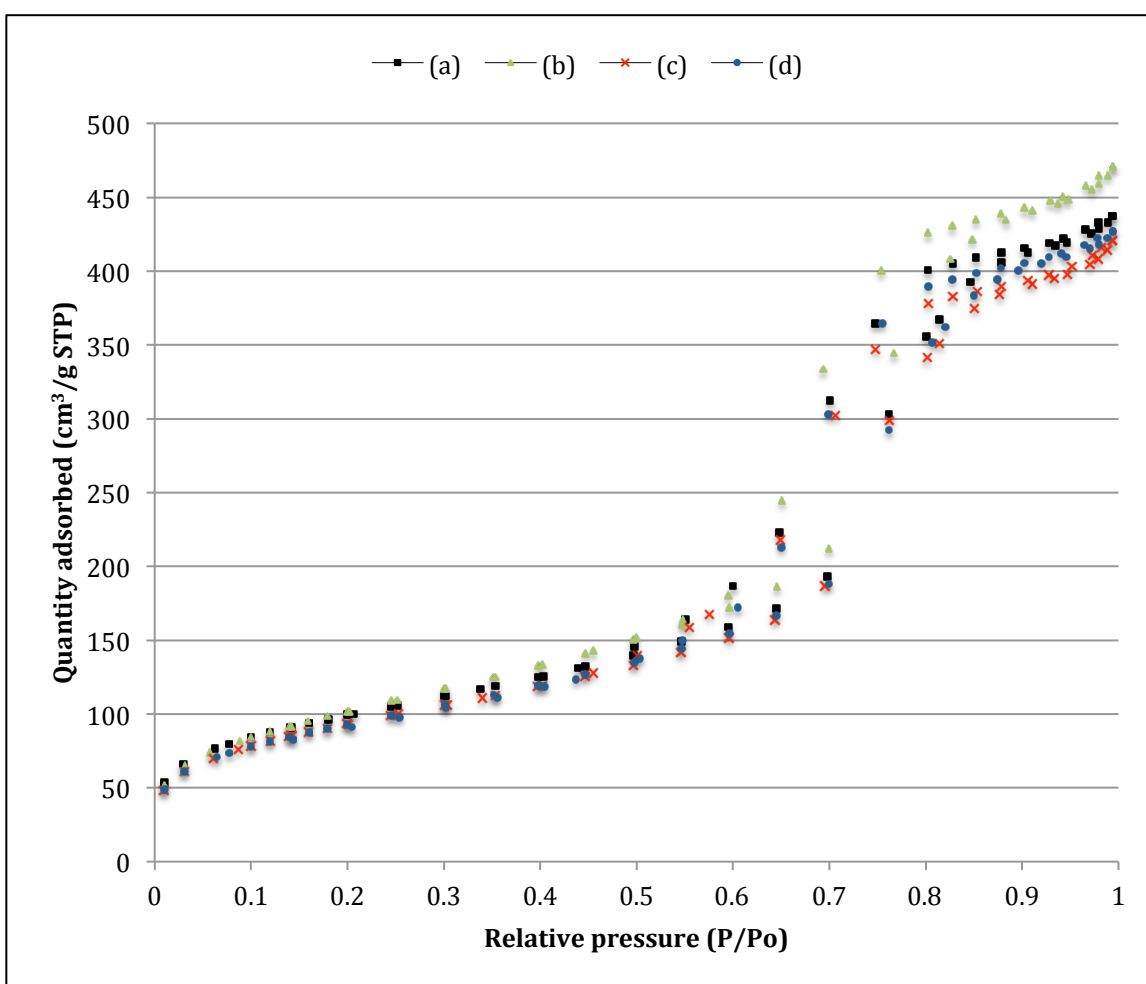
Figure 14. N_2 sorption isotherms of NiWC/Al-SBA-15 prepared by the impregnation method: (a) Ni-W = 1:1, (b) Ni-W = 1:9, (c) Ni-W = 2:1, and (d) Ni-W = 9:1.

Table 3. Physical properties of NiWC/Al-SBA-15 for different Ni-W ratios.

Ni-W Ratio	S_{BET} (m^2 g^{-1})	pore size (nm)	pore volume (cm^3 g^{-1})
1:9	376	6.91	0.74
1:1	361	7.30	0.69
2:1	342	7.32	0.66
9:1	340	7.13	0.67

SEM and EDS were used to characterize the catalysts that were prepared by the impregnation method to determine Ni and W distributions on the support (Al-SBA-15). Figure 15 shows the distribution of Ni particles on the support which are well- dispersed, with no particle agglomeration observed at any area. On the other hand, W particles had poor distribution, especially for the catalysts with high W content (Figure 16). It is likely that the surface energy of the W particles, which is higher than that of Ni particles, leads to W particle aggregation.[98,99]
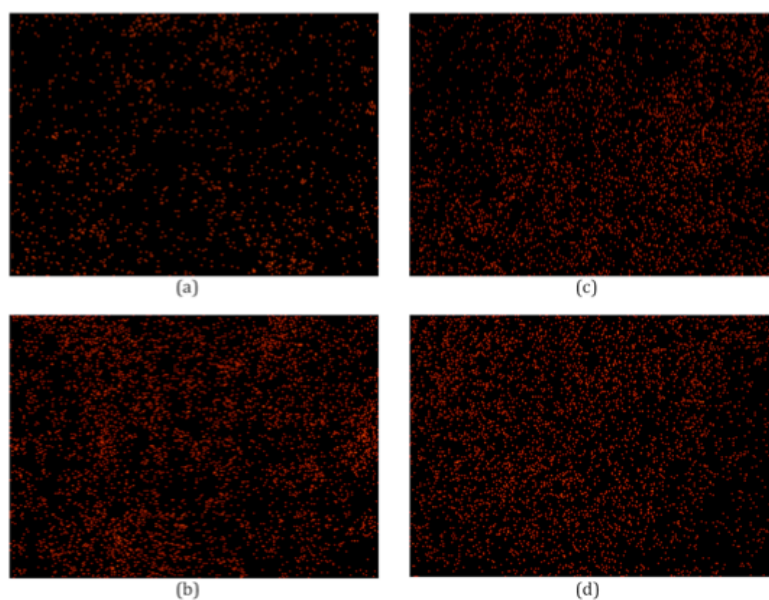
Figure 15. Distribution of Ni particles in the catalysts prepared by impregnation method: (a) Ni-W=1:9, (b) Ni-W=1:1, (c) Ni-W=2:1, and (d) Ni-W=9:1.

Figure 17 shows the XRD patterns of the catalysts prepared by the DENP method for three different ratios of Ni−W (1:9, 1:1, and 2:1). The figure indicates that the three peaks that were found at 2θ of 44.2°, 51.9°, and 76.1° correspond to Ni particles. The peaks for tungsten carbides did not appear, which indicates that the phase either did not exist or the carbide phase was very well-dispersed on the support; therefore, SEM and EDS were used to study the existence of WC phase. In addition, the peak of Ni−W alloy was not observed.
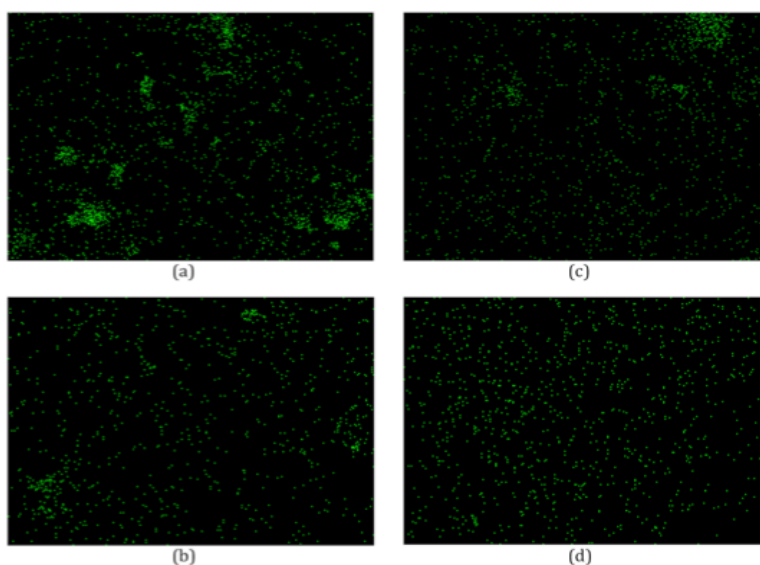
Figure 16. Distribution of W particles in the catalysts prepared by impregnation method:
(a) Ni-W=1:9, (b) Ni-W=1:1, (c) Ni-W=2:1, and (d) Ni-W=9:1.

SEM and EDS (Figure 18) confirmed that the W particles are present in the catalysts prepared by the DENP method and the W particles are very well dispersed on the support. Also, the particle size of the catalysts prepared by the DENP method are in the range of 5−20 nm (Figure 19a), which is smaller than the particle size of the catalysts prepared by the impregnation method (Figure 19b). Thus, the DENP method produces a smaller particle size.
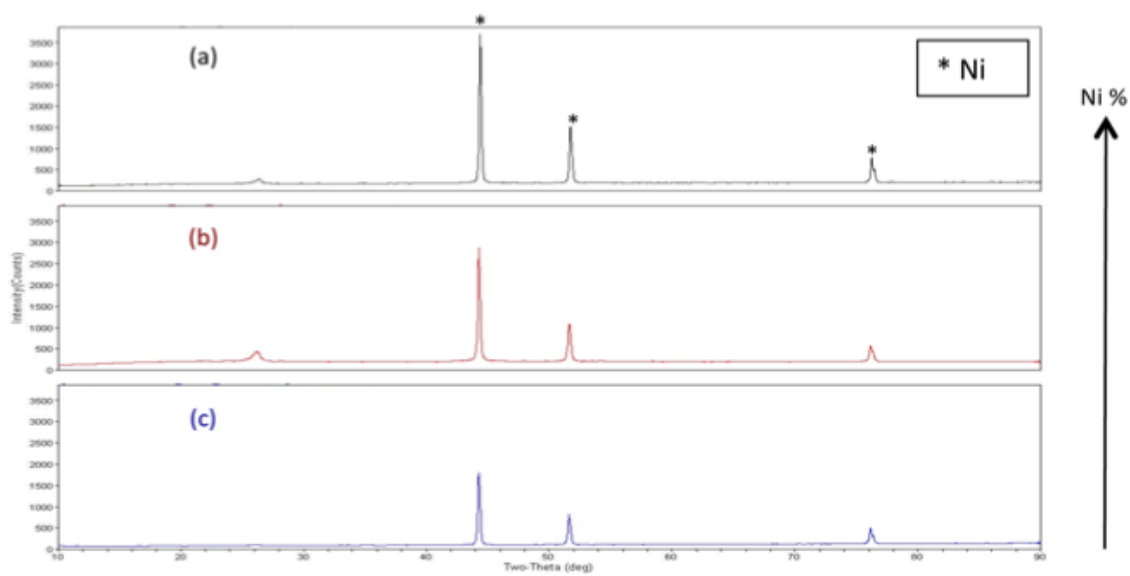
Figure 17. XRD patterns of the catalysts prepared by DENP method: (a) Ni-W=9:1, (b) Ni-W=2:1, and (c) Ni-W=1:1.
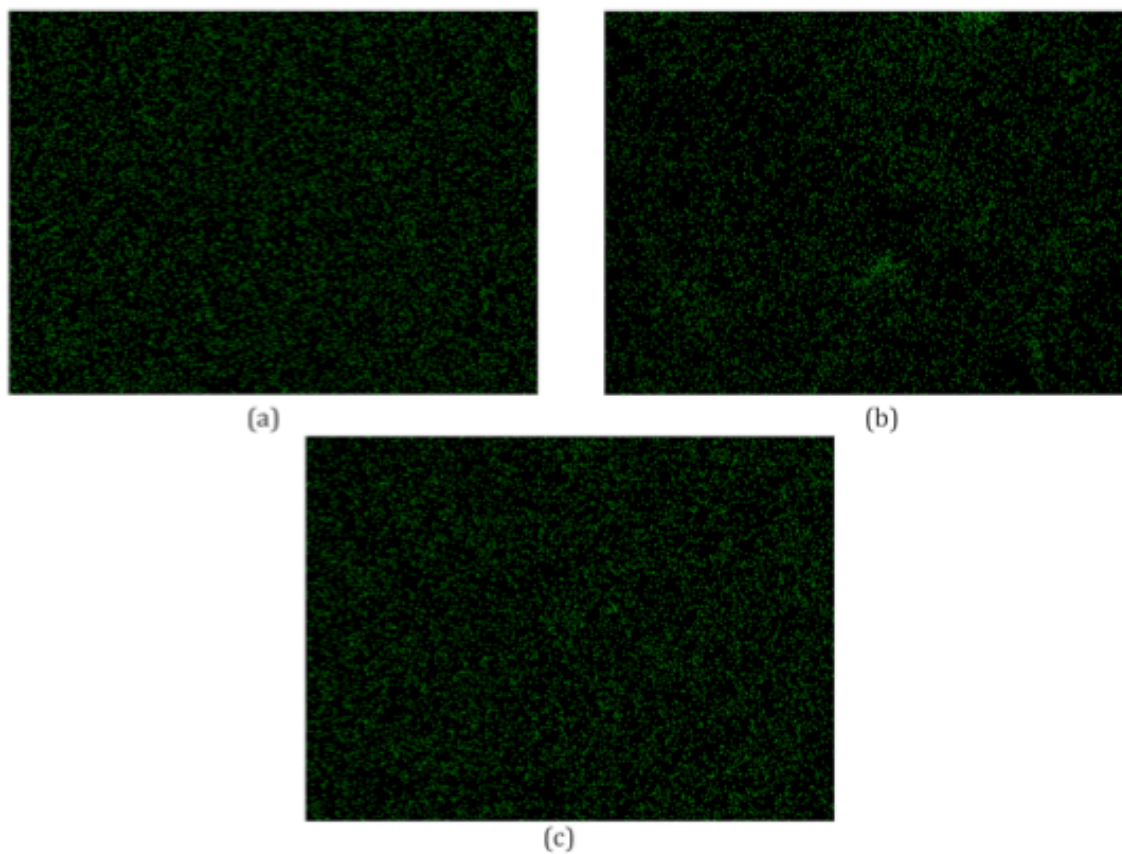
Figure 18. Distribution of W particles in the catalysts prepared by DENP method: (a) Ni-W=1:9, (b) Ni-W=1:1, and (c) Ni-W=2:1.
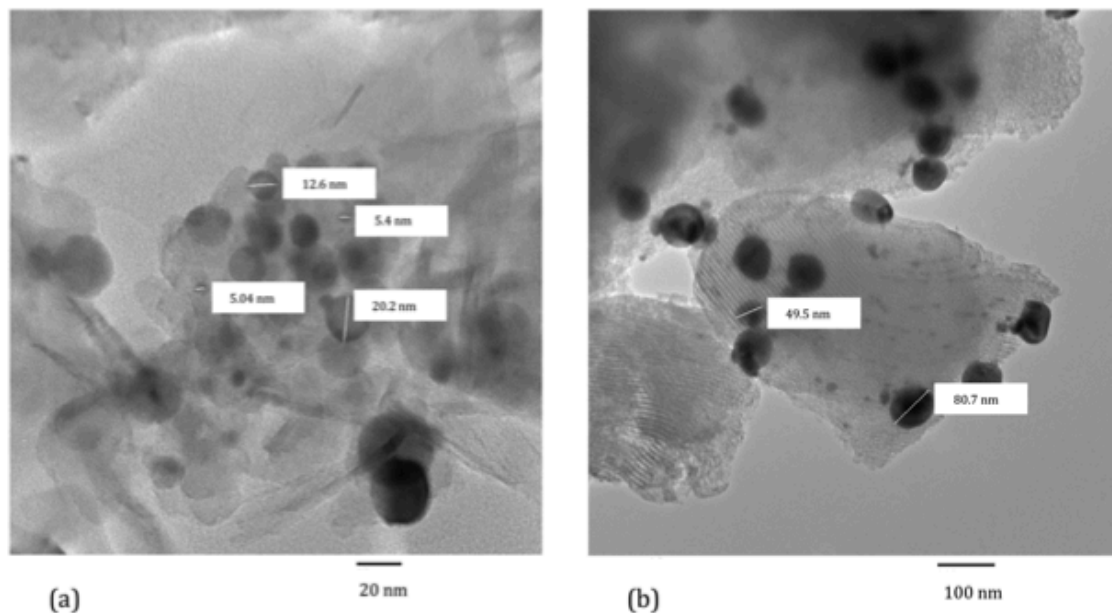
Figure 19. TEM image of NiWC/Al-SBA-15 prepared by: (a) the DENP method and (b) the impregnation method.

3.3.2 Catalyst performance evaluation

The performance of the prepared catalysts was evaluated for hydrocracking of DDGS corn oil at a reaction temperature of 400 °C, pressure of 650 psi (4.48 MPa), H_2 flow rate of 30 mL min^{-1}, and DDGS corn oil LHSV of 1 h^{-1}. The OLPs that were obtained from the catalysts prepared by the impregnation method were analyzed by using GC-FID to determine the conversion of DDGS corn oil and the selectivity of diesel (Table 4). The conversion of corn oil for the first day was high for every Ni−W ratio except for the Ni−W ratio of 1:9. Also, the catalysts with Ni−W ratios of 1:1 and 2:1 deactivated very fast, which can be attributed to the deposition of coke.[100] However, the catalyst with Ni−W ratio of 9:1 showed the best conversion of corn oil (100% for the first 2 days) and showed a significant resistance against deactivation. Table 4 indicates that the selectivity of diesel was low for every ratio except for the Ni−W ratio of 9:1 (almost 100% for the first 2

days).

Table 4. Conversion and liquid product selectivity of hydrocracking of DDGS corn oil over NiWC/Al-SBA-15 catalysts prepared by the impregnation method.

Ni-W ratio	Conversion (%)		Selectivity of diesel (%)	
	First day	Second day	First day	Second day
1:9	29.6	31.2	47.7	34.1
1:1	99.8	23.4	83.7	73.5
2:1	95.1	17.5	62.9	55.4
9:1	100	100	100	98.5

The stability of the catalyst was studied by comparing the XRD pattern of the fresh catalyst versus that of the used catalyst (Figure 20). The catalysts with Ni−W ratios of 1:1 and 2:1 experienced changes in their structures after 2 days of reaction. There is a peak shift in each pattern of Ni−W ratios of 1:1 and 2:1 at 2θ of 43.8° and 31.4°, respectively. On the other hand, the most stable catalyst was the catalyst with Ni−W ratio of 9:1, with the pattern of new and used catalyst remaining unchanged. Characterization results show the impregnation catalyst with Ni−W of 9:1 has the highest dispersion of W particles and no Ni−W alloy formed. Thus, having well-dispersed W particles and minimizing Ni−W alloys could lead to higher conversion of DDGS corn oil, higher selectivity of diesel, and greater stability. Although the acid properties and hydrocracking activity of the catalysts are enhanced by increasing the load of the active component (W), the promoter (Ni) is important for enhancing metal dispersion and catalyst selectivity.[101] The observation that higher particle dispersion leads to higher catalyst activity is in a good agreement with results obtained by Halachev et al.[102] Upon alloying, the lattice constant of W adopts the

lattice constant of Ni, resulting in an increase in W−W bond length; therefore, the center of the W d-band shifts away from the Fermi level, which weakens the interaction between the reactants and the surface of W atoms.[103-105]
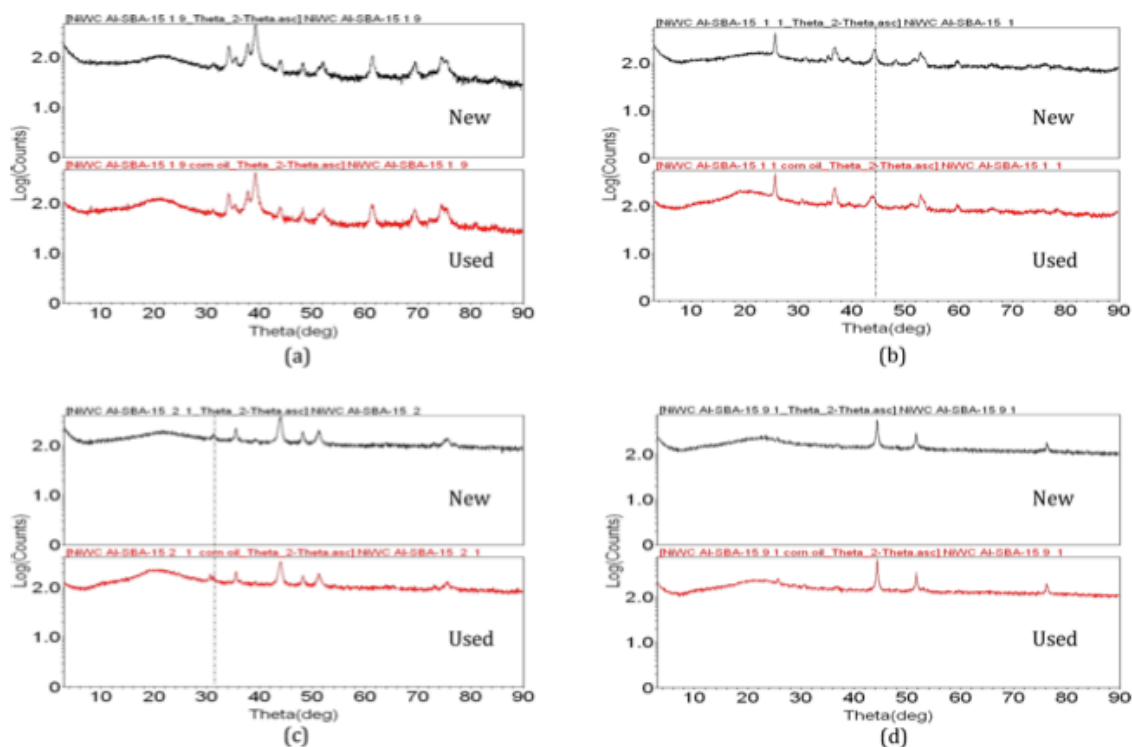
Figure 20. XRD patterns of new and used catalysts prepared by the impregnation method: (a) Ni-W=1:9, (b) Ni-W=1:1, (c) Ni-W=2:1, and (d) Ni-W=9:1.

Dramatic effects on the catalytic activity have been observed as a result of the modification of the catalysts prepared by the DENP method in metal dispersion and minimizing alloy formation. A very high conversion of corn oil (almost 100%) was observed for every catalyst prepared by the DENP method (Figure 21). The catalysts prepared by the DENP method showed activity higher than that of the catalysts that were prepared by the impregnation method, which can be attributed to the absence of Ni−W alloy. Even though the catalyst characterization showed high metal dispersion and no alloy formation, these catalysts exhibited different diesel selectivity (Figure 21). The

catalyst with a Ni−W ratio of 2:1 showed the highest selectivity to diesel in comparison to that of other Ni−W ratios. The selectivity of diesel was high (100%) for the first 2 days, then decreased. The catalyst with Ni−W ratio of 1:1 was steadier than the others; however, the selectivity of diesel was less than 80%. The differences in selectivity could be attributed to the changing Ni−W ratio. Changing the metal ratio results in varying the strength of Lewis sites and the number of Brønsted sites, which significantly influences the catalytic activity, coke formation, and thermal stability.[101,106] Also, Figure 21 indicates that the selectivity of diesel is proportional to the Ni content in the catalyst because nickel has the ability to adsorb and activate hydrogen.[107] Although dendrimer-based catalysts are relatively more expensive than catalysts prepared by the impregnation method and some other commercial catalysts, they can still be used as model systems to investigate structure−function relationships.[95] It may be possible to recover and recycle the dendrimers, perhaps making it applicable for some industrial applications.[93] Regardless, the cost of the preparation methods was not a focus of this study.

The FTIR spectra of the OLP was obtained for NiWC/Al- SBA-15 prepared by the DENP method with Ni−W ratio of 1:9 (Figure 22a), Ni−W ratio of 1:1 (Figure 22b), and Ni−W ratio of 2:1 (Figure 22c). All showed a similar trend, which indicates that the conversion of triglycerides was 100% for all catalysts prepared by the DENP method. They show that the peak at 722.34 cm^{-1}, which corresponds to C=C, for the products was smaller than the one for the corn oil. Therefore, most of the double bonds were saturated to form single bonds. Also, it could be noticed from the FTIR spectra that most of the triglycerides in corn oil were converted because the peak at 1743.89 cm^{-1} was diminished. However, the increase in the peak at 1712.89 cm^{-1} indicates that a larger

amount of esters was produced along with a longer reaction time. This result is in agreement with Albuquerque et al.[108] This fact indicates that the deoxygenating activity of the catalysts decreased as the time increased.[109] On the other hand, the FTIR spectra of day 2 in Figure 22c showed no ester group absorption, which is consistent with the result from GC-FID that the diesel selectivity was 100%.
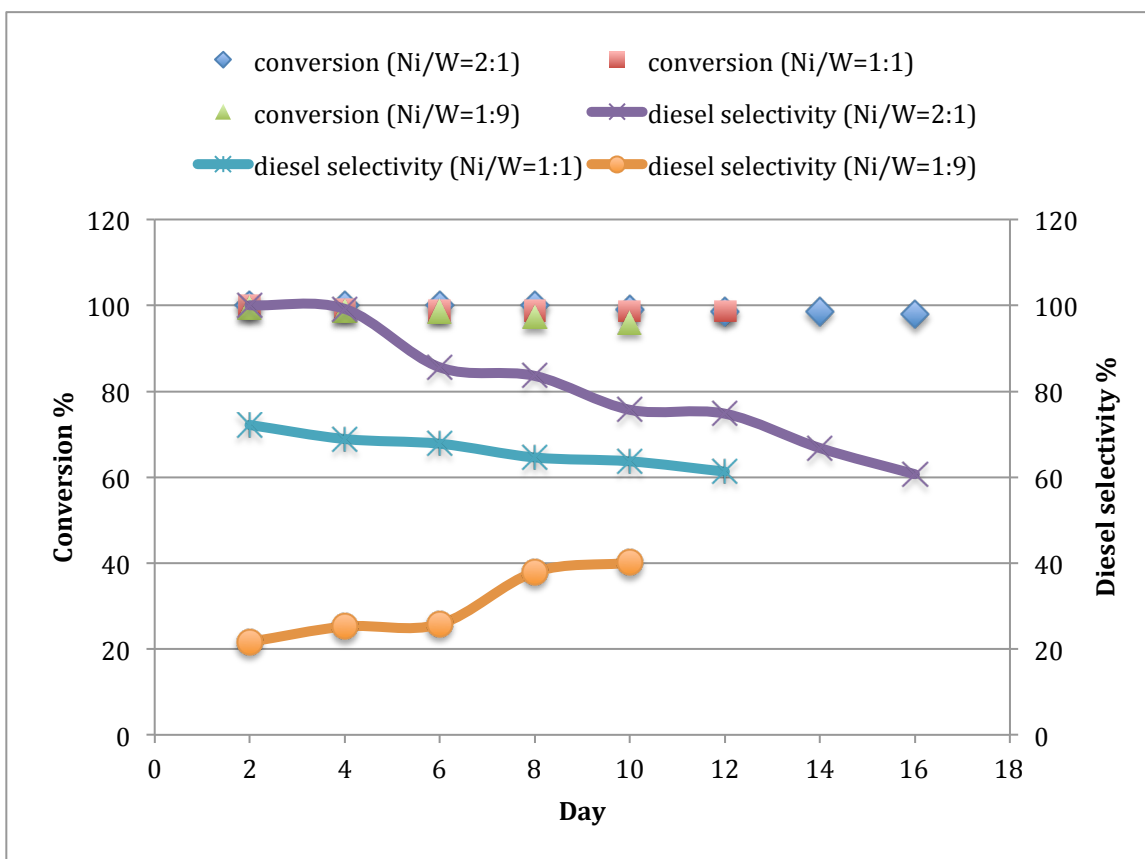
Figure 21. Conversion of DDGS corn oil and the diesel selectivity over NiWC/Al-SBA-15 prepared by the DENP method.

Figure 23 shows the GC-MS qualitative analysis of the products obtained from the catalyst prepared by the DENP method with Ni−W ratio of 1:9, 1:1, and 2:1. The spectra in Figure 23c corresponds to a Ni−W ratio of 2:1 and confirmed that the OLP was in the diesel hydrocarbon range for the first two products, which led to 100% selectivity of

diesel. However, other compounds were produced along with a longer reaction time, indicating a decrease in diesel selectivity. Figure 23a,b shows that not only alkanes but also other compounds were observed for every sample. Thus, it is clear that the diesel selectivity of the catalyst with Ni−W ratio of 1:9 or 1:1 was lower than that of the catalyst with Ni−W ratio of 2:1.

(a)

(b)

(c)
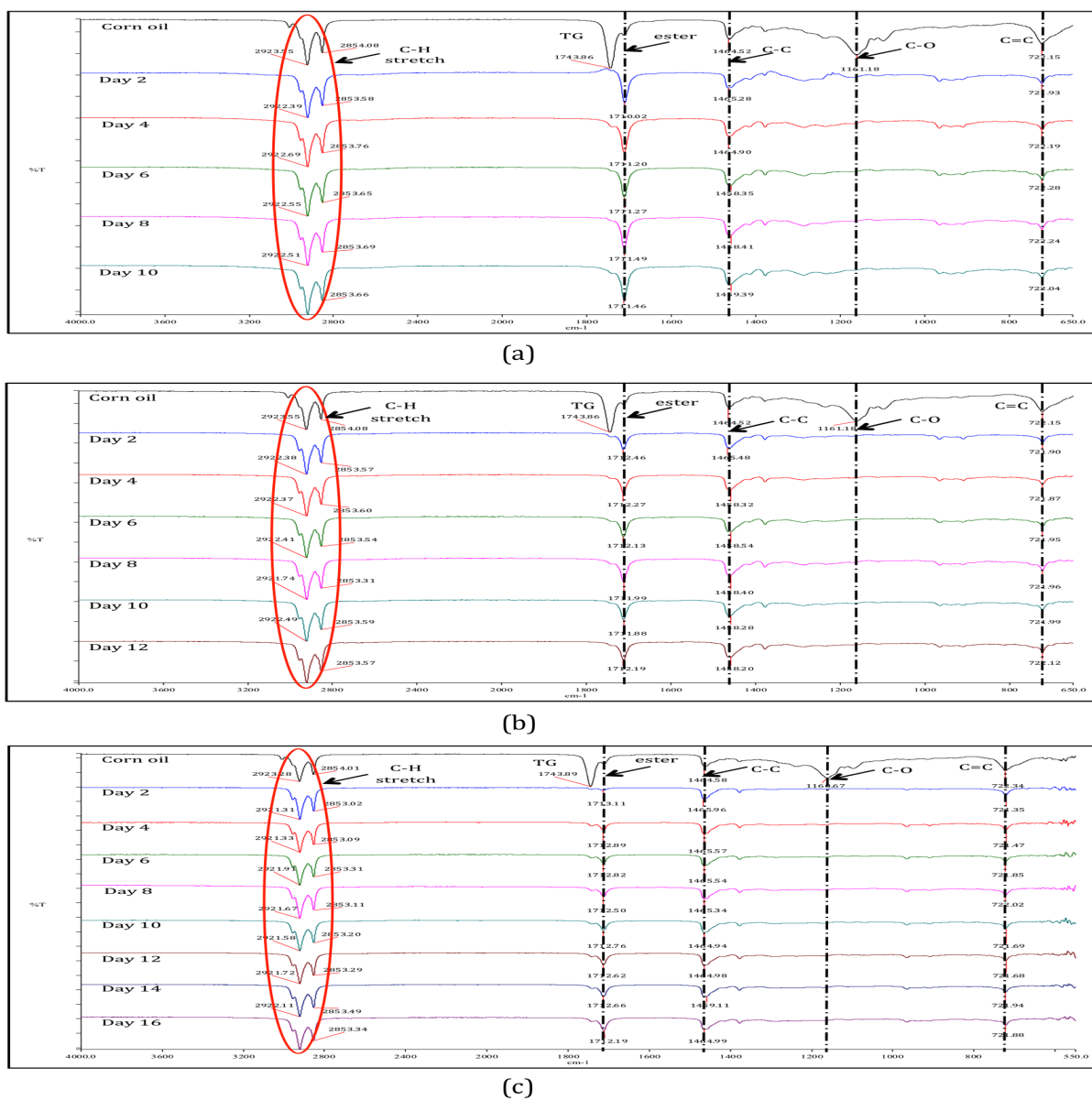
Figure 22. FTIR spectra of the products over NiWC/Al-SBA-15 prepared by the DENP method with Ni-W ratio of (a) 1:9, (b) 1:1, and (c) 2:1.
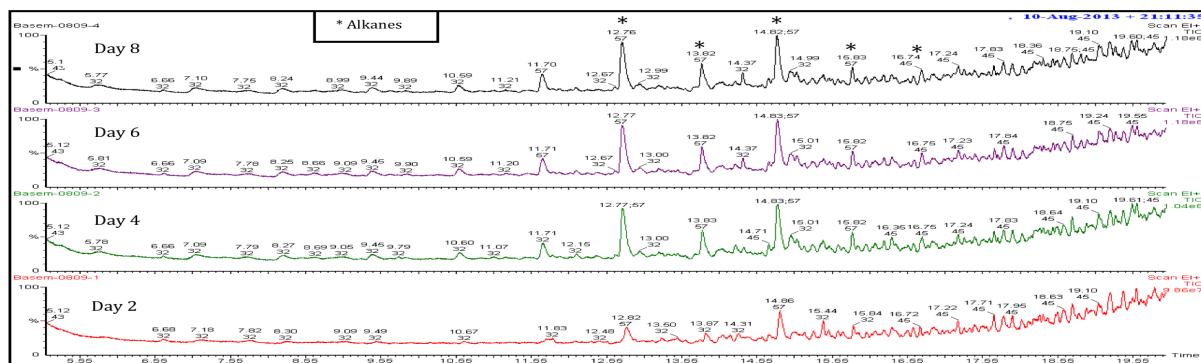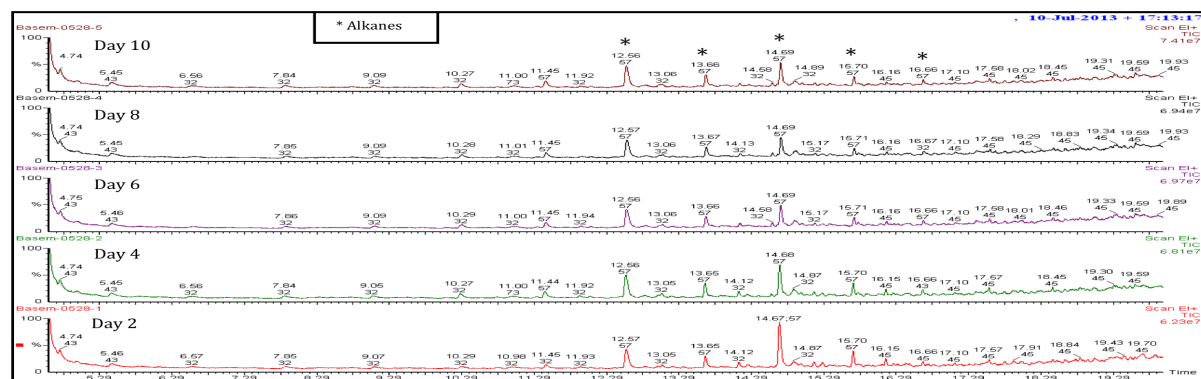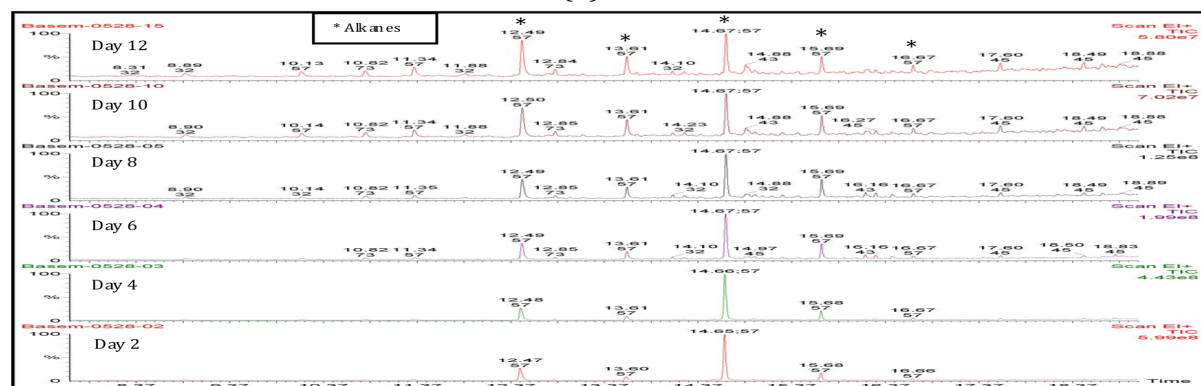
Figure 23. GC-MS analysis of the products over NiWC/Al-SBA-15 prepared by the DENP method with Ni-W ratio of (a) 1:9, (b) 1:1, and (c) 2:1.

In addition, the peaks that are shown in Figure 23 were identified in order to propose a possible mechanism of how these compounds were formed. Most of the other compounds produced are alcohols or esters as a result of high temperature, high pressure, and existence of water.[110] One of the possible mechanisms of forming alcohols consists

of two reactions: cracking and hydration.[110] The long saturated hydrocarbon chains are cracked in the presence of catalyst and high temperature to form saturated and unsaturated hydrocarbon chains. Then, the unsaturated hydrocarbons are hydrated in the presence of water to produce alcohols. A free radical mechanism is another mechanism that could be a responsible for converting hydrocarbons to alcohols.[111,112] In that mechanism, the alkane produces a radical at the surface of metal active sites which then reacts with the dissolved oxygen to make a peroxo radical species that leads to alcohol.[113]

Inductively coupled plasma spectrometry was used to determine the Ni and Si concentration in the OLP (Table 5). The concentration of Ni was less than 1.0 ppm in every sample, which could be deemed negligible. Although the concentration of Si in the second day was very small, the concentration of Si increased over time. This suggests that Si may have leached out of the catalyst, leading to a collapse of the Al-SBA-15 structure, a reduction in pore diameter, and resultant drop in diesel selectivity.[114]

Table 5. ICP results for the liquid products obtained from NiWC/Al-SBA-15 catalysts prepared by DENP method.

NiWC/Al-SBA-15 (Ni/W=2:1)			NiWC/Al-SBA-15 (Ni/W=1:1)		
Product (OLP)	Concentration of Ni (ppm)	Concentration of Si (ppm)	Product (OLP)	Concentration of Ni (ppm)	Concentration of Si (ppm)
Day 2	0.836	1.11	Day 2	0.59	2.479
Day 6	0.611	4.25	Day 4	0.712	16.31
Day 10	0.583	12.62	Day 6	0.853	10.55
Day 14	0.272	13.03	Day 8	0.435	12.182

The NiWC/Al-SBA-15 catalyst with a Ni−W ratio of 2:1 prepared by the DENP method maintained a high hydrocracking conversion of DDGS corn oil up to 16 days on

stream. However, Gong et al.[115] reported that NiMoP/Al$_2$O$_3$ catalyst started deactivation after a reaction time of 120 h for the hydrocracking of jatropha oil at LHSV = 2 h^{-1}, 3 MPa H$_2$, and 350 °C. Lower diesel selectivities were obtained from NiMoC catalyst over different supports for the hydrocracking of soybean oil at LHSV = 1 h^{-1}, 4.48 MPa H$_2$, and 400 °C.[22] For example, NiMoC/USY catalyst showed low diesel selectivity (about 55−60%) up to 7 days. As mentioned previously, the composition of the green diesel produced by this method was purely hydrocarbons of (C$_{12}$−C$_{22}$). The properties of the hydrocarbons in the range of (C$_{12}$−C$_{22}$) are quite similar to those for petroleum diesel; thus, this method produced a high-quality green diesel.[116]

3.4 Conclusions

A 10% NiWC/Al-SBA-15 catalyst is highly active for the hydrocracking of DDGS corn oil. Metal dispersion, alloy formation, and Ni content are important factors for improving the behavior of the catalysts. Both metal ratio and preparation method control the degree of metal dispersion and alloy formation. Enhancing the degree of metal dispersion and suppressing the formation of metal alloys results in essentially 100% conversion and green diesel selectivity. A proper Ni content is essential for providing sufficient activated hydrogen for the hydrocracking reactions and enhancing the metal dispersion. The decrease in green diesel selectivity can be attributed to the secondary reactions that convert the green diesel to alcohols. Thus, NiWC supported on Al-SBA-15 could be a prospective catalyst for the hydrocracking of waste oil under relatively mild operation conditions, which leads to lower operating costs.

CHAPTER 4

Hydrocracking of DDGS corn oil over transition metal carbides supported on Al-SBA-15: Effect of fractional sum of metal electronegativities[†]

4.1 Introduction

The search for alternative energy sources that are sustainable and renewable has been motivated by increasing petroleum prices, diminishing fossil fuel reserves, and environmental issues associated with greenhouse gas emissions. Biofuels (in particular, green diesel) produced from the hydroprocessing of vegetable oils typically display properties that are similar to petroleum diesel and can be directly used in existing infrastructures with no modifications.[8,85] Low quality vegetable oils such as distillers dried grains with solubles (DDGS) corn oil could be appropriate alternatives to fresh vegetable oils as feedstocks because they are inexpensive and non-food-competitive.

During the catalytic hydrocracking of vegetable oils, the triglycerides can be converted to hydrocarbons in the boiling range of diesel as a result of the following reactions:[9,10]

$$C_{57}H_{104}O_6 \xrightarrow{+3H_2} C_{57}H_{110}O_6 \xrightarrow{+3H_2} C_3H_8 + C_{17}H_{35}COOH \quad \text{(Hydrogenation)}$$

$$C_{17}H_{35}COOH \longrightarrow C_{17}H_{36} + CO_2 \quad \text{(Decarboxylation)}$$

$$C_{17}H_{35}COOH + H_2 \longrightarrow C_{17}H_{36} + H_2O + CO \quad \text{(Decarbonylation)}$$

$$C_{17}H_{35}COOH + 3 H_2 \longrightarrow C_{18}H_{38} + 2H_2O \quad \text{(Hydrodeoxygenation)}$$

$$n\text{-RH} \longrightarrow iso\text{-RH} \quad \text{(Hydroisomerization)}$$

$$iso\text{-RH} \longrightarrow iso\text{-R}_1\text{H} + iso\text{-R}_2\text{H} \quad \text{(Hydrocracking)}$$
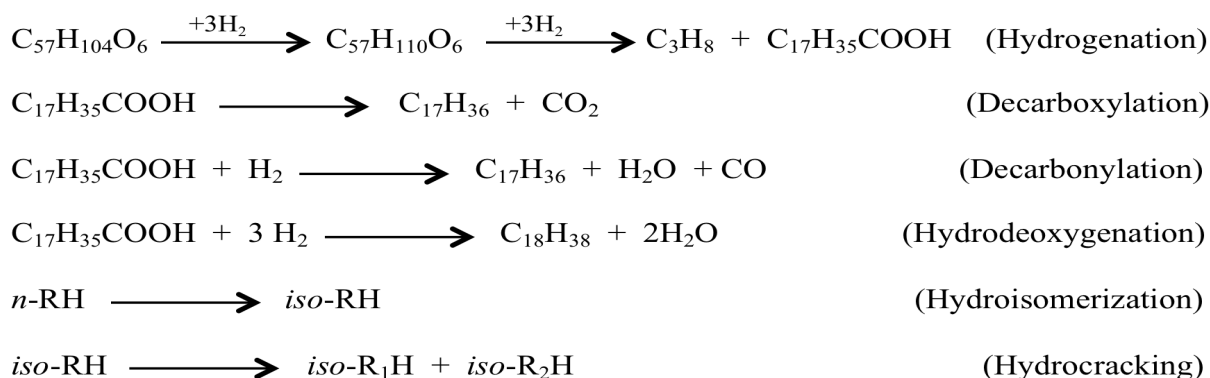
The hydrogenation reaction dominates initially by converting triglyceride molecules

to free fatty acids (FFA), followed by hydrodeoxygenation, hydrodecarboxylation, and hydrodecarbonylation of FFA to green diesel. Supported noble metal catalysts[11] and metal sulfide catalysts[12,13] have been investigated in the hydrocracking of vegetable oils to produce green diesel. The noble metal catalysts are not viable for the large-scale processes because of their limited availability, high cost, and sensitivity to contaminants (such as oxygenated compounds) in the feedstock.[14] Although metal sulfide catalysts overcome the issues with noble metal catalysts, the addition of sulfur-containing compounds such as H_2S is required to maintain the catalysts in the active form.[15]

Recently, supported metal carbide and nitride catalysts have received considerable attention as mediators for the hydrocracking of vegetable oils.[16] The presence of carbon or nitrogen atoms in the transition metal lattice extends the lattice parameter and increases the d-band electron density of the metals.[17,18] However, only 86% yield of paraffin and 46% selectivity for branched paraffins were obtained from rapeseed oil feedstock when a molybdenum carbide catalyst supported on carbon nanotubes (20% Mo_2C/CNTs) was used.[88] Bimetallic carbide and nitride catalysts have shown higher activities and stabilities than the monometallic ones.[19] It has been claimed that the carbide form of the NiMo/ZSM-5 catalyst produced a lower amount of CO and CO_2 from soybean oil feedstock than the nitride form; there- fore, more hydrodeoxygenation took place on the carbide catalyst compared to the nitride catalyst.[20] Most recently, Wang et al.[22] investigated the effect of several supports on the activity of a NiMo carbide catalyst for the hydrocracking of soybean oil. The conversion of soybean oil reached 100% and the selectivity for green diesel was 97% for the NiMo carbide catalyst over Al-SBA-15 during 7 days at 400 ° C and 4.48 MPa. Our earlier study investigated the effect of

catalyst preparation method and Ni-W ratio on the carbide form of the NiW/Al-SBA-15 catalyst activity and selectivity.[117] The catalyst prepared by Dendrimer-Encapsulated-Nanoparticles (DENP) method with a Ni-W ratio of 2:1 led to a complete conversion of DDGS corn oil for 16 days and 100% diesel selectivity for 4 days at 400 ° C and 4.48 MPa.

Electronegativity is defined as the tendency of an atom to attract an electron to itself. The ability of the tetrachloroaluminate catalyst to attract and retain hydrocarbon feedstock at the reaction sites then simultaneously release formed products can be attributed to the electronegativity of the catalyst.[118] According to Sabatier's principle, the maximum rate of catalytic activity is obtained when the rate of reactant adsorption on the catalyst is equal to the rate of product desorption from the catalyst.[119] Nwosu[119] claims that all the noble metals are considered to be good catalysts based on their performance on the Sabatier's volcano scale, and they have almost the same electronegativity. The electronegativity of noble metals is neutral, between the electropositive and electronegative elements; therefore, their ability to adsorb reactants and desorb products is almost equal. Also, this study shows that the closer the electronegativity of transition metals to the range of noble metals (2.0–2.2), the better performance on the Sabatier's volcano scale. However, this study indicates that other factors like particle sizes and synergy pattern hindered the performance of the catalysts. In this respect, noble metal catalysts have shown excellent performance in the hydrocracking of vegetable oils. Since chemical reactions depend on the ability of the reactants to donate, receive, or share electrons; the electronegativity of the material would appear to have a role in this process. For bimetallic catalysts, the ensemble and ligand (electronegativity) effects have the main

roles of enhancing the catalyst performance in comparison to monometallic types.[104] The dibenzothiophene conversion for the hydrodesulfurization (HDS) reaction over a Pd-Au bimetallic catalyst was higher than over either Pd or Au alone (84, 16, and 22%, respectively).[120] Due to the difference in electronegativities between Pd and Au, the sulfur is selectively adsorbed on the Au sites, leaving the Pd sites available for activating hydrogen and accomplishing the HDS reaction.

In the present work, a wet co-impregnation method was used to prepare various catalysts on an Al-SBA-15 support by combining metals with both lower and higher electronegativities, to achieve catalysts with fractional sums of their components' electronegativity values lying in the electronegativity range of the noble metals. We hypothesized that by mimicking the electronegativity of noble metals, the performance of bimetallic carbide catalysts for the hydrocracking of vegetable oils might improve. The empirical formula used for calculating the fractional sum of the electronegativities of the metals is presented in (Eq. (1)):

$$\vartheta_T = \frac{\sum_i^n \vartheta_i * \varphi_i}{\sum_i^n \varphi_i} \qquad\qquad (eq.\,1)$$

where ϑ_T is the electronegativity of the catalyst, ϑ_i is the electronegativity of the individual metal, and φ_i (mol%) is the quantity of the corresponding metal in the catalyst.[119] The effect of the fractional sum of the metals' electronegativities on the activity and selectivity of the catalyst for green diesel production via the hydrocracking of DDGS corn oil was investigated under relatively mild reaction conditions.

4.2 Experimental

4.2.1 Materials

Ammonium (*para*)tungstate hydrate ($(NH_4)_{10}(H_2W_{12}O_{42}) \cdot 4H_2O$, 99.99%, Aldrich), ammonium niobate(V) oxalate hydrate ($C_4H_4NNbO_9 \cdot xH_2O$, 99.99%, Aldrich), ammonium molybdate ($(NH_4)_6Mo_7O_{24} \cdot 4H_2$, Sigma-Aldrich), zirconium(IV) oxynitrate hydrate ($ZrO(NO_3)_2 \cdot xH_2O$, 99%, Aldrich), nickel(II) nitrate hexahydrate ($Ni(NO_3)_2 \cdot 6H_2O$, Sigma-Aldrich), and cerium(III) nitrate hexahydrate ($Ce(NO_3)_3 \cdot 6H_2O$, 99.99%, Aldrich) were used as W, Nb, Mo, Ni, and Ce sources, respectively. Carbon disulfide (HPLC grade ≥99.9%), aluminum isopropoxide ($C_9H_{21}AlO_3$, 99.99%), and the mesoporous silica SBA-15 were purchased from Sigma-Aldrich, Aldrich, and Advanced Chemicals Supplier (ACS), respectively.

4.2.2 Catalyst preparation

A neutral support, SBA-15, with a 9 nm pore diameter and Brunauer-Emmett-Teller (BET) surface area of 600 m^2/g, was modified by aluminum isopropoxide to adjust its acidity. SBA-15 (20 g) was suspended in hexane (150 mL); then, aluminum isopropoxide (0.067 g) was added to the solution and stirred for 24 h. The mixture was filtered, dried, and calcined at 550 °C for 4 h. According to our previous work,[117] the catalysts NiNb, NiMo, NiW, and NiZr were prepared in the ratio of 6.67 wt% Ni:3.33 wt% M (M = Nb, Mo, W, Zr) by the wet co-impregnation of aqueous solutions of ($Ni(NO_3)_2 \cdot 6H_2O$, $C_4H_4NNbO_9 \cdot xH_2O$), ($Ni(NO_3)_2 \cdot 6H_2O$, $(NH_4)_6Mo_7O_{24} \cdot 4H_2$), ($Ni(NO_3)_2 \cdot 6H_2O$, $(NH_4)_{10}(H_2W_{12}O_{42}) \cdot 4H_2O$), and ($Ni(NO_3)_2 \cdot 6H_2O$, $ZrO(NO_3)_2 \cdot xH_2O$) on the modified Al-SBA-15 support. The resulting solids were dried and calcined at 450 °C for 4 h. The catalysts promoted with Ce were prepared by impregnation of the NiNb/Al-SBA-15, NiMo/Al-SBA-15, NiW/Al-SBA-15, and NiZr/Al-SBA-15 catalysts with an approximate

amount of 10 wt% $(Ce(NO_3)_3 \cdot 6H_2O)$ solution. The impregnated samples were dried and calcined at 450 °C for 4 h.

Carburization was conducted using temperature-programmed reduction (TPR) according to the method of Claridge et al.[90] Each metal oxide precursor was placed in a quartz tube and subjected to a flow of 20% CH_4/80% H_2 at 30 cm^3/min and a heating rate of 10 K/min to 250 °C, followed by 2.0 K/min to 730 °C. The temperature was maintained at 730 °C, the optimal temperature for carbide formation, for 30 min to complete the reaction.[90] After cooling, the catalyst was passivated under a mixture of 1% O_2 in Ar for 1 h to eliminate its pyrophoricity[19] and protect the bulk of the catalyst against deep oxidation.[91]

4.2.3 Material characterization

The BET surface area, Barrett–Joyner–Halenda (BJH) pore size, and pore volume were determined using a Micromeritics model ASAP 2010 surface area analyzer with 99.9% purity nitrogen gas, and the results were collected on a Tristar 3020 analyzer. The samples were degassed at 400 °C at a heating rate of 10 °C/min for 2 h prior to analysis. X-Ray diffraction (XRD) patterns were collected using a Rigaku RU2000 rotating anode powder diffractometer (Rigaku Americas Corporation, TX) with SmartLab Guidance and MDI Jade 8 software at a scan rate of 8° /min.

4.2.4 Hydrocracking reaction procedures

4.2.4.1 Batch reactor

The catalytic hydrocracking conversion of DDGS corn oil was carried out in a 100 mL Hanwoul stirred batch reactor (Geumjeong- dong, South Korea). To investigate the activity of each catalyst, the reactor was loaded with catalyst (2 g) and reduced in situ

under a 30mL/min flow of H_2 for 3h at 350°C. The gas flow rate was controlled by a metal-sealed mass flow controller (Brooks, Warren, MI). After cooling to room temperature, DDGS corn oil (50 mL) was fed into the reactor by a pump (Chrom Tech, Series III) at a rate of 5 mL/min for 10 min. The temperature was increased to 350 °C at a rate of 10 °C/min, and the H_2 pressure in the vessel was increased to 4.48 MPa. The oil is mostly liquid at 350 °C and 4.48 MPa. The agitation speed was maintained at 1100 rpm throughout the reaction. A liquid sample was collected every 30 min for analysis. The sample was allowed to phase separated for 12 h at room temperature and atmospheric pressure.

4.2.4.2 Flow reactor

This DDGS corn oil hydrocracking reaction was also performed in a BTRS-Jr. system (Autoclave Engineers, PA) that consisted of a fixed bed reactor with an internal diameter of 1.31 cm and a length of 61 cm, a heater, a pressure regulator, and a condenser. The experimental conditions were similar to those from a previous study,[20] in which biofuels were produced via the hydrocracking of soybean oil over transition metal carbides and nitrides supported on ZSM-5. The catalyst (2 g) and quartz beads (4.5 g) were loaded in the reactor and reduced under an H_2 flow of 30 STP mL/min at 450 °C for 3h. The quartz beads were used to dilute the catalyst bed, prevent plugging, and enhance heat and mass transfer. The reaction was carried out at 400 °C and 4.48 MPa. The hydrogen flow was maintained at a constant 30 mL/min and the DDGS corn oil was fed at a liquid hourly space velocity (LHSV) of $1h^{-1}$. The outlet liquid phase was separated from the gas phase via a condenser maintained at room temperature and 4.48 MPa. The collected liquid samples consisted of two phases: organic liquid product (OLP) and aqueous phase. The

OLP samples were analyzed qualitatively and quantitatively. The produced jet fuel and green diesel fractions were identified as (C_8–C_{16}) and (C_{12}–C_{22}), respectively.

4.2.5 Analysis method

The samples of OLP were dissolved in carbon disulfide and analyzed using a Perkin Elmer Clarus 500 gas chromatograph (GC) equipped with a flame ionization detector (FID) and an Elite-Biodiesel 5HT column (Perkin Elmer, N9316690, length: 15 m; internal diameter: 0.31 mm; phase film thickness: 0.10 μm). For triglycerides analysis, the GC oven temperature was programmed as follows: 1 min hold at 80 °C, 30 °C/min ramp to 240 °C, 10 °C/min ramp to 360 °C, and 15 min hold at 360 °C. The detector temperature was maintained at 360 °C. Samples (0.5 μL) were injected into the column with a 10:1 split ratio. For hydrocarbons analysis, the GC oven temperature was programmed as follows: 5 min hold at 35 °C, 10 °C/min ramp to 360 °C, and 15 min hold at 360 °C. The detector temperature was maintained at 370 °C. Samples (0.5 μL) were injected into the column with a 10:1 split ratio.

4.3 Results and discussion

4.3.1 Catalyst characterization

The XRD patterns of the nickel carbide catalyst and the nickel-based carbide catalysts with four different metals supported on Al-SBA-15 are shown in Figure 24. For all the catalysts, the broad peak between 2θ = 15–30° corresponds to the mesoporous silica. The XRD patterns of the catalysts show three main peaks at 2θ = 44.6°, 52.2°, and 76.3°, corresponding to the (111), (200), and (220) diffractions of the Ni particles, respectively.[121] The carbide phases of Mo, Nb, and W can be observed as shown in Figure 24(b), (c), and (d), respectively. Surprisingly, the carbide phase of Zr was not

observed in the XRD pattern (Figure 24(e)), which suggests that the phase was very well dispersed on the support. SEM-EDAX was used to characterize the catalyst in order to determine Zr and C distributions on the support (Al-SBA-15). Figure 25 shows that the distributions of Zr and C on the support are well dispersed with no agglomeration observed at any area. Also, Figure 26 shows that the atomic weight percentages of the Zr (40.01%) and C (59.99%) in the catalyst were close to that in the most stable phase of ZrC.[122] There is no indication of Ni carbide formation, as shown in Figure 24(a), confirming that Ni metal was easily reduced to form Ni particles, in agreement with the findings of Gajbhiye et al.[96] Figure 24(b) and (d) shows that NiMoC/Al-SBA-15 and NiWC/Al-SBA-15 are the only catalysts that form alloys, as indicated by the peaks at 2θ = 47.3° and 48.1°, respectively.
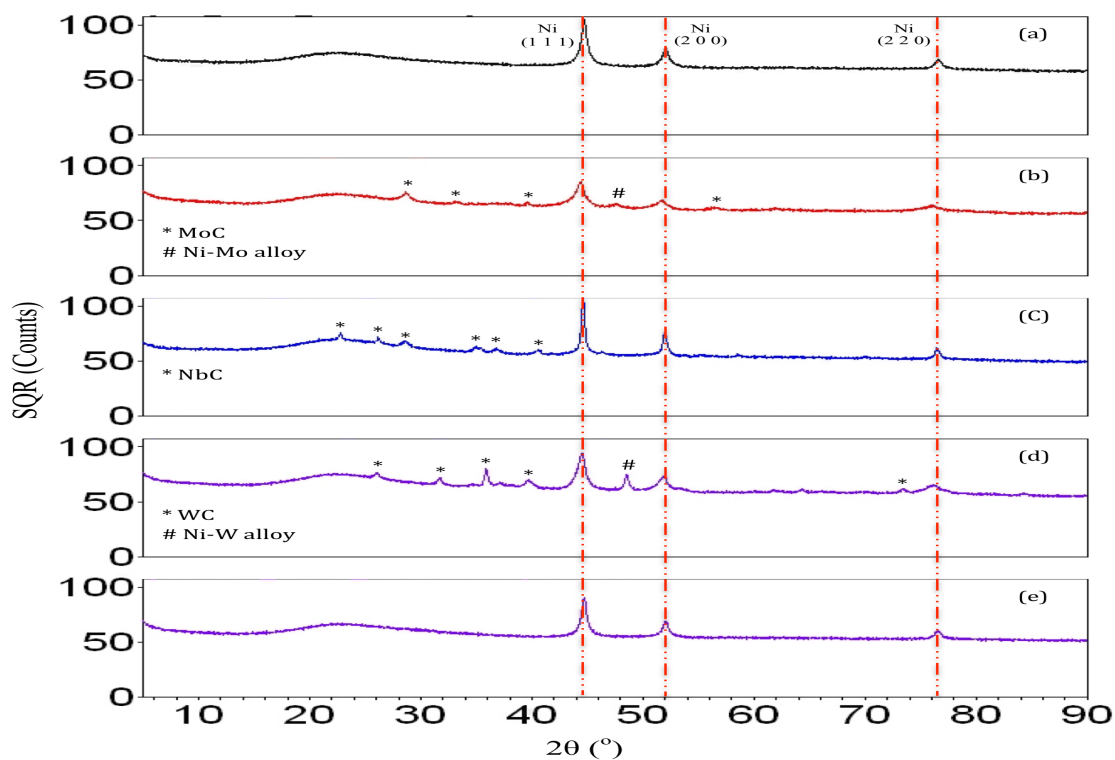
Figure 24. XRD patterns of NiC/Al-SBA-15 (a), NiMoC/Al-SBA-15 (b), NiNbC/Al-SBA-15 (C), NiWC/Al-SBA-15 (d), NiZrC/Al-SBA-15 (e).

Figure 27 shows the XRD patterns of the catalysts promoted with Ce. The broadening of peaks of the promoted catalysts suggests smaller crystal sizes and higher metal carbide dispersions than the non-promoted catalysts. Moreover, there is a decrease in the intensities of the diffraction peaks as well as the disappearance of some peaks. Therefore, the Ce additive increases the metal dispersion, leading to the formation of more active centers and greater hydrogen adsorption.[109,123] No peak assignable to a Ce carbide phase is seen in Figure 27(b), which indicates that the phase either was not formed or the particles were too small to be detected by the XRD technique.[124] The peak corresponding to the Ni-Mo alloy disappeared and that corresponding to Ni-W alloy decreased, which provides another indication of the enhancement in metal dispersion after adding Ce.

(a)   (b)
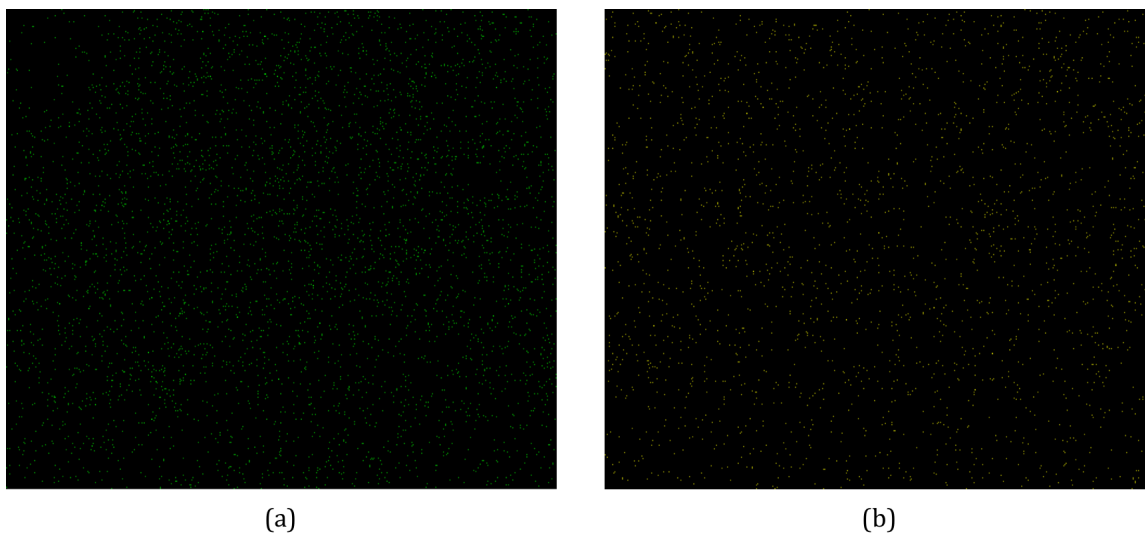
Figure 25. The distribution of Zr and C in the NiZrC/Al-SBA-15: Zr (a) and C (b).

The effect of the loading of the Ce promoter on the structure of NiNbC/Al-SBA-15 was also investigated by XRD (Figure 28). The higher the loading of Ce, the weaker were the peaks in the XRD pattern of NiNbC/Al-SBA-15, and more peaks disappeared ($2\theta =$ 26.3°, 35.5°, and 40.8°) as the Ce amount increased. The particle sizes were estimated by

using the Debye-Scherrer equation in order to show the extent to which the peaks have broadened. Table 6 indicates that the increasing in the peak broadening was caused by the decreasing in particle size; therefore, the dispersion of NiNbC increases with the increase in Ce content.
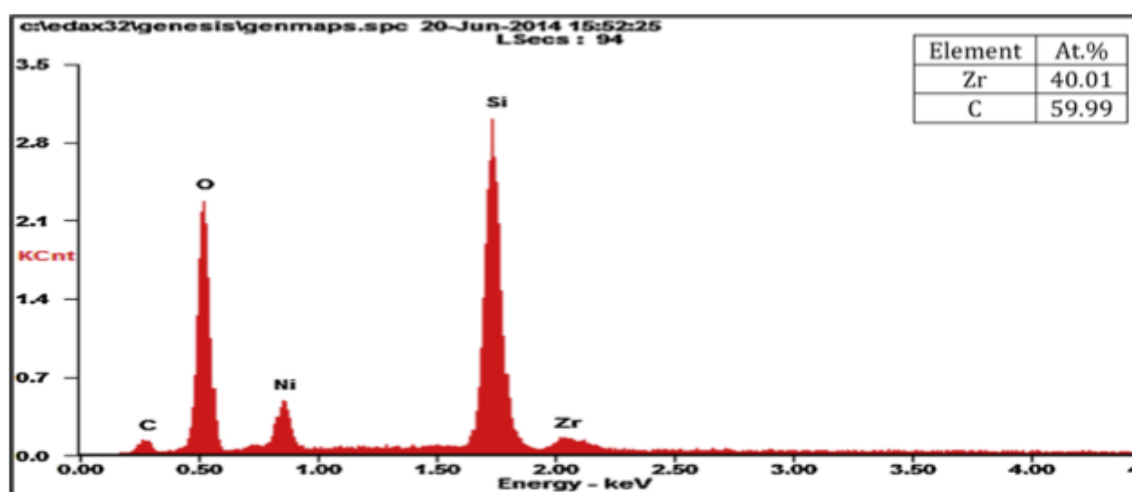
Figure 26. EDAX spectra of NiZrC/Al-SBA-15 catalyst.

Table 6. Effect of Ce loading on particle size.

		Particle size (nm)						Mean crystallite size (nm)
	$2\theta(^o)$	22.9	28.3	36.4	44.6	52.2	76.3	-
Catalyst	NiNbC 0% Ce	33	27	31	29	23	24	27
	NiNbC 5% Ce	31	21	28	18	15	18	19
	NiNbC 10% Ce	29	19	25	17	14	17	16
	NiNbC 20% Ce	28	16	23	17	13	15	15

The surface area, pore size, pore volume, and average particle size of the catalysts are summarized in Table 7. The surface area and pore size of the catalysts decreased as compared to the Al-SBA-15 support (surface area: 600 m^2/g; pore size: 9 nm), which

could be caused by loss of structure and/or pore blockage.[97] All of the catalysts have relatively high surface areas and suitable pore sizes that would readily allow the diffusion of bulky triglyceride molecules.[109] The BET surface area of the Ce-promoted catalysts increased compared to the non-promoted catalysts, while the average particle size decreased. These results are in accord with the results obtained from the XRD characterization. Table 8 shows that the surface area increases after adding Ce; however, the surface area decreases as the Ce loading increases further. These decreases in surface area as the Ce loading increases suggest that the addition of Ce may block some pores in the Al-SBA-15 support.[125] Moreover, the average particle size decreases after adding Ce can be attributed to the increase in metal dispersion.

Table 7. Textural properties of non-promoted catalysts and promoted catalysts with 10%. Ce.

Catalyst	Non-promoted			
	S_{BET} (m^2/g)	Pore size (nm)	Pore volume (cm^3/g)	Avg. particle size (nm)
NiWC/Al-SBA-15	342	7.32	0.66	21.3
NiMoC/Al-SBA-15	302	5.85	0.43	17.5
NiNbC/Al-SBA-15	343	5.89	0.48	19.8
NiZrC/Al-SBA-15	299	5.98	0.48	16.9
Catalyst	Promoted with 10% Ce			
	S_{BET} (m^2/g)	Pore size (nm)	Pore volume (cm^3/g)	Avg. particle size (nm)
NiWC/Al-SBA-15	388	5.36	0.54	15.4
NiMoC/Al-SBA-15	454	5.84	0.59	13.2
NiNbC/Al-SBA-15	402	6.07	0.55	14.9
NiZrC/Al-SBA-15	353	6.10	0.43	15.1

S_{BET}: BET surface area

Table 8. Effect of Ce loadings on textural properties of catalysts.

NiNbCeC/Al-SBA-15	S_{BET} (m^2/g)	Pore size (nm)	Pore volume (cm^3/g)	Avg. particle size (nm)
0% Ce	343	5.89	0.48	19.8
5% Ce	424	5.4	0.55	14.1
10% Ce	402	5.44	0.53	14.9
20% Ce	346	5.38	0.45	17.3

S_{BET}: BET surface area
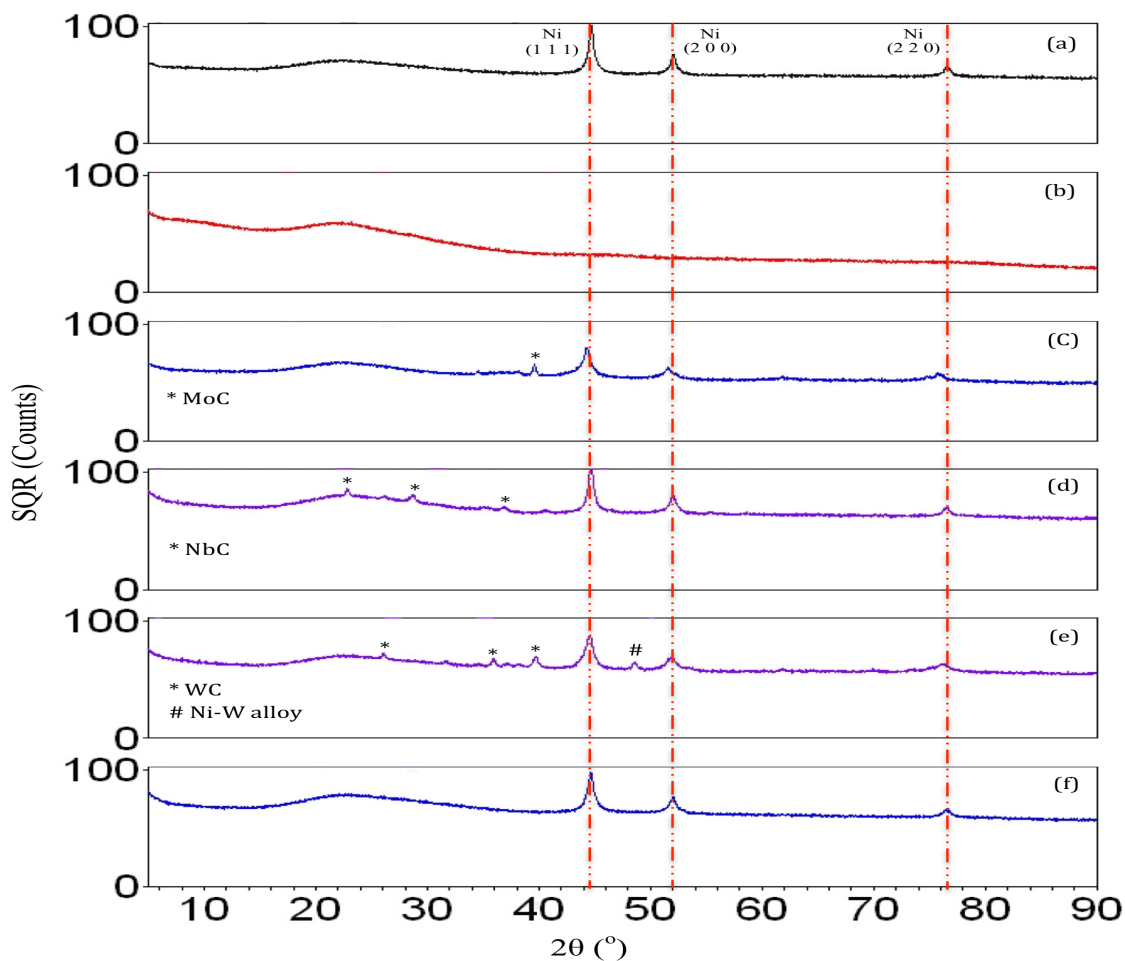
Figure 27. XRD patterns of (10% Ce) NiC/Al-SBA-15 (a), CeC/A-SBA-15 (b), (10% Ce) NiMoC/Al-SBA-15 (C), (10% Ce) NiNbC/Al-SBA-15 (d), (10% Ce) NiWC/Al-SBA-15 (e), (10% Ce) NiZrC/Al-SBA-15 (f).
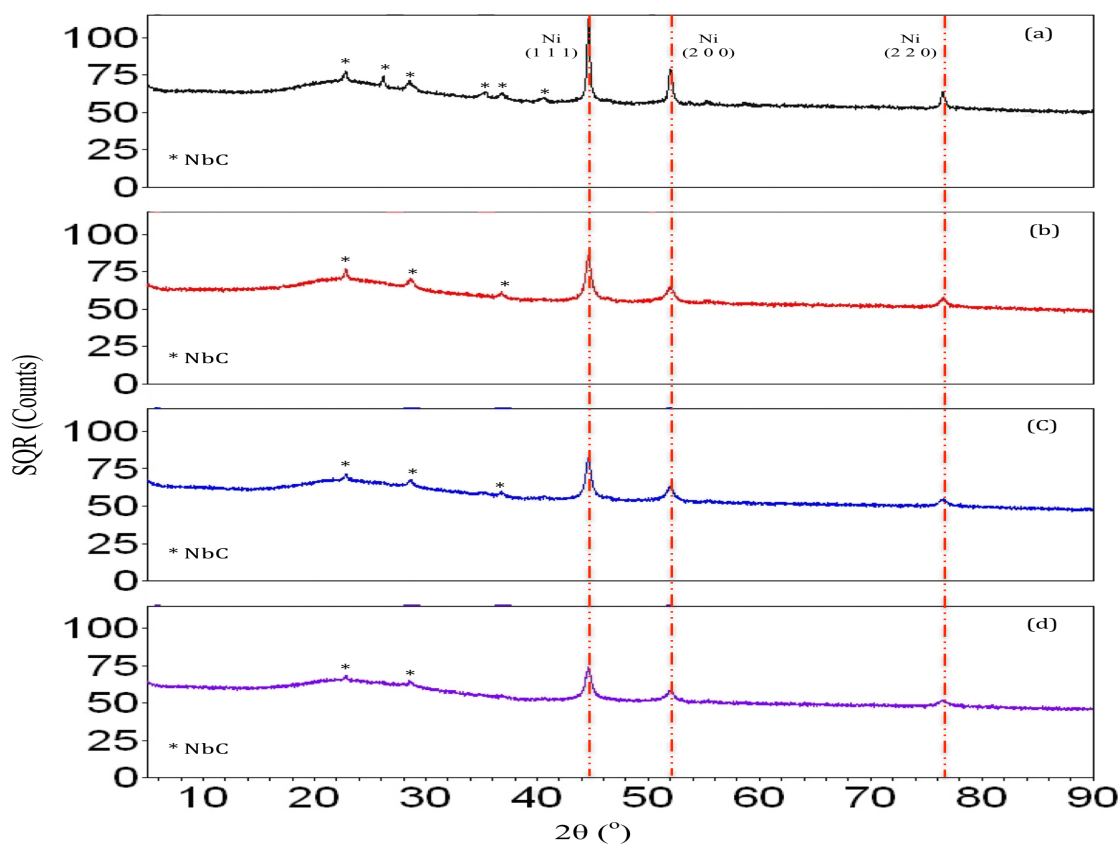
Figure 28. XRD patterns of the promoted NiNbC/Al-SBA-15 catalyst with: 0% Ce (a), 5% Ce (b), 10% Ce (c), 20% Ce (d).

4.3.2 Hydrocracking of DDGS corn oil

4.3.2.1 Relationship between nickel-based catalysts, electronegativity, and catalytic activity

The performance of NiMoC/Al-SBA-15, NiZrC/Al-SBA-15, NiNbC/Al-SBA-15, and NiWC/Al-SBA-15 was evaluated for the hydrocracking of DDGS corn oil in a batch reactor at 350 °C and 4.48 MPa. Table 9 shows the typical fatty acid compositions and the elemental analysis of DDGS corn oil. The collected samples were analyzed by GC-FID to determine the DDGS corn oil conversion and the selectivity for diesel; the results are shown in Figure 29 as a function of time. The 30 min data point corresponds to the

time at which the temperature reaches 350 °C. However, hydrocracking had started before the temperature reached 350 °C because the DDGS corn oil conversion at 30 min was more than 30% for all the catalysts. The conversion at time t (C_t) was calculated as:

$$C_t \, (\%) = 100\% - C_{TG,t} \qquad\qquad (eq.\,2)$$

where $C_{TG,t}$ is the concentration of triglycerides (%) in the OLP determined by GC-FID analysis at time t. There were no significant differences in the conversion of DDGS corn oil for all the catalysts; however, the selectivity for green diesel varied, and the maximum green diesel selectivity (100%) was obtained from NiWC/Al-SBA-15 after 180 min, as shown in Figure 29 (d). The green diesel selectivity at time t ($S_{d,t}$) is defined as:

$$S_{d,t} \, (\%) = \frac{C_{d,t}}{C_{p,t}} * 100 \qquad\qquad (eq.\,3)$$

where $C_{d,t}$ and $C_{p,t}$ are the concentrations of green diesel and OLP at time t, respectively. Although Figure 29 (a) shows that the diesel selectivity obtained from NiMoC/Al-SBA-15 reached 86% at 150 min, the diesel selectivity dropped to 69% after 3.5 h. The diesel selectivities of the NiZrC/Al-SBA-15 and NiNbC/Al-SBA-15 catalysts both increased with time; however, NiNbC/Al-SBA-15 reached 90% earlier than NiZrC/Al-SBA-15. The differences in selectivity could be related to the fractional sum of the electronegativities of the metals. The fractional sum of the electronegativities in a catalyst was calculated using (eq. 1), as shown in Table 10. The catalyst producing the highest diesel selectivity, NiWC/Al-SBA-15, has a fractional sum of electronegativities within the electronegativity range of the noble metal catalysts (2.0–2.2), a result in agreement with Nwosu et al.[119] On the other hand, the other catalysts did not behave the same way. The catalyst with the second highest fractional sum of the electronegativities of metals did not lead to the second highest diesel selectivity. This suggests electronegativity is not

the determining factor for activity and selectivity, and the differences in metal compositions, particle size and surface area may also play a role.

Table 9. Fatty acid compositions and elemental analysis of DDGS corn oil.

Fatty acid composition wt.%		Element analysis (ppm)	
C14:0	0.1	Fe	0.4
C16:0	5.8	Na	3.9
C16:1	0.1	Ca	0.2
C18:0	2.5	P	1.8
C18:1	31.3	S	27.6
C18:2	49.1		
C18:3	4.8		
C20:0	3.7		
C22:1	2.6		
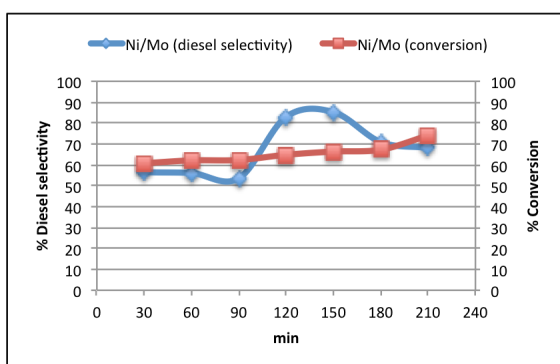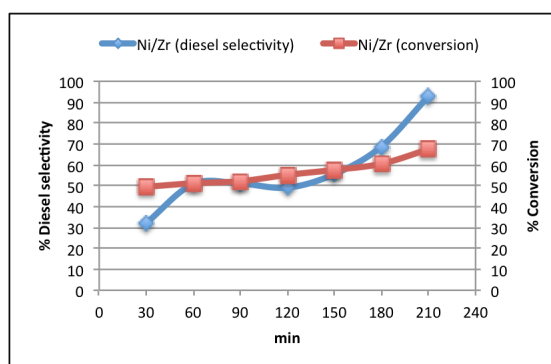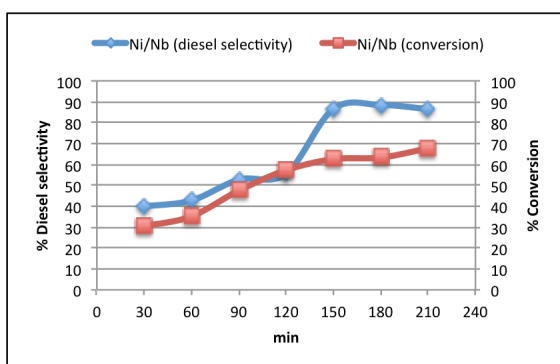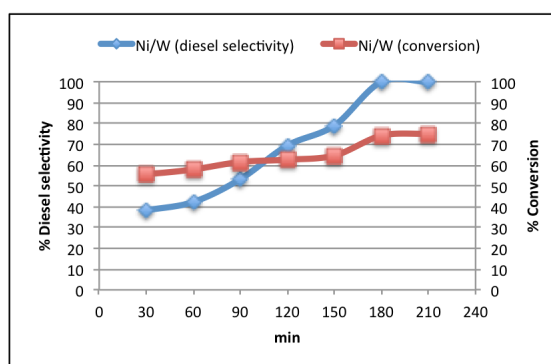
Figure 29. DDGS corn oil conversion and diesel selectivity in batch reaction at 350 ^{o}C and 650 psi on NiMoC/Al-SBA-15 (a), NiZrC/Al-SBA-15 (b), NiNbC/Al-SBA-15 (C), NiWC/Al-SBA-15 (d).

Table 10. Values of the fractional sum of transition metal electronegativities in the non-promoted and Ce-promoted catalysts.

	Fractional sum of electronegativity values (ϑ_T)			
Catalyst	Non-promoted		Promoted with 10% Ce	
NiZrC/Al-SBA-15	1.72		1.83	
NiNbC/Al-SBA-15	1.81		1.92	
NiMoC/Al-SBA-15	1.99		2.10	
NiWC/Al-SBA-15	2.06		2.17	
Catalyst	0% Ce	5% Ce	10% Ce	20% Ce
NiNbC/Al-SBA-15	1.81	1.87	1.92	2.03

4.3.2.2 Effect of doping 10% Ce on electronegativity and activity of catalysts

To understand the effect of Ce doping on the catalyst performance for the hydrocracking of DDGS corn oil, the reaction was conducted over a catalyst that contained only cerium (CeC/Al-SAB-15). Both the DDGS corn oil conversion and the diesel selectivity obtained from this catalyst were low (Figure 30), indicating that adding Ce to the catalysts did not significantly contribute to the hydrocracking reaction.

The Ce-promoted hydrocracking reaction of DDGS corn oil over the NiMoC/Al-SBA-15, NiZrC/Al-SBA-15, NiNbC/Al-SBA-15, and NiWC/Al-SBA-15 catalysts was investigated in a batch reactor at 350 °C and 4.48 MPa to examine the effect of 10% Ce doping. Figure 31 shows that there was a slight increase in the conversion for the promoted catalysts compared to the non-promoted catalysts. However, a significant improvement in the diesel selectivity was obtained with the promoted catalysts, reaching 100%. Indeed, the Ce-promoted NiNbC/Al-SBA-15 catalyst reached 100% diesel selectivity only after 90 min. The improvement in diesel selectivity for the promoted catalysts could be attributed to several factors, including the value of the fractional sum

of the electronegativities. This sum increases after catalyst promotion by Ce (Table 10).
As mentioned previously, the optimal electronegativity should be noble-metal-like (2.0–
2.2) to equalize the rates of reactant adsorption and product desorption,[119] and obtain the
highest catalytic activity. The Ce-promoted NiWC/Al-SBA-15 catalyst exhibited
approximately similar diesel selectivity to the non-promoted one since the fractional sum
of the electronegativities in the non-promoted catalyst already approximated that of the
noble catalysts. Nevertheless, other catalysts showed greater diesel selectivity as their
fractional sums of electronegativities approached 2.0–2.2. Moreover, based on the XRD
and BET analysis, metal dispersion and surface area in the promoted catalysts are
enhanced which may lead to the formation of more active centers and the adsorption of
more hydrogen.[109,123] These factors may additionally contribute to the improved diesel
selectivity of the promoted catalysts.
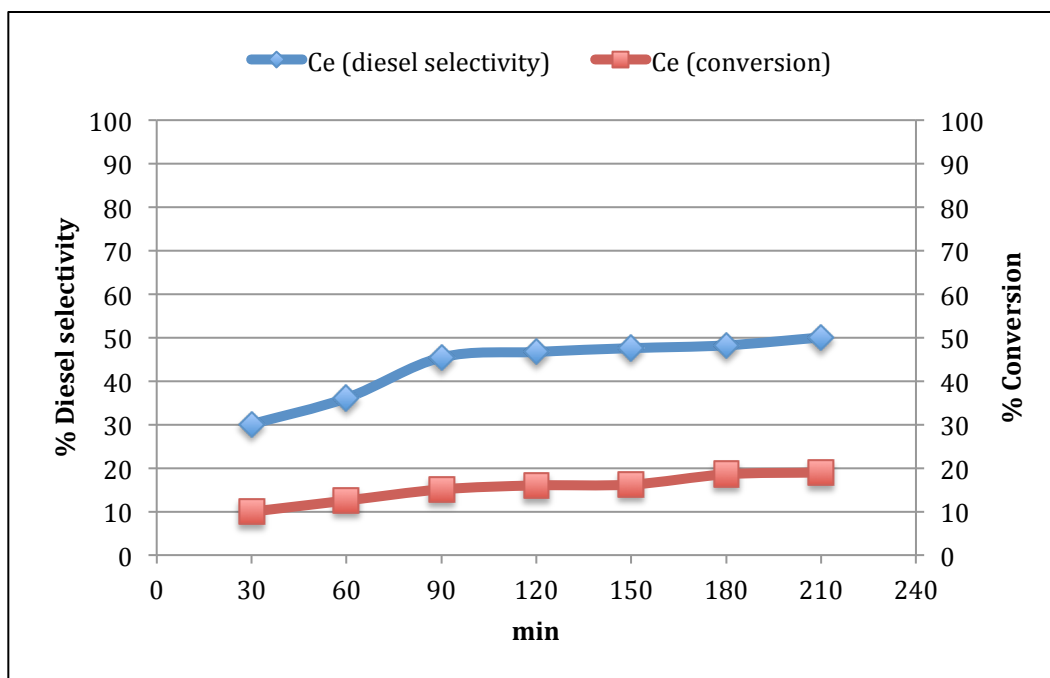
Figure 30. DDGS corn oil conversion and diesel selectivity in batch reaction at 350 $^{\circ}$C
and 650 psi on CeC/Al-SBA-15.
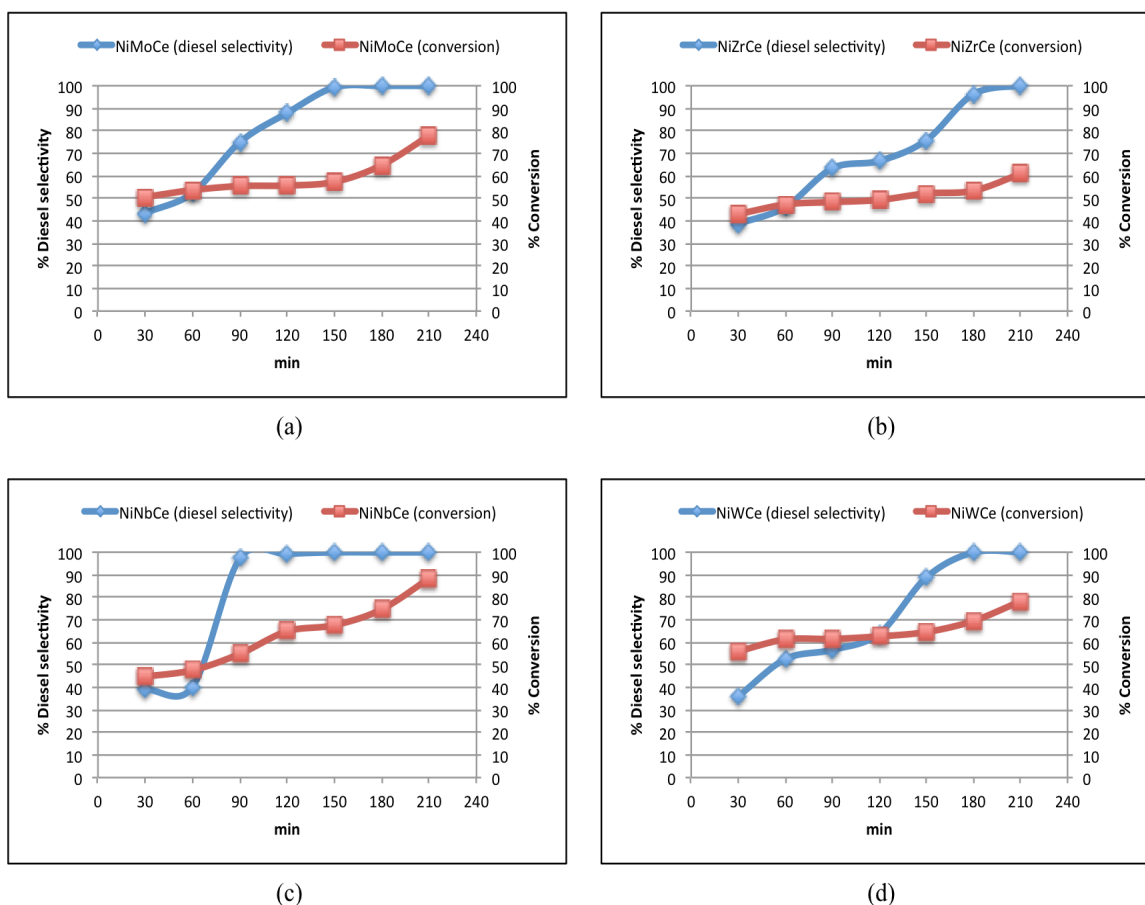
Figure 31. DDGS corn oil conversion and diesel selectivity in batch reaction at 350 ^{o}C and 650 psi on Ce promoted catalysts with (10% Ce): NiMoC/Al-SBA-15 (a), NiZrC/Al-SBA-15 (b), NiNbC/Al-SBA-15 (C), NiWC/Al-SBA-15 (d).

4.3.2.3 Effect of Ce loading on electronegativity and catalyst activity

The NiNbC/Al-SBA-15 catalyst was promoted with four different Ce loadings to study the effect of the fractional sum of the electronegativities on the catalytic activity. Table 10 shows that this fractional sum increases as the Ce loading increases. The catalyst with 20% Ce should have exhibited the best performance since its fractional sum of electronegativities fell in the electronegativity range of the noble catalysts; however, the catalyst with 10% Ce displayed higher performance, as shown in Figure 32 (c) and (d), respectively. The catalyst with 10% Ce reached 88% DDGS corn oil conversion after

210 min whereas only 78% conversion was obtained from the 20% loading. In addition, the diesel selectivity reached 100% for the catalysts with 10 and 20% Ce after 90 min and 120 min, respectively. The variation in the catalyst performance could be attributed to the opposing effects of the fractional sums of the electronegativities and the textural properties of the catalysts such as surface area and particle size. Therefore, the enhancement of the catalyst performance due to the electronegativity could be limited by the decrease in surface area and increase in particle size, as shown in Table 8. The diesel yield of the Ce-promoted and non-promoted catalysts was calculated as shown in Table 11. The diesel yield was observed to increase with time, with the catalyst (NiNbCeC/Al-SBA-15 with 10% Ce) achieving the highest diesel yield (88.4%) after 210 min. Based on the hydrogenation reaction, the maximum hydrocarbon gas (propane) produced could be as high as 13% for complete conversion. As indicated from Table 11, total liquid product (weight %) from each catalyst was about 90%.

4.3.2.4 Catalyst stability

The stability of the NiNbC/Al-SBA-15 catalyst promoted with 5% Ce was investigated in a continuous flow reactor at 400 °C and 4.48 MPa. The conversion of DDGS corn oil over seven days of operation is shown in Figure 33. The catalyst was stable over the entire duration. The selectivity for jet fuel was higher than for diesel, perhaps due to the higher temperature, which favors higher cracking activity. During the first day, the jet fuel selectivity was 85%, with no production of diesel. The jet fuel selectivity decreased as the diesel selectivity increased with time. This might be due to the retention of deoxygenated and cracked intermediates that are not hydrocracked to produce jet fuel (light HC's); but rather, are retained in the range of diesel because more

of the Ni surface is covered by the adsorbed reactants with time.[20] Wang et al.[20] studied

the hydrocracking of soybean oil over NiMoC/ZSM-5 at 450 °C and 4.48 MPa and

obtained only 42% jet fuel selectivity. The NiNbC/Al-SBA-15 catalyst promoted with

5% Ce shows greater jet fuel selectivity than NiMoC/ZSM-5 under similar reaction

conditions albeit at lower temperature (400 °C).

Table 11. Diesel yield and total liquid product weight percentage.

Non-promoted catalyst	Diesel Yield (%)							Liquid product wt. (%)
	30 min	60 min	90 min	120 min	150 min	180 min	210 min	
NiMoC	35.4	36.5	34	52.7	59.8	48.3	49.7	86
NiZrC	15.5	25	25.5	28.4	31.9	41.4	62.6	89
NiNbC	12.4	14.8	24.9	27.6	53.7	55.2	59.8	87
NiWC	21.8	24.2	31.1	42.8	48.9	71.9	73.2	89
Promoted catalyst								
NiMoCeC (10% Ce)	21	26.4	40.3	50.7	58.4	62.1	78.3	93
NiZrCeC (10% Ce)	15.9	21.2	30.4	34	37.7	50.9	61.8	83
NiNbCeC (5% Ce)	25.1	26.1	36.6	51.4	67.3	70	71.9	92
NiNbCeC (10% Ce)	18	19.6	51.5	64.3	68.6	71.9	88.4	95
NiNbCeC (20% Ce)	19.2	20.4	28.9	69.3	75.2	76.1	78.6	93
NiWCeC (10% Ce)	22.1	31.6	35.4	37.8	56.1	68.3	78.4	92
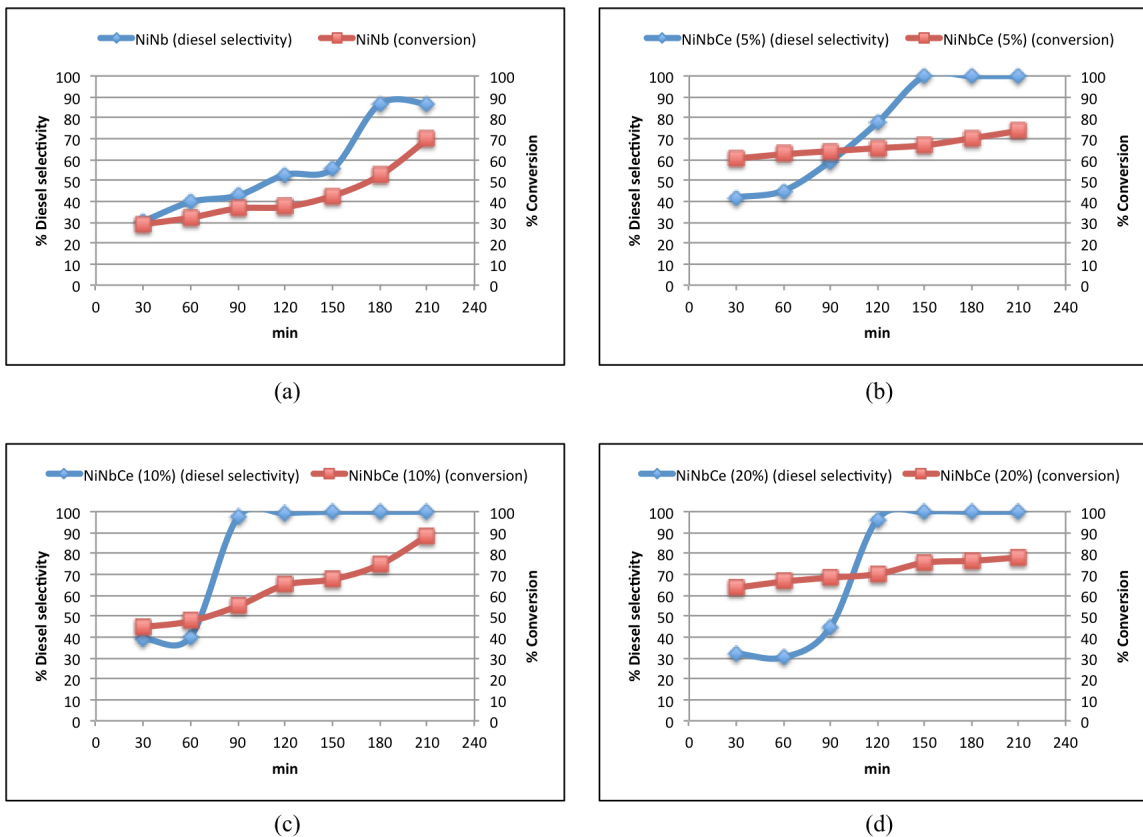
Figure 32. DDGS corn oil conversion and diesel selectivity in batch reaction at 350 $^{\circ}$C and 650 psi on Ce promoted NiNbC/Al-SBA-15 catalyst with: 0% Ce (a), 5% Ce (b), 10% Ce (c), 20% Ce (d).
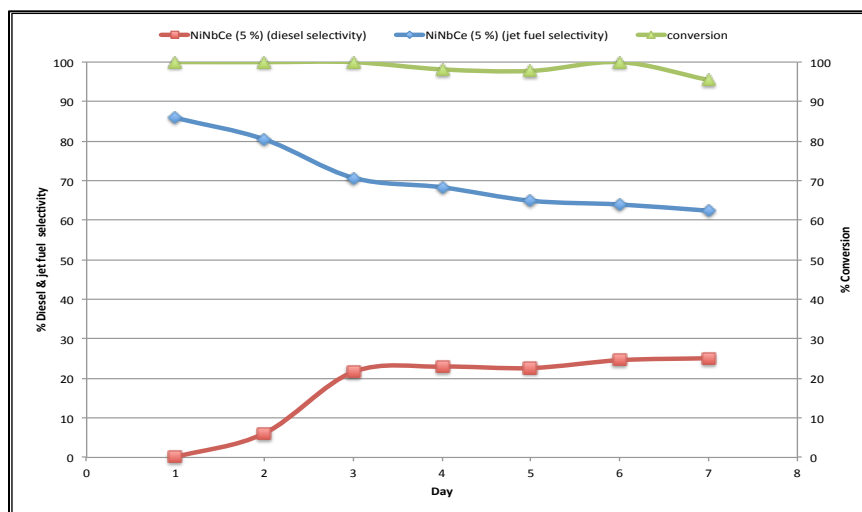
Figure 33. DDGS corn oil conversion and diesel selectivity in flow reaction with liquid hourly space velocity (LHSV) of 1 h^{-1} at 400 $^{\circ}$C and 650 psi on Ce promoted NiNbC/Al-SBA-15 catalyst with 5% Ce.

4.4 Conclusion

The fractional sum of the electronegativities of the transition metals were correlated with the performance of these catalysts because it affects the reactant adsorption and product desorption steps. The maximum rate of catalytic activity can be obtained when the rates of adsorption and desorption are similar to those observed for the noble metals. It is possible to posit that the closer the fractional sum of the transition metal electronegativities is to the electronegativity range of the noble catalysts (2.0–2.2), the better the catalyst performance will be. However, this is not the only factor that controls the catalyst activity. The BET surface area, particle size, pore size, and metal composition can also affect the activity and selectivity.

Several catalysts were investigated to evaluate the effect of the fractional sum of electronegativity values on the hydrocracking of DDGS corn oil. The catalyst with the fractional sum of electronegativity values in the range 2.0–2.2, NiWC/Al-SBA-15, was the most active. Doping different loadings of Ce brought the electronegativity closer to the 2.0–2.2 range and improved the catalyst performance. However, not every catalyst followed this trend because the improvement obtained from the electronegativity values could be inhibited by other factors, such as surface area and particle size. The NiNbC/Al-SBA-15 catalyst promoted with 5% Ce was studied in a fixed bed reactor over 7 days and achieved high conversions of triglycerides and free fatty acids. Thus, this promoted catalyst may be regarded as a prospective hydrocracking catalyst for inexpensive feedstocks such as brown grease.

CHAPTER 5

Biofuels Production from Hydrothermal Decarboxylation of Oleic Acid and Soybean Oil Over Ni-based Transition Metal Carbides Supported on Al-SBA-15[‡]

5.1 Introduction

Biofuels production has been attracting considerable attention because of increases in petroleum prices and the world's energy demand, declines in petroleum reserves, and concerns about the environmental issues associated with greenhouse gas emissions. Triglycerides and fatty acids (from plants, animal fat, and waste oil/grease) can be used as renewable fuel feedstocks.[126,127] Eliminating oxygen from triglycerides and fatty acids in the form of H_2O, CO, or CO_2 produces renewable liquid biofuels that are similar to petroleum fuels and can be directly used in existing infrastructure with no modifications.[8,85] The cost of biofuels production from new vegetable oils is not likely to be competitive with the cost of petroleum fuels. Therefore, using inexpensive and inedible feedstocks such as waste oil and brown grease is necessary to produce biofuels that are fungible with petroleum fuels. The hydrocracking process is the most developed route for removal of oxygen from triglycerides and fatty acids to produce biofuels.[62,128,129] Our previous study[117] has shown that bimetallic carbide catalysts (NiWC/Al-SBA-15) prepared by a Dendrimer-Encapsulated-Nanoparticles (DENP) method with a Ni-W ratio of 2:1 led to a complete conversion of DDGS corn oil (>95% triglycerides) over 16 continuous days with 100% diesel selectivity for 4 days at 400 °C and 4.48 MPa. However, this process requires high pressure of H_2 and has issues related to catalyst deactivation due to the presence of water.[130,131]

[‡] This chapter has been submitted to *Applied Catalysis A: General*.

An alternative method for removing oxygen is decarboxylation of fatty acid, a method which proceeds under lower H_2 pressure.[64] Most reports have focused on the use of noble metal catalysts, Pd[132-134] or Pt.[135-137] Also, some early studies focused on the decarboxylation of fatty acids in hydrocarbon solvents such as dodecane over Pd-supported catalysts.[138-142] Several studies showed that using water as solvent for the decarboxylation of fatty acids is more advantageous than hydrocarbon solvents,[143-145] not only because water is an environmentally friendlier solvent but also the avoidance of a water removal step after triglycerides hydrolysis that generates fatty acids in an aqueous stream. Watanabe et al.[71] studied the effect of the addition of alkali hydroxide (NaOH and KOH) and metal oxides (CeO_2, Y_2O_3, and ZrO_2) on the decarboxylation of stearic acid in super-critical water at 400 °C. KOH promoted the monomolecular decarboxylation of stearic acid to produce C_{17} alkane and CO_2, while ZrO_2 was effective for bimolecular decarboxylation into C_{16} alkene and CO_2 because long chain ketone was observed. For the decarboxylation of palmitic acid in sub-critical water at 370 °C, 63% and 76% pentadecane molar yields were obtained over 5% Pd/C and 5% Pt/C, respectively.[72] Although the catalysts experienced a reduction in metal dispersion after the reaction, these changes did not seem to reduce their activities. However, the cost and rapid deactivation due to catalyst coking[139] and lack of H_2,[146] hindered the use of these catalysts commercially.

Fu et al.[74] reported that activated carbons could be an alternative to the expensive noble metal catalysts to convert saturated and unsaturated fatty acids to alkanes in sub and super-critical water. Although the major products were alkanes that are produced via

decarboxylation and hydrogenation of oleic acid after 3 h at 370 °C, only 6% molar yield of decarboxylation product was obtained.

Triglycerides, a type of neutral lipids, can be rapidly hydrolyzed in hydrothermal media to produce saturated and unsaturated free fatty acids, as well as glycerol.[75] Some studies examined hydrothermal catalytic reforming of glycerol, commonly referred to as aqueous phase reforming (APR), to generate hydrogen.[76-81] Utilizing glycerol APR for *in situ* hydrogen production can promote the hydrogenation of unsaturated fatty acids. The addition of Re to Pt/C catalyst can motivate the glycerol APR due to the reduction of the affinity for CO.[79,82] A complete conversion of oleic acid was achieved over Pt-Re/C catalyst when a 1:3 glycerol-to-oleic acid molar ratio was applied in a 2 h reaction. The catalyst experienced moderate sintering, suggesting additional work is needed to investigate its hydrothermal stability with time on stream. Vardon et al.[75] proposed an integrated catalytic hydrothermal reaction for the conversion of triglycerides to hydrocarbon fuels with *in situ* hydrogen production from glycerol. A continuous hydrogen supply can be obtained by the APR of glycerol released from triglyceride hydrolysis.

To the best of our knowledge, there has been no study of the hydrothermal decarboxylation of fatty acids over Ni-based transition metal carbide catalysts supported on Al-SBA-15. If sufficiently active, these catalysts could be suitable low cost catalysts for the hydrothermal decarboxylation of fatty acids. Also, unlike noble metal catalysts, these catalysts are not sensitive to CO that is produced during fatty acid decarbonylation.[147] In the present work, we investigate the use of Ni-based transition metal carbide catalysts on an Al-SBA-15 for the decarboxylation in sub and super-critical

water of unsaturated fatty acid (oleic acid) and triglycerides (soybean oil) to produce hydrocarbons in the diesel range without adding hydrogen.

5.2 Experimental

5.2.1 Materials

Ammonium (*para*)tungstate hydrate ($H_{42}N_{10}O_{42}W_{12}$. xH_2O, 99.99%, Aldrich), ammonium niobate(V) oxalate hydrate ($C_4H_4NNbO_9$. xH_2O, 99.99%, Aldrich), ammonium molybdate ($H_{24}Mo_7N_6O_{24}$. $4H_2O$, Sigma-Aldrich), zirconium(IV) oxynitrate hydrate (N_2O_7Zr. xH_2O, 99%, Aldrich), and nickel(II) nitrate hexahydrate (N_2NiO_6. $6H_2O$, Sigma-Aldrich) were used as W, Nb, Mo, Zr, and Ni sources, respectively. Oleic acid (technical grade 90%), aluminum isopropoxide ($C_9H_{21}AlO_3$, 99.99%), heptane (UN1206, 99%), the mesoporous silica SBA-15, glycerin (Class IIIB) were purchased from Sigma-Aldrich, Aldrich, EMD Chemicals, Advanced Chemicals Supplier (ACS), and Fisher-Scientific, respectively.

5.2.2 Catalyst preparation

A neutral support, SBA-15, with a 9 nm pore diameter and Brunauer-Emmett-Teller (BET) surface area of 600 m^2/g, was modified by aluminum isopropoxide to adjust its acidity. SBA-15 (20 g) was suspended in hexane (150 mL); then, aluminum isopropoxide (0.067 g) was added to the solution and stirred for 24 h. The mixture was filtered, dried, and calcined at 550 °C for 4 h. According to our previous work,[117] the catalysts NiNb, NiMo, NiW, and NiZr were prepared in the ratio of 6.67 wt% Ni:3.33 wt% M (M = Nb, Mo, W, Zr) by the wet co-impregnation of aqueous solutions of ($Ni(NO_3)_2$. $6H_2O$, $C_4H_4NNbO_9$. xH_2O), ($Ni(NO_3)_2$. $6H_2O$, $(NH_4)_6Mo_7O_{24}$. $4H_2$), ($Ni(NO_3)_2$. $6H_2O$,

$(NH_4)_{10}(H_2W_{12}O_{42})\cdot 4H_2O)$, and $(Ni(NO_3)_2. 6H_2O, ZrO(NO_3)_2\cdot xH_2O)$ on the modified Al-SBA-15 support. The resulting solids were dried and calcined at 450 °C for 4 h.

Carburization was conducted using temperature-programmed reduction (TPR) according to the method of Claridge et al.[90] Each metal oxide precursor was placed in a quartz tube and subjected to a flow of 20% CH_4/80% H_2 at 30 cm^3/min and a heating rate of 10 K/min to 250 °C, followed by 2.0 K/min to 730 °C. The temperature was maintained at 730 °C, the optimal temperature for carbide formation, for 30 min to complete the reaction.[90] After cooling, the catalyst was passivated under a mixture of 1% O_2 in Ar for 1 h to eliminate its pyrophoricity[19] and protect the bulk of the catalyst against deep oxidation.[91]

5.2.3 Material characterization

X-Ray diffraction (XRD) patterns were collected using a Rigaku RU2000 rotating anode powder diffractometer (Rigaku Americas Corporation, TX) with SmartLab Guidance and MDI Jade 8 software at a scan rate of 8 °/min.

5.2.4 Reaction procedure

The catalytic hydrothermal decarboxylation of oleic acid was conducted in mini-reactors assembled from 3/8-inch stainless steel Swagelok parts, sealed with a cap on each end to give a reactor volume of 1.52 mL.[72] Prior to use in any experiments, the reactors were washed with acetone and water to remove any residual materials. In typical experiments, 10 mg catalyst, 0.642 mL water, and 0.156 mmol oleic acid were loaded in the reactors. The reactors were sealed in a glove box to avoid their exposure to air. The loaded reactors were placed in a pre-heated furnace (400 °C) and (350 °C) to achieve super-critical and sub-critical conditions, respectively. After the desired reaction time was

completed (4 h), the reactors were submerged in a water bath to quench the reaction. The products were transferred to volumetric flasks, and the reactors were rinsed with repeated heptane washes until the total volume collected was 10 mL.

Additional experiments were performed with the same catalysts that were reduced in H_2 before being loaded to the reactors to investigate the effect of a catalyst reduction step. During the reduction, the catalysts were placed in a quartz tube reactor and reduced in H_2 (30 mL/min) at 450 ^{o}C for 3 h. After cooling to ambient temperature, the ends of the tube were quickly sealed and placed in a glove box to minimize the likelihood of re-oxidation of the reduced catalysts.

Another set of experiments was conducted by adding different loadings of glycerol to the reactants to determine the impact of glycerol as a hydrogen donor. Three different glycerol loading were applied (0.12, 0.24, and 0.48 mmol glycerol). The experiments were carried out under super-critical conditions.

Finally, soybean oil was used as a feedstock to investigate the ability of the catalysts to hydrolyze the triglycerides to form fatty acids and glycerol; and then produce hydrogen *in situ* from the generated glycerol. Therefore, no addition glycerol is required for the hydrothermal decarboxylation of triglycerides. These experiments were conducted under super-critical conditions.

5.2.5 Analysis method

The liquid products were analyzed using a Perkin Elmer Clarus 500 gas chromatograph (GC) equipped with flame ionization detector (FID) and an Rtx-65 TG column (Restek, 17008, length: 30 m, internal diameter: 0.25 mm, phase film thickness: 0.10 μm). For fatty acid separation, the GC oven temperature was programmed as

follows: 1 min hold at 80 ^{o}C, 30 ^{o}C/min ramp to 240 ^{o}C, 0 min hold at 240 ^{o}C, 10 ^{o}C/min ramp to 360 ^{o}C, 15 min hold at 360 ^{o}C. The detector temperature was maintained at 360 ^{o}C. Samples (1.5 μL) were injected into the column with a 5:1 split ratio. For hydrocarbon analysis, the GC oven temperature was programmed as follows: 2 min hold at 40 ^{o}C, 10 ^{o}C/min ramp to 300 ^{o}C, 5 min hold at 300 ^{o}C. The injector and detector temperatures were 250 ^{o}C and 300 ^{o}C, respectively, and the split ratio was 5:1. Concentrations were determined by the external standard method.

In order to identify the products, a gas chromatography-mass spectrometer (GC-MS) (Clarus 500 GC-MS, Perkin-Elmer) with a capillary wax Rtx-WAX column (length: 60 m, diameter: 0.25 mm, thickness of stationary phase 0.25 μm) was also used.

5.3 Results and discussion

5.3.1 Catalyst characterization

The XRD patterns of the nickel-based carbide catalysts with four different metals (Mo, Nb, W, and Zr) supported on Al-SBA-15 are shown in Figure 34. For all the catalysts, the broad peak between 2θ = 15–30° corresponds to the mesoporous silica. The XRD patterns of the catalysts show three main peaks at 2θ = 44.6^o, 52.2^o, and 76.3^o, corresponding to the (111), (200), and (220) diffractions of the Ni particles, respectively.[144] There is no indication of Ni carbide formation, confirming that Ni metal was easily reduced to form Ni particles, in agreement with the findings of Gajbhiye et al.[71] The carbide phases of Mo, Nb, and W were observed; however, the carbide phase of Zr was not observed, which may suggest that the Zr carbide phase was very well dispersed on the support or the particles were too small to be detected by XRD.[74]
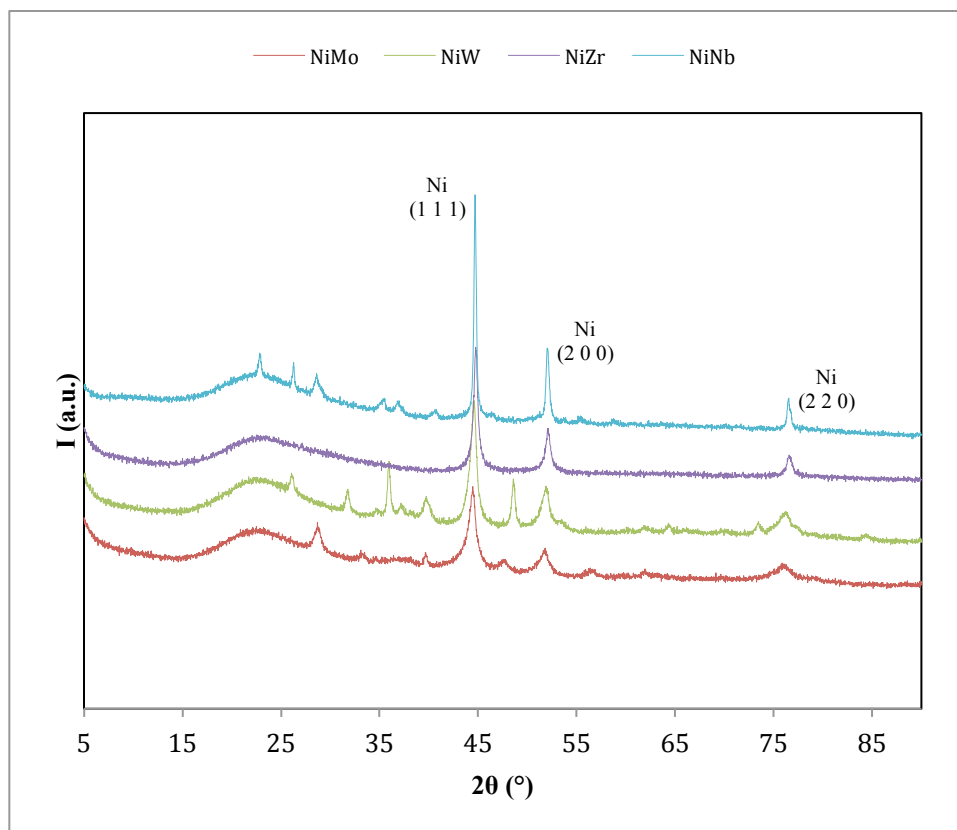
Figure 34. XRD patterns of NiMoC/Al-SBA-15, NiWC/Al-SBA-15, NiZrC/Al-SBA-15, and NiNbC/Al-SBA-15.

5.3.2 Effect of sub- and super-critical water on hydrothermal decarboxylation of oleic acid

Four different catalysts for the hydrothermal decarboxylation of oleic acid under sub-critical conditions (350 $^{\circ}$C and 16.5 MPa) and super-critical conditions (400 $^{\circ}$C and 32 MPa) were evaluated. As a control experiment, hydrothermal decarboxylation of oleic acid in super-critical water was conducted in the absence of catalyst with only 4.7% conversion observed, which is in agreement with Fu et al.[74] Also, the influence of the support (Al-SBA-15 with no metals) on the hydrothermal decarboxylation of oleic acid

was studied under supercritical conditions and showed similar conversion to that observed for the control experiment.

Table 12 summarizes the results for the hydrothermal decarboxylation of oleic acid under super-critical conditions after 4 h reaction time for the four catalysts supported on Al-SBA-15. All of the catalysts exhibited similar conversion of oleic acid (30-33 %) which can be attributed to the absence of rich H_2 environment. The major product of the reaction from every catalyst was unsaturated C17 arising directly from decarboxylation and decarbonylation reactions. The NiWC/Al-SBA-15 produced heptadecane with a selectivity of 0.72%; while less than 0.1% heptadecane selectivity was obtained from the other catalysts. These results suggest that the NiWC/Al-SBA-15 has slightly higher activity for the hydrogenation reaction than others. This may be attributed to the variation in the valence shell for tungsten and the other metals (Mo, Nb, and Zr). The electrons in tungsten's valence shell (5d) have higher average energy than the electrons in the other metal's valence shell (4d). Therefore, the hydrogenation activity of tungsten catalyst was higher than the other metal catalysts. The GC-FID spectrum of the product obtained from the NiWC/Al-SBA-15 catalyst, Figure 35, shows that an oxygenated compound (γ-Stearolactone) was observed in the product at a level of roughly 21-35% for all of the catalysts. The double bond in the oleic acid migrates from the position of (Δ9) to the (Δ4) position before ring closure resulted in the γ-Stearolactone.[148] The presence of the double bond in oleic acid may promote oligomerization paths that produce higher molecular weight materials, which do not elute from the GC-FID. Although Fu et al.[74] shows that the conversion of oleic acid over activated carbon after 3 h at 370 ^{o}C was 80%, the

selectivity of heptadecane was only 7%. Also, only partial hydrogenation of oleic acid

(31%) to stearic acid took place over Pt/C after 9 h at 300 °C.[72,75]

Table 12. Conversion and product selectivity for the hydrothermal decarboxylation of oleic acid after 4 h reaction in super-critical water.

Catalyst on (Al-SBA-15)	Conversion (%)	Selectivity (%)			
		C17	Unsaturated C17	C18	Unsaturated C18
NiMoC	32.8	0.08	62.5	0	3.1
NiNbC	30.7	0	67.6	0	1.9
NiWC	30.7	0.72	53.6	0.04	1.8
NiZrC	30.1	0.09	67.7	0	1.1
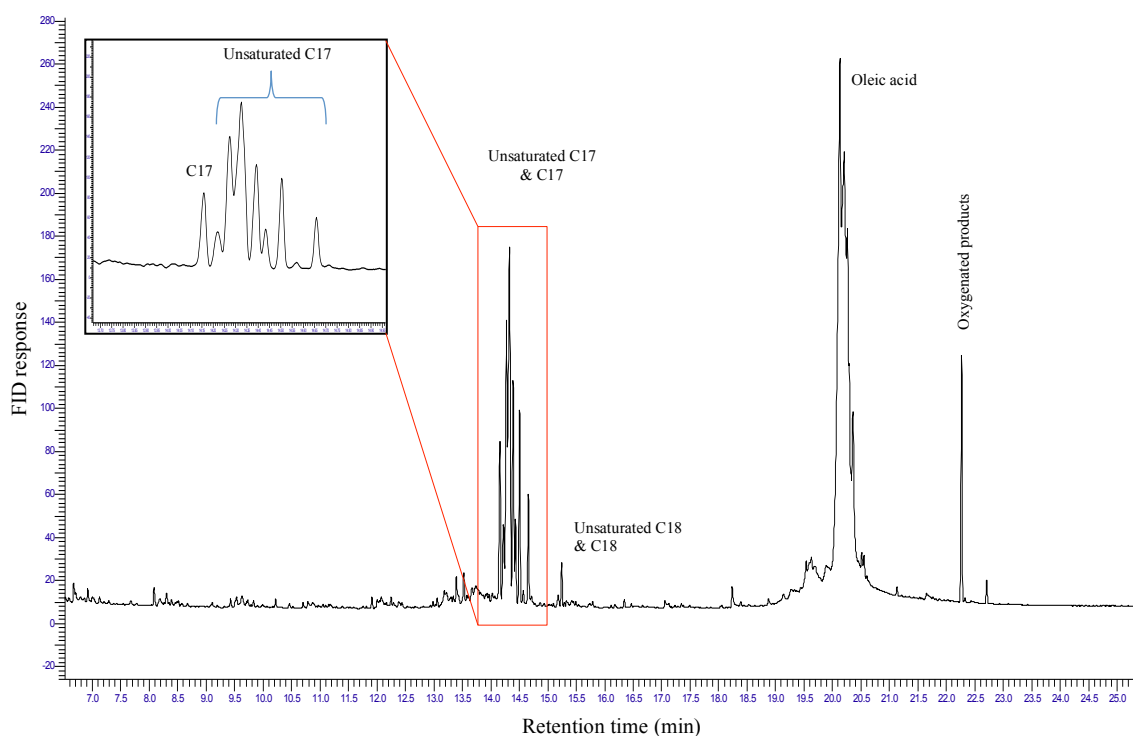
Figure 35. GC-FID spectrum of the product obtained from the hydrothermal decarboxylation of oleic acid after 4 h reaction in super-critical water over the NiWC/Al-SBA-15 catalyst.

A proposed mechanism of hydrothermal decarboxylation of oleic acid in super-critical water based on the previous results is shown in Figure 36. During the hydrothermal decarboxylation of oleic acid, the carboxylic acid donates protons by the heterolytic cleavage of the O-H bond, generating a carboxylate and hydrogen ions. Heptadecenes (unsaturated C17) are produced due to the removal of CO_2. The *in situ* generated hydrogen (as a result of heterolytic cleavage of the O-H bond in oleic acid) is consumed by the hydrogenation of oleic acid or unsaturated C17 to form stearic acid or heptadecane, respectively. The produced stearic acid is then decarboxylated to generate more heptadecane. Moreover, hydrogen molecules can also be generated from water-gas shift reactions.[149] A similar sequential hydrogenation–decarboxylation pathway for oleic acid in dodecane solvent was proposed by Immer et al.[150]
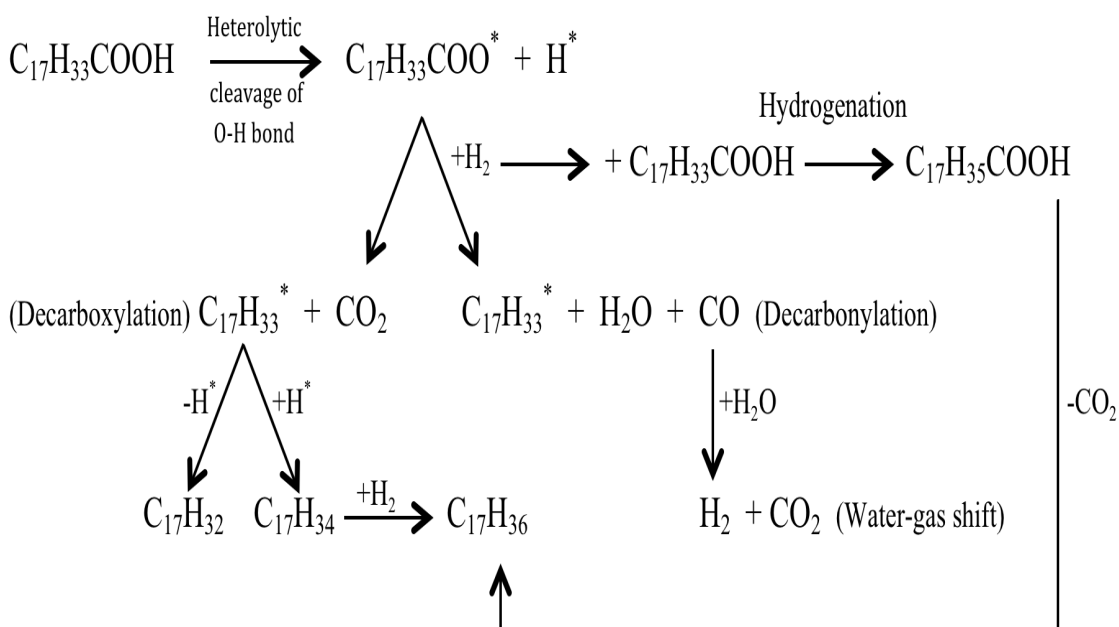
Figure 36. Proposed reaction mechanism for the hydrothermal decarboxylation of oleic acid in super-critical water.

The catalysts were evaluated for the hydrothermal decarboxylation activities of oleic acid in sub-critical water (350 °C) (Table 13). Under sub-critical conditions, all of the catalysts exhibited lower conversion and product selectivity for the hydrothermal decarboxylation of oleic acid than for super-critical conditions. The major products were oxygenated compounds, with no measurable amount of stearic acid. These results suggest that higher temperature promotes the hydrogenation-decarboxylation reactions of oleic acid. The decarboxylation of oleic acid over Pt/SAPO-11 after 2 h increased from 20% to 90% as the temperature increased from 200 °C to 325 °C. Also, the heptadecane selectivity increased by a factor of 4 when the temperature increased to 325 °C.[151] At super-critical conditions, water becomes a highly reactive medium due to the reduction in dielectric constant and increasing in self-dissociation constant.[75]

Table 13. Conversion and product selectivity for the hydrothermal decarboxylation of oleic acid after 4 h reaction in sub-critical water.

Catalyst on (Al-SBA-15)	Conversion (%)	Selectivity (%)			
		C17	Unsaturated C17	C18	Unsaturated C18
NiMoC	13.1	0	34.6	0	0.96
NiNbC	15.3	0	31.1	0	0.83
NiWC	15.6	0.01	35.8	0.03	1.01
NiZrC	12.9	0	28.5	0	0.77

The pretreatment (pre-reduction) of the catalysts did not significantly affect the hydrothermal decarboxylation of oleic acid at super-critical conditions (400 °C) for 4 h reaction (Figure 37), which indicates that the pre-reduction step was not necessary because there was not much oxide on the catalyst surface. A similar finding by Fu et al.[72] shows that the pre-reduction step of Pt/C and Pd/C catalysts did not alter the catalyst

activity for the hydrothermal decarboxylation of palmitic acid. Also, the pre-reduction of activated carbon did not show a significant effect on the hydrothermal decarboxylation of palmitic acid.[74]

(a)　　　　　　　　　　　　　　　　　　　(b)
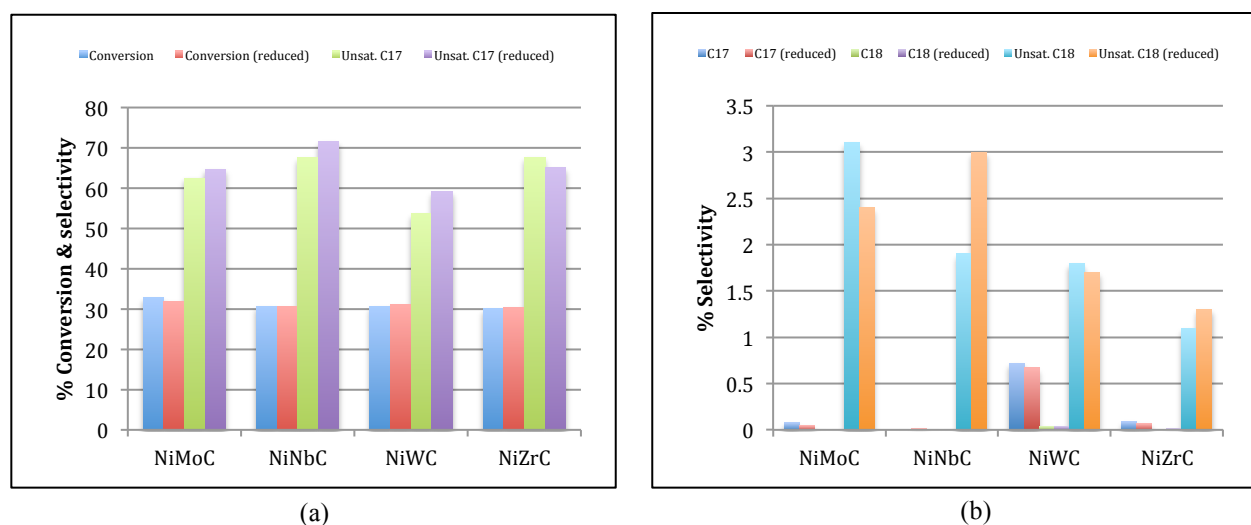
Figure 37. Effect of the catalyst pre-reduction on the hydrothermal decarboxylation of oleic acid after 4 h reaction in super-critical water. Conversion of oleic acid and selectivity of unsaturated C17 (a), Selectivity of C17, C18, and unsaturated C18 (b).

5.3.3 Effect of adding glycerol on hydrothermal decarboxylation of oleic acid

The effect of *in situ* H_2 production via glycerol APR (Rxn. 1) on the hydrothermal decarboxylation of oleic acid in super-critical water was examined. The need for external hydrogen is a basic challenge for conventional lipid hydrotreatment processes;[63,64] however, the production of *in situ* hydrogen may alleviate this challenge.

$$C_3H_8O_3 + 3\ H_2O \longrightarrow 7\ H_2 + 3\ CO_2 \qquad \text{(Rxn. 1)}$$

Three different initial glycerol loadings were investigated for the hydrothermal decarboxylation of oleic acid at super-critical condition as shown in Figure 38. Theoretically, the 0.156 mmol of oleic acid requires 0.156 mmol of H_2 to completely hydrogenate the oleic acid into stearic acid as shown in (Rxn. 2).

$$C_{18}H_{34}O_2 + H_2 \longrightarrow C_{18}H_{36}O_2 \qquad \text{(Rxn. 2)}$$
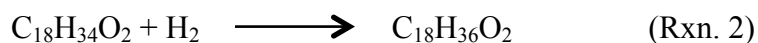
Based on Rxn. 1, the three initial glycerol loadings (0.12 mmol, 0.24 mmol, and 0.48 mmol) can generate H_2 of 0.84 mmol, 1.68 mmol, and 3.36 mmol, respectively. The NiMoC, NiNbC, and NiZrC supported on Al-SBA-15 performed similarly with the three different glycerol loadings as shown in Figure 38. A slight increase in the stearic acid selectivity (Figure 38 b) and decrease in the unsaturated C17 selectivity (Figure 38 d) were observed when 0.12 mmol of glycerol was added. Also, the NiMoC, NiNbC, and NiZrC catalysts required higher glycerol loading (0.48 mmol) in order to obtain higher oleic acid conversion (Figure 38 a). However, a significant improvement in the conversion of oleic acid (Figure 38 a), selectivity of stearic acid (Figure 38 b), and selectivity of heptadecane (Figure 38 c) was observed for the reaction over NiWC catalyst with the addition of only 0.12 mmol of glycerol. The conversion of oleic acid and selectivity of heptadecane over NiWC catalyst reached 97.3% and 5.2% after adding 0.48 mmol glycerol. However, the production of unsaturated C17 decreased with the addition of glycerol (Figure 38 d), which suggests that the direct decarboxylation of oleic acid decreased. These results suggest that hydrogenation of oleic acid dominates the reaction in the presence of excess H_2 to produce stearic acid. A complete hydrogenation of oleic acid into stearic acid and partial decarboxylation of stearic acid to produce heptadecane (24%) was observed when the reaction was carried out over Pt/C at 300 $^{\circ}$C for 9 h, suggesting that the hydrogen concentration greatly affects the catalyst decarboxylation performance.[75]

The addition of glycerol to the reactants of the hydrothermal decarboxylation of oleic acid improved the conversion of oleic acid and the selectivity of heptadecane. Figure 38

illustrates a comparison of the catalyst performance before and after adding glycerol, indicating that all the catalysts utilized the glycerol for generating hydrogen. However, the NiWC/Al-SBA-15 exhibited the greatest potential for utilizing the *in situ* produced H_2 from glycerol to hydrogenate the oleic acid and then decarboxylate the produced stearic acid to produce heptadecane. The higher hydrogenation activity of the NiWC/Al-SBA-15 catalyst in comparison to others may be attributed to its fractional sum of electronegativity that falls in the range of electronegativity of noble metal catalysts.[152] Therefore, the rates of adsorption and desorption are similar to those observed for the noble metals. In addition, the high electron energy in the outermost shell of tungsten may be another reason for the higher activity of NiWC/Al-SBA-15 in comparison to the other catalysts.

A reaction sequence as shown in Figure 39 is likely wherein the hydrogenation of oleic acid initially takes place to produce stearic acid followed by decarboxylation of stearic acid to form heptadecane. A similar finding by Vardon et al.[75] suggested that the hydrogenation of oleic acid to produce stearic acid, and followed by decarboxylation of the stearic acid over (Pt/C and Pt-Re/C) increased after adding glycerol. Although Pt/C and Pt-Re/C showed higher production of heptadecane than the catalysts in this study, the CO produced during fatty acid decarbonylation can inhibit the activity of those noble catalysts.[147]

The product distributions obtained from the NiWC/Al-SBA-15 catalyst were influenced by the glycerol addition (0.48 mmol) as shown in Figure 40. The oxygenated products that were produced from the hydrothermal decarboxylation of oleic acid with no glycerol addition diminished after adding the glycerol. Also, some shorter hydrocarbons

(C10-C16) were apparent in the GC-FID spectrum, suggesting that the NiWC/Al-SBA-15

catalyst exhibited some cracking activity.

(a)

(b)

(c)

(d)
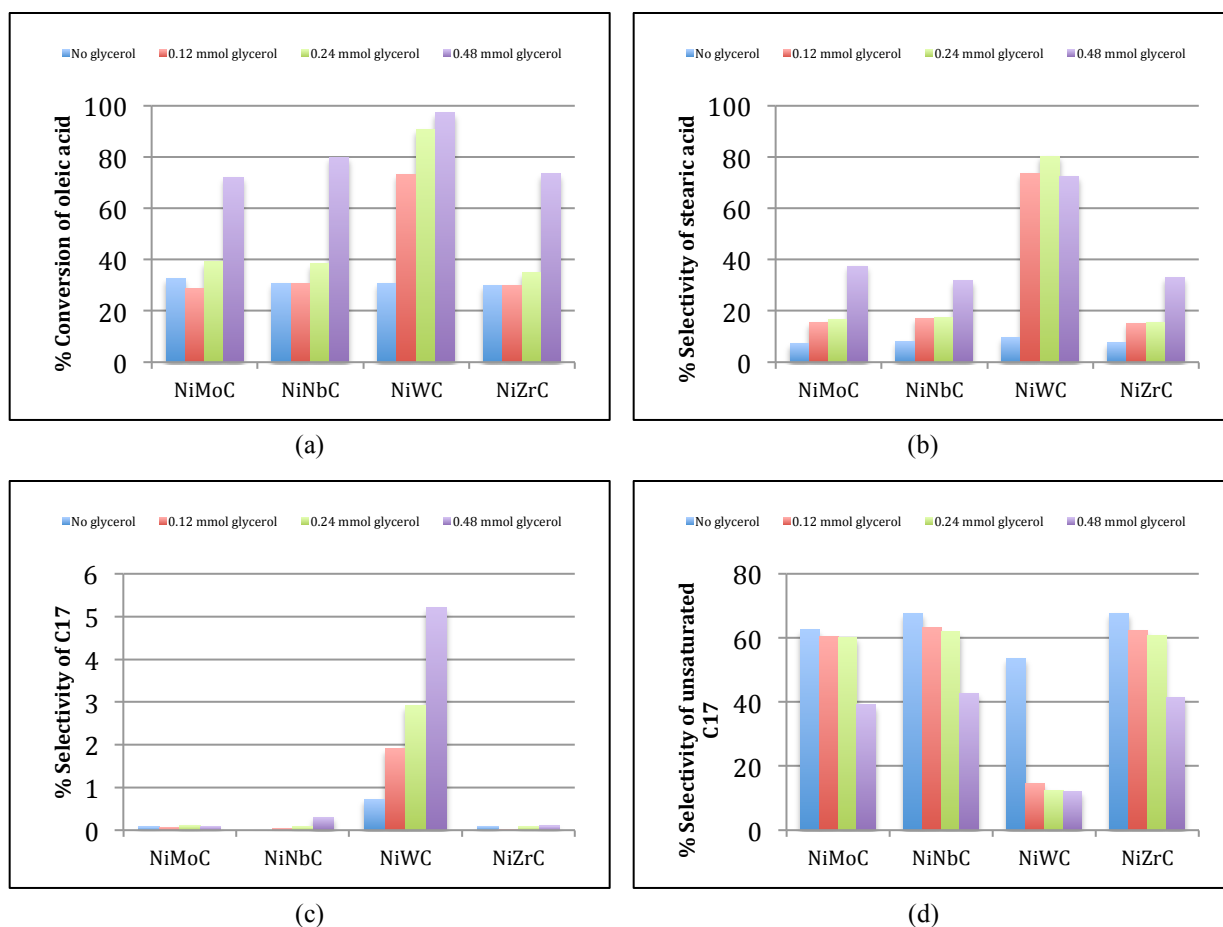
Figure 38. Conversion and product selectivity for the hydrothermal decarboxylation of
oleic acid with different initial glycerol loading after 4 h reaction in super-critical water.
Conversion of oleic acid (a), selectivity of stearic acid (b), selectivity of C17 (c),
selectivity of unsaturated C17 (d).

$$C_3H_8O_3 + 3\,H_2O \longrightarrow 7\,H_2 + 3\,CO_2$$

$$C_{17}H_{33}COOH + H_2 \longrightarrow C_{17}H_{35}COOH$$

$$C_{17}H_{35}COOH \longrightarrow C_{17}H_{36} + CO_2$$
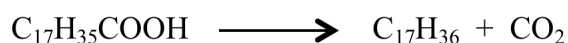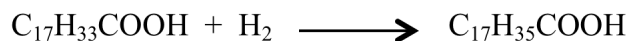
Figure 39. Reaction sequence for the hydrothermal decarboxylation of oleic acid in the
presence of glycerol in super-critical water.
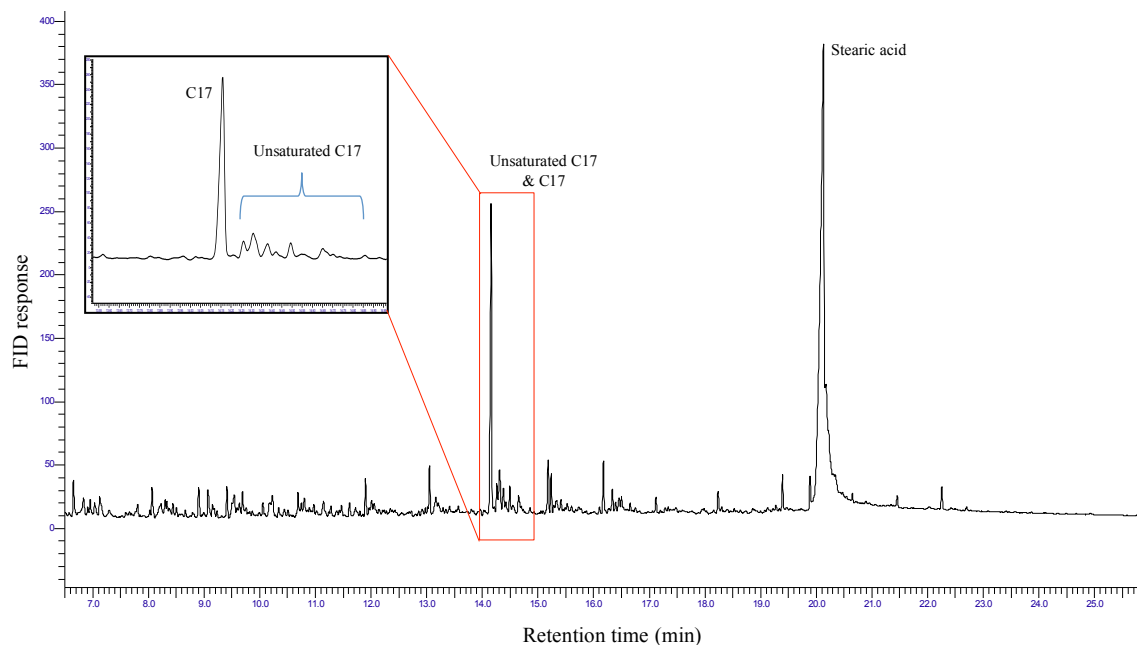
Figure 40. GC-FID spectrum of the product obtained from the hydrothermal decarboxylation of oleic acid with glycerol addition (0.48 mmol) after 4 h reaction in super-critical water over the NiWC/Al-SBA-15 catalyst.

5.3.4 Conversion of lipids (soybean oil) to hydrocarbons

The process that is used to hydrolyze triglycerides to produce free fatty acids and glycerol in hydrothermal media is commonly called "fat-splitting".[149,153,154] The previous experimental results support the idea of using triglyceride-based biomass such as soybean oil as a feedstock to produce hydrocarbons via hydrothermal decarboxylation reaction. No additional glycerol is required since glycerol molecules are generated from the hydrolysis of triglycerides. Following hydrolysis, liberated glycerol can undergo catalytic APR reactions to generate H_2.[75] Also, glycerol can be catalytically decomposed to generate CO that is consumed to produce additional H_2 from the water-gas shift reaction.

A nearly complete conversion of soybean oil (>95% triglycerides) was obtained from the hydrothermal decarboxylation reaction to produce heptadecane, unsaturated C17, unsaturated C18, stearic acid, oleic acid, and linoleic acid as shown in Table 14. The

soybean oil used in this study had a fatty acid profile of 2-5% stearic acid, 20-30% oleic acid, 50-60% linoleic acid and 5-11% linolenic acid. All of the catalysts exhibited good hydrolysis activities of triglycerides. The soybean oil (triglycerides) is converted to its major fatty acids (oleic acid and linoleic acid) in addition to other fatty acids such as stearic acid and linolenic acid. Also, the presence of stearic acid suggests that some of the oleic acid and linoleic acid were hydrogenated to produce stearic acid. Although several studies show that the rate of hydrogenation of linoleic acid is greater than oleic acid,[155-157] the selectivity for hydrogenation of linoleic acid decreases as temperature increases.[158] A 19-31% selectivity to unsaturated C17 was observed for each catalyst, indicating a decarboxylation of oleic acid and linoleic acid took place. No oleic acid was observed when the reaction was carried out over the NiWC/Al-SBA-15. Also, the highest stearic acid selectivity was obtained from the NiWC/Al-SBA-15; therefore, this catalyst has the best hydrogenation activity, as observed previously. The results for the NiWC/Al-SBA-15 suggest that heptadecane was produced from either the decarboxylation of stearic acid or from the hydrogenation of unsaturated C17.

Table 14. Product selectivity for the hydrothermal decarboxylation of soybean oil after 4 h reaction in super-critical water.

Catalyst	Selectivity (%)						
	C17	C17*	C18	C18*	Stearic acid	Oleic acid	Linoleic acid
NiMoC	0.04	31.1	0	2.9	19.3	9.6	20.1
NiNbC	0.04	31.1	0	2.9	16.2	14.4	19.7
NiWC	2.1	19.7	0	3.7	39.6	0	15
NiZrC	0.03	30.5	0	2.6	14.3	18.2	21

* Unsaturated components

5.4 Conclusion

Catalytic hydrothermal decarboxylation processing is a promising method for converting low-quality lipid feedstocks, such as brown grease, which are typically high in free fatty acids and triglycerides, into hydrocarbon fuels. Several catalysts, Ni-based transition metal carbides supported on Al-SBA-15, were investigated for the hydrothermal decarboxylation of oleic acid. The effect of catalyst reduction, sub- and super-critical conditions on the catalysts performance was examined. Super-critical water promotes the hydrogenation-decarboxylation reactions of oleic acid due to the increase of water reactivity at super-critical temperature. Water at super-critical condition becomes a more reactive medium with lower dielectric constant and higher self-dissociation constant. The utilization of APR of glycerol for *in situ* hydrogen production motivates the hydrogenation of oleic acid to stearic acid and production of heptadecane especially over NiWC-Al-SBA-15. The NiWC/Al-SBA-15 showed higher hydrogenation activity than other catalysts, which may be attributed to its fractional sum of electronegativity that falls in the range of electronegativity of noble metal catalysts and the high electron energy in the outermost shell of tungsten. The NiWC/Al-SBA-15 shows a great potential to hydrolyze triglycerides, generate *in situ* H_2 from glycerol, hydrogenate oleic acid and linoleic acid to form stearic acid, and produce heptadecane. However, further hydrothermal decarboxylation of stearic acid is needed to enhance the selectivity to green diesel hydrocarbons. It is envisioned a bifunctional catalyst, or a two-step process can be developed for hydrothermal decarboxylation of triglycerides: first step for hydrogenation of unsaturated fatty acids over a modified NiWC/Al-SBA-15, and second step for decarboxylation of saturated fatty acid to produce alkanes. Thus, modified NiWC/Al-SBA-15 catalysts may provide an economically viable process for the

hydrothermal decarboxylation of fatty acids and triglycerides derived from low-quality sources without the need of additional H_2.

CHAPTER 6

CONCLUSIONS AND RECOMMENDATIONS

6.1 Conclusions

Relatively inexpensive bimetallic catalysts, nickel-based carbide catalysts combined with other metals (Mo, Nb, W, and Zr) and supported on Al-SBA-15, exhibited great performances for producing green diesel from hydrocracking of non-edible vegetable oils (DDGS corn oil). Also, these catalysts showed promising results for producing green diesel from hydrothermal decarboxylation of oleic acid and soybean oil. However, several factors can contribute in determining and improving the activity and selectivity of the catalysts for the hydrocracking and hydrothermal decarboxylation reactions. The following conclusions can be obtained according to the results from the three accomplished projects:

Effect of Metal Ratio and Preparation Method on Nickel−Tungsten Carbide Catalyst for Hydrocracking of Distillers Dried Grains with Solubles Corn Oil

- The activity and selectivity of NiWC/Al-SBA-15 catalyst for the hydrocracking of DDGS corn oil are significantly varied with the metal ratio (Ni-W) and the preparation method.

- The activity and selectivity of NiWC/Al-SBA-15 catalyst for the hydrocracking of DDGS corn oil are improved with enhancing the degree of metal dispersion on the support and suppressing the formation of metal alloys.

- Both the metal ratio and preparation method influence the metal dispersion and metal alloy formation.

- Ni content is an important factor in designing NiWC/Al-SBA-15 catalyst for the

hydrocracking of DDGS corn oil because it is essential for activating hydrogen and increasing the metal dispersion.

- Not only did the DENP method enhance the metal dispersion and prevented alloy formation, it also decreased the particle size of the catalyst.

Hydrocracking of DDGS corn oil over transition metal carbides supported on Al-SBA-15: Effect of fractional sum of metal electronegativities

- The closer the fractional sum of the transition metal electronegativities is to the electronegativity range of the noble catalysts (2.0–2.2), the better the catalyst performance will be. However, this is not the only factor that controls the catalyst activity. The BET surface area, particle size, pore size, and metal composition can also affect the activity and selectivity.

- The catalyst, NiWC/Al-SBA-15, with the fractional sum of the electronegativities value within the range of noble metal electronegativity (2.0-2.2) exhibited the highest catalytic performance.

- Doping a promoter (Ce) brought the fractional sum of the electronegativities of the transition metals closer to the (2.0-2.2) range, and improved the catalyst performance.

This study shows a promising approach for producing biofuels (green diesel) from low quality (non-edible) renewable sources under relatively mild reaction conditions. Also, this study shows that the bimetallic carbide catalysts can replace noble catalysts (expensive catalysts) and sulfided catalysts. Therefore, this study overcomes some of the challenges that are associated with biofuel productions.

Biofuels Production from Hydrothermal Decarboxylation of Oleic Acid and Soybean Oil Over Ni-based Transition Metal Carbides Supported on Al-SBA-15

- The activity of transition metal carbide catalyst supported on Al-SBA-15 for the hydrogenation-decarboxylation of oleic acid was promoted on super-critical water.

- The catalysts, especially NiWC/Al-SBA-15, showed a great potential for utilizing APR of glycerol for *in situ* hydrogen production. The *in situ* hydrogen production motivates the hydrogenation of oleic acid to stearic acid and production of heptadecane.

- The NiWC/Al-SBA-15 catalyst exhibited higher hydrogenation activity than the other catalysts, which may be attributed to its fractional sum of electronegativity that falls in the range of electronegativity of noble metal catalysts and the high electron energy in the outermost shell of tungsten in comparison to the other metals.

6.2 Recommendations

For the hydrocracking of DDGS corn oil over NiWC/Al-SBA-15, there are two possible reasons for declining the diesel selectivity over the time: the secondary reactions that convert the green diesel to alcohols and the Si leaching out of the catalyst that leads to a collapse of the Al-SBA-15 structure. The following recommendations are for the future study:

- Minimize the effect of the produced water, from the hydrodeoxygenation reaction, on changing the catalyst structure and promoting the secondary reactions that convert green diesel to alcohols.

- Modify the support by combining Al-SBA-15 and zeolite to improve the mechanical and thermal stability of the support.

- Develop a cost model in order to study the possibility of the process to be commercialized.

After adding glycerol for the hydrothermal decarboxylation of oleic acid, the conversion of oleic acid increases toward forming stearic acid (hydrogenation reaction) rather than forming decarboxylation products. Moreover, the decarboxylation products were produced from the decarboxylation of stearic acid. The following suggestions are to help in understanding the mechanism of the hydrothermal decarboxylation reaction:

- Synthesize a tri-metallic carbide catalyst (NiWPdC) supported on Al-SBA-15. Therefore, NiW will be responsible for the hydrogenation of oleic acid to stearic acid, while Pd will be responsible for the decarboxylation of stearic acid to produce heptadecane.

- Use a two-step process: first, using NiWC/Al-SBA-15 catalyst to hydrogenate oleic acid to produce stearic acid. Second, use Pd/C or NiWC/Al-SBA-15 catalyst for the hydrothermal decarboxylation of stearic acid to produce heptadecane.

REFERENCES

[1] *International Energy Agency. World Energy and Economic Outlook. International Energy Outlook 2009,* DOE/EIA, 2009.

[2] *Statistical Review of World Energy 2009*. Available from. <http://www.bp.com/liveassets/bp_internet/globalbp/globalbp_uk_english/reports_and_p ublications/statistical_energy_review_2008/ST AGING/local_assets/2009_downloads/sta tistical_review_of_world_energy_full_report_2009.xls#'Primary>. Accessed October 24, 2009.

[3] *U.S. Energy information administration (eia). AER Energy Perspectives and MER*. Available from. <http://www.eia.gov/totalenergy/data/annual/#summary>. Accessed May 23, 2014.

[4] *Basic Research Needs: Catalysis for Energy*; U.S. Department of Energy: Maryland, August 6-8, 2007.

[5] L. Dandik, H. A. Aksoy, A. Erdem-Senatalar, Energy & Fuels 12 (1998) 12 1148-1152.

[6] G. Knothe, J. V. Gerpen, J. Krahl, *The Biodiesel Handbook*. AOCS Press: 2005.

[7] Y. S. Prasad, N. N. Bakhshi, Applied Catalysis 18 (1985) 71.

[8] J. Gusmão, D. Brodzki, G. Djéga-Mariadassou, R. Frety, Catal. Today 5 (1989) 533–544.

[9] P. Priecel, D. Kubička, L. Čapek, Z. Bastl, P. Ryšánek, Appl. Catal. A-Gen. 397 (2011) 127–137.

[10] Y. Liu, R. Sotelo-Boyás, K. Murata, T. Minowa, K. Sakanishi, Chem. Lett. 38 (2009) 552–553.

[11] K. Murata, Y. Liu, M. Inaba, I. Takahara, Energy Fuels 24 (2010) 2404–2409.

[12] M. Krar, S. Kovacs, D. Kallo, J. Hancsok, Bioresour. Technol. 101 (2010) 9287–9293.

[13] D. Kubicˇka, M. Bejblová, J. Vlk, Top. Catal. 53 (2010) 168–178.

[14] N. Choudhary, D.N. Saraf, Prod. R&D 14 (1975) 74–83.

[15] V. A. Yakovlev, S. A. Khromova, O. V. Sherstyuk, V. O. Dunduch, D. Y. Ermakov, V. M. Novopashina, Catal. Today 144 (2009) 362–366.

[16] B. Diaz, S. J. Sawhill, D. H. Bale, R. Main, D. C. Phillips, S. Korlann, R. Self, M. E. Bussell, Catal. Today 86 (2003) 191–209.

[17] J. S. Choi, G. Bugli, G. D. Mariadassou, J. Catal. 193 (2000) 238–247.

[18] E. Furimsky, Appl. Catal. A 240 (2003) 1–28.

[19] W. Zhang, Y. Zhang, L. Zhao, W. Wei, Energy Fuels 24 (2010) 2052–2059.

[20] H. Wang, S. Yan, S. Salley, S. Ng, I&EC Res. 51 (2012) 10066–10073.

[21] M. Nasikin, B. H. Susanto, M. A. Hirsaman, A. Wijanarko, World Appl. Sci. J. 5 (2009) (Special Issue for Environment) 74−79.

[22] H. Wang, S. Yan, S. Salley, S. Ng, Fuel 111 (2013) 81–87.

[23] *Sustainable Oils Inc*. Available from. <http://www.susoils.com>. 2009.

[24] STRATEGIC PETROLEUM RESERVE. Available from.
<http://energy.gov/fe/services/petroleum-reserves/strategic-petroleum-reserve>.

[25] D. Malloy, K. Mayowski, *In Ninth Annual freshman Conference*. University of Pittsburgh, 2009.

[26] A. E. Barron, J. A. Melo, J. M. Dominguez, Catalyst Today (2011) 102-110.

[27] N. O. Nylund, P. A. Saksa, K. Sipila, *Status and Outlook for Biofuels, Other Alternative Fuels and New Vehicles*; Espoo 2008. VTT Tiedotteita- Research Notes 2426.

[28] G. Knothe, J. V. Gerpen, J. Krahl, *The Biodiesel Handbook*. AOCS Press: 2005.

[29] B. Smith, H. C. Greenwell, A. Whiting, Energy & Environmental Science 2 (2009) 262-271.

[30] Jet Fuel. Available from. *<http://www.algaelink.com/jet-fuel.htm>*. (accessed 10/06/2009).

[31] C. Ratledge, Biochimie 86 (2004) 807.

[32] S. K. Hoekman, Renewable Energy 34 (2009) 14-22.

[33] C. Leonard, Not a tiger, but maybe a chicken in your tank. *The Washington Post* 2007.

[34] G. Knothe, J. V. Gerpen, J. Krahl, J., *The Biodiesel Handbook*. AOCS Press: 2005.

[35] R. Boyas, Y. Liu, T. Minowa, Available from.

<http://www.nt.ntnu.no/users/skoge/prost/proceedings/aiche2008/data/papers/P134226.pdf>.

[36] B. Donnis, R. G. Egeberg, P. Blom, K. G. Knudsen, Topics in Catalysis 52 (2009) 229-240.

[37] M. Nasikin, B. H. Susanto, M. A. Hirsaman, A. Wijanarko, World Appl. Sci. J. 5 (2009) (Special Issue for Environment) 74−79.

[38] G. E. Dolbear, *Abstracts of Papers of the American Chemical Society* 1995, 210, 9.

[39] F. Morel, S. Kressmann, V. Harle, S. Kasztelan, G. F. Froment, B. Delmon, P. Grange, Eds. 1997, P 1.

[40] J. W. Ward, Fuel Processing Technology 35 (1993) 55.

[41] G. N. da RochFilho, D. Brodzki, G. Djega-Mariadassou, Fuel 72 (1993) 543-549.

[42] S. Ooi, R. Zakaria, A. R. Mohamed, S. Bhatia, Catal. Lett. 84 (2005) 295-302.

[43] P. Simacek, D. Kubicka, G. Sebor, M. Pospisil, Fuel (2010) 611-615.

[44] M. Stumborg, A. Wong, E. Hogan, Bioresource Technology (1996) 13-18.

[45] S. Bezergianni, A. Kalogianni, Bioresource Technology (2009) 3927-3932.

[46] R. J. O'Brien, L. Xu, X. X. Bi, P. C. Eklund, B. H. Davis, Blackie, Glasgow 1996; p 362.

[47] S. T. Oyama, Handbook of heterogeneous catalysis, vol. 1, VCH, Weinheim, Germany, 1997; p 39.

[48] J. C. Chen, B. Fruhberger, M. D. Weisel, J. E. Baumgartner, B. D. De Vries, Blackie, Glasgow 1996; p 439.

[49] D. J. Sajkowski, S. T. Oyama, Applied catalyst (1996) 339-349.

[50] V. Heine, Phys. Rev. 153 (1967) 673.

[51] H. O. Pierson, Handbook of Refractory Carbides and Nitrides, Noyes Publ., Westwood, Nj, USA.

[52] J. S. Choi, G. Bugli, G. J. Djega-Maradassou, Catal. 193 (2000) 238.

[53] M. Nagai, Y. Goto, A. Miyata, M. Kiyoshi, K. Hada, K. Oshikawa, S. J. Omi, Catal. 182 (1999) 292.

[54] T. C. Xiao, A. P. E. York, V. C. Williams, H. Al-Megren, A. Hanif, X. Y. Zhou, M. L. H. Green, Chem. Mater. 12 (2000) 3896.

[55] G. W. Hadix, J. A. Reimer, A. T. J. Bell, Catal. 108 (1987) 50.

[56] C. W. Colling, J. G. Choi, L. T. J. Thompson, Catal. 160 (1996) 35.

[57] Y. J. Zhang, Q. Xin, I. Rodrigues-Amos, A. Guerrero-Ruiz, Appl. Catal. 180 (1999) 237.

[58] Y. Li, Y. J. Zhang, R. Rawal, C. Li, R. Zhai, Q. Xin, Catal. Lett. 48 (1997) 239.

[59] A. I. Reyes de la Torre, J. M. Dominguez, J. A. Melo-Banda, C. E. Ramos, G. Sandoval, R. C. Angeles, M. R. Torres, Catal. Today 148 (2009) 55-62.

[60] J. S. Choi, R. L. Curls, L. T. J. Thompson, Catal. 146 (1994) 218.

[61] M. Breysse, E. Furimsky, S. Kasztelan, M. Lacroiz, G. Perot, Catal. Rev.-Sci. Eng. 44 (2002) 649.

[62] http://www.nesteoil.com/default.asp?path = 141, 11,991, 12,243, 15,658. 12,335.

[63] A. Berenblyum, V. Danyushevsky, E. Katsman, T. Podoplelova, V. Flid, Pet. Chem. 50 (2010) 305–311.

[64] E. Santillan-Jimenez, M. Crocker, J. Chem. Technol. Bio-technol. 87 (2012) 1041–1050.

[65] E. Sari, Green diesel production via catalytic hydrogenation/decarboxylation of triglycerides and fatty acids of vegetable oil and brown grease 2013. *Wayne State University Dissertations.*

[66] J. G. Immer, Liquid-phase deoxygenation of free fatty acids to hydrocarbns using supported palladium catalysts. North Carolina State University, 2010.

[67] J. B. Dunn, M. L. Burns, S. E. Hunter, P. E. Savage, J. Supercrit. Fluids 27 (2003) 263–274.

[68] J. Fu, P. E. Savage, X. Lu, Ind. Eng. Chem. Res. 48 (2009) 10467.

[69] J. Li, T. B. Brill, J. Phys. Chem. A. 107 (2003) 2667.

[70] A. A. Peterson, F. Vogel, R. P. Lachance, M. Froling, M. J. Antal, J. W. Tester, Energy Environ. Sci. 1 (2008) 32–65.

[71] M. Watanabe, T. Iida, H. Inomata, Energy Convers. Manage. 47 (2006) 3344–3350.

[72] J. Fu, X. Lu, P. E. Savage, Energy Environ. Sci. 3 (2010) 311–317.

[73] J. Fu, X. Lu, P. E. Savage, Chem. Sus. Chem. 4 (2011) 481– 486.

[74] J. Fu, F. Shi, L. T. Thompson, Jr., X. Lu, P. E. Savage, ACS Catal. 1 (2011) 227–231.

[75] R. Vardon, B. Sharma, H. Jaramillo, D. Kim, J. Choe, P. Ciesielski, T. Strathmann, Green Chem. 16 (2014) 1507-1520.

[76] R. D. Cortright, R. R. Davda, J. A. Dumesic, Nature 418 (2002) 964–967.

[77] J. Shabaker, G. Huber, J. Dumesic, J. Catal. 222 (2004) 180–191.

[78] N. Luo, X. Fu, F. Cao, T. Xiao, P. P. Edwards, Fuel 87 (2008) 3483–3489.

[79] D. L. King, L. Zhang, G. Xia, A. M. Karim, D. J. Heldebrant, X. Wang, T. Peterson, Y. Wang, Appl. Catal. B 99 (2010) 206–213.

[80] D. Ö. Özgür, B. Z. Uysal, Biomass Bioenergy 35 (2011) 822–826.

[81] L. Zhang, A. M. Karim, M. H. Engelhard, Z. Wei, D. L. King, Y. Wang, J. Catal. 287 (2012) 37–43.

[82] E. L. Kunkes, D. A. Simonetti, J. A. Dumesic, W. D. Pyrz, L. E. Murillo, J. G. Chen, D. J. Buttrey, J. Catal. 260 (2008) 164–177.

[83] S. Fernando, S. Adhikari, C. Chandrapal, N. Murali, Energy Fuels 20 (2006) 1727−1737.

[84] G. W. Huber, S. Iborra, A. Corma, Chem. Rev. (Washington, DC, U.S.) 106 (2006) 4044−4098.

[85] R. Sotelo-Boyás, Y. Liu, T. Minowa, Ind. Eng. Chem. Res. 50 (2010) 2791–2799.

[86] E. Koivusalmi, R. Piilola, P. Aalto, P. Process for Producing Branched Hydrocarbons. U.S. Patent Publication US20080302001, 2008.

[87] R. G. Egeberg, K. Knudsen, S. Nystrom, E. Lind, K. Efraimsson, Pet. Technol. Q. Q3 (2011) 59− 65.

[88] J. Han, J. Duan, P. Chen, H. Lou, X. Zheng, H. Hong, Green Chem. 13 (2011) 2561–2568.

[89] S. Wu, J. Huang, T. Wu, K. Song, H. Wang, L. Xing, H. Xu, L. Xu, J. Guan, Q. Kan, Chin. J. Catal. 27 (2006) 9−14.

[90] J. B. Claridge, A. P. E. York, A. J. Brungs, Chem. Mater. 12 (2000) 132–142.

[91] L. Leclercq, A. Almazouari, M. Dufour, G. Leclercq, in: S.T. Oyama (Ed.), The Chemistry of Transition Metal Carbides and Nitrides, Springer, Netherlands, 1996, pp. 345–361.

[92] M. Q. Zhao, R. M. Crooks, Chem. Mater. 11 (1999) 3379−3385.

[93] Y. Niu, R. M. Crooks, C. R. Chim. 6 (2003) 1049− 1059.

[94] Z. V. Feng, J. L. Lyon, J. S. Croley, R. M. Crooks, D. A. V. Bout, K. J. Stevenson, J. Chem. Educ. 86 (2009) 368−372.

[95] X. Peng, Q Pan, G. Rempel, Chem. Soc. Rev. 37 (2008) 1619−1628.

[96] N. S. Gajbhiye, R. S. Ningthoujam, J. Weissmuller, Phys. Stat. Sol. 189 (2002) 691–695.

[97] S. Chatterjee, H. L. Greene, Appl. Catal. A 98 (1993) 139–158.

[98] E. N. Hodkin, M. G. Nicholas, D. M. Poole, J. Less-Common Met. 20 (1970) 93−103.

[99] V. M. Kuznetsov, R. I. Kadyrov, G. E. Rudenskii, J. Mater. Sci. Technol. 14 (1998) 320−322.

[100] Y. Rezgui, M. Guemini, Ind. Eng. Chem. Res. 47 (2008) 4056−4062.

[101] A. M. Alsobaai, R. Zakaria, B. H. Hameed, Chem. Eng. J. 132 (2007) 77−83.

[102] T. Halachev, P. Antanasova, A. L. Agudo, M. G. Arias, J. Ramirez, Appl. Catal. A 136 (1996) 161− 175.

[103] F. Gao, D. W. Goodman, Chem. Soc. Rev. 41 (2012) 8009−8020.

[104] P. Liu, J. K. Norskov, Phys. Chem. Chem. Phys. 3 (2001) 3814-3818.

[105] P. Quaino, E. Santos, G. Soldano, W. Schmickler, Adv. Phys. Chem. 2011 (2011) 1− 14.

[106] T. Kabe, A. Isshihara, W. Qian, Hydrodesulfurization and Hydrodenitrogenation; Wiley-VCH: Singapore, 1999.

[107] A. L. Cabrera, W. H. Garrido, U. G. Volkmann, Catal. Lett. 25 (1994) 115−126.

[108] M. L. Albuquerque, I. Guedes, P. Alcantara, S. G. Moreira, Vib. Spectrosc. 33 (2003) 127−131.

[109] J. Liu, K. Fan, W. Tian, C. Liu, L. Rong, Int. J. Hydrogen Energ. 37 (2012) 17731−17737.

[110] T. Okuhara, M. Kimura, T. Kawai, Z. Xu, T. Nakato, Catal. Today 45 (1998) 73−77.

[111] J. A. Labinger, J. Mol. Catal. A: Chem. 220 (2004) 27−35.

[112] G. Fu, X. Xu, H. Wan, Catal. Today 117 (2006) 133−137.

[113] M. Sun, J. Zhang, P. Putaj, V. Caps, F. Lefebvre, J. Pelletier, J. Basset, Chem. Rev. (Washington, DC, U.S.) 104 (2014) 981−1019.

[114] K. Mouli, K. Soni, A. Dalai, J. Adjaye, Appl. Catal. A 404 (2011) 21−29.

[115] S. Gong, A. Shinozaki, M. Shi, E. Qian, Energy Fuels 26 (2012) 2394−2399.

[116] T. Kalnes, K. Koers, T. Marker, D. Shonnard, Sustainable Energy 28 (2009) 111−120.

[117] B. Al. Alwan, E. Sari, S. Salley, K.Y.S. Ng, I&EC Res. 53 (2014) 6923–6933.

[118] Plummer, Mark A. CRACKING PROCESS CATALYST SELECTION BASED ON CATION ELECTRONEGATIVITY. Marathon Oil Company, Findlay, Ohio, assignee. Patent 4,557,803. 10 Dec. 1985. Print.

[119] C. Nwosu, J. Tech. Sci. Tech. 1 (2012) 25–28.

[120] A. M. Venezia, V. La Parola, G. Deganello, B. Pawelec, J. L. Fierro, J. Catal. 215 (2003) 317–325.

[121] S. Mitra, A. Mandal, A. Datta, S. Banerjee, D. Chakravorty, EPL 92 (2010) 26003.

[122] F. Baker, E. Storms, C. Holley Jr., J. Chem. Eng. Data 14 (1969) 244–246.

[123] J. Zhu, X. Peng, L. Yao, J. Shen, D. Tong, C. Hu, Int. J. Hydrogen Energ. 36 (2011) 7094–7104.

[124] K. Chayakul, T. Srithanratana, S. Hengrasmee, Catal. Today 175 (2011) 420–429.

[125] P. Priecel, L. Capek, D. Kubicka, F. Homola, P. Rysanek, M. Pouzar, Catal. Today 176 (2011) 409–412.

[126] F. Ma, M. A. Hanna, Bioresour. Technol. 70 (1999) 1–15.

[127] X. Meng, J. Yang, X. Xu, L. Zhang, Q. Nie, M. Xian, Renewable Energy 34 (2009) 1–5.

[128] http://www.uop.com/processing-solutions/biofuels/green-diesel/#green- diesel biodiesel.

[129] http://www.dynamicfuelsllc.com/compare.aspx.

[130] B. Peng, X. Yuan, C. Zhao, J. A. Lercher, J. Am. Chem. Soc. 134 (2012) 9400–9405.

[131] E. Laurent, B. Delmon, J. Catal. 146 (1994) 281–291.

[132] I. Kubicková, M. Snåre, K. Eränen, P. Mäki-Arvela, D. Y. Murzin, Catal. Today 106 (2005) 197–200.

[133] M. Snåre, I. Kubicková, P. Mäki-Arvela, K. Eränen, J. Wärnå, D.Y. Murzin, Chem. Eng. J. 134 (2007) 29–34.

[134] P. Mäki-Arvela, M. Snåre, K. Eränen, J. Myllyoja, D.Y. Murzin, Fuel 87 (2008) 3543–3549.

[135] P. T. Do, M. Chiappero, L. L. Lobban, D. E. Resasco, Catal. Lett. 130 (2009) 9–18.

[136] M. Chiappero, P. T. M. Do, S. Crossley, L. L. Lobban, D. E. Resasco, Fuel 90 (2011) 1155–1165.

[137] J. G. Na, B. E. Yi, J. K. Han, Y. K. Oh, J. H. Park, T. S. Jung, S. S. Han, H. C. Yoon, J. N. Kim, H. Lee, C. H. Ko, Energy 47 (2012) 25–30.

[138] M. Snare, I. Kubickova, P. Maki-Arvela, D. Chichova, K. Eranen, D. Y. Murzin, Fuel 87 (2008) 933-945.

[139] M. Snare, I. Kubickova, P. Maki-Arvela, K. Eranen, D. Y. Murzin, Ind. Eng. Chem. Res. 45 (2006) 5708-5715.

[140] S. Lestari, P. Maki-Arvela, K. Eranen, J. Beltramini, G. Q. M. Lu, Murzin, D. Y, Catal Lett 134 (2010) 250-257.

[141] I. Simakova, O. Simakova, P. Maki-Arvela, A. Simakov, M. Estrada, D. Y. Murzin, Applied Catalysis A: General 355 (2009) 100-108.

[142] W. L. Roberts, H. H. Lamb, L. F. Stikeleather, T. L. Turner, US 7,816,570 B2, 2010.

[143] G. W. Huber, J. A. Dumesic, Catalysis Today 111 (2006) 119–132.

[144] D. Kusdiana, S. Saka, Appl. Biochem. Biotechnol. 115 (2004) 781–91.

[145] L. Li, E. Coppola, J. Rine, J. L. Miller, D. Walker, Energy Fuels 24 (2010) 1305–1315.

[146] H. Bernas, K. Eranen, I. Simakova, A. R. Leino, K. Kordas, J. Myllyoja, P. Maki-Arvela, T. Salmi, D. Y. Murzin, Fuel 89 (2010) 2033–2039.

[147] R. R. Soares, D. A. Simonetti, J. A. Dumesic, Angew. Chem., Int. Ed. 118 (2006) 4086–4089.

[148] S. C. Cermak, T. A. Isbell, JAOCS 77 (2000) 243-248.

[149] R. L. Holliday, J. W. King, G. R. List, Ind. Eng. Chem. Res. 36 (1997) 932–935.

[150] J. G. Immer, M. J. Kelly, H. H. Lamb, Applied Catalysis A: General 375 (2010) 134-139.

[151] M. Ahmadi, E. E. Macias, J. B. Jasinski, P. Ratnasamy, M. A. Carreon, J. of Molec. Catal. A: Chemical 386 (2014) 14-19.

[152] B. Al Alwan, S. Salley, K.Y.S. Ng, Applied Catalysis A: General 485 (2014) 58–66.

[153] L. Lascaray, Ind. Eng. Chem. 41 (1949) 786–790.

[154] T. A. Patil, D. N. Butala, T. S. Raghunathan, H. S. Shankar, Ind. Eng. Chem. Res. 27 (1988) 727–735.

[155] A. J. Dijkstra, J. of the American Oil Chemists' Society 77 (2000) 1329-1331.

[156] A. Šmidovnik, I. Plazl, T. Koloini, Chemical Engineering Journal 51 (1993) B51-B56.

[157] M. B. Fernández, G. M. Tonetto, G. Crapiste, D. E. Damiani, Journal of Food Engineering 82 (2007) 199-208.

[158] G. Díaz, R. Perez, N. Tapanes, D. Aranda, A. Arceo, Natural Science 3 (2011) 530-534.

ABSTRACT

BIOFUELS PRODUCTION VIA CATALYTIC HYDROCRACKING OF DDGS CORN OIL AND HYDROTHERMAL DECARBOXYLATION OF OLEIC ACID OVER TRANSITION METAL CARBIDES SUPPORTED ON Al-SBA-15

by

BASEM AL ALWAN

December 2014

Advisors: Dr. K. Y. Simon Ng and Dr. Steven O. Salley

Major: Chemical Engineering

Degree: Doctor of Philosophy

The purpose of this research is to minimize the gap between the production of biofuels and the production of petroleum-based fuels by developing catalysts that can utilize renewable non-food based feedstocks (waste vegetable oils, algal oil, brown grease, etc.) and have great performance under low operation conditions. In particular, green diesel has become an attractive biofuel due to its superior properties that are quite similar to petroleum diesel. Therefore, no modifications are required to existing infrastructures. Three distinct experimental phases have been identified in order to achieve the objective of this work as follow:

First, the hydrocracking of distillers dried grains with solubles (DDGS) corn oil over bimetallic carbide catalysts was explored for green diesel production. A catalyst composed of nickel−tungsten (Ni−W) carbide supported on Al-SBA-15 was designed based on the ability of nickel to adsorb and activate hydrogen and the potential of tungsten for hydrogenation reactions. Four different Ni−W ratios (1:9, 1:1, 2:1, and 9:1) were prepared by the impregnation method to study the effect of metal ratio on the

catalyst structure, activity, and selectivity. Catalyst activity was evaluated in a fixed bed reactor at 400 °C and 650 psi (4.48 MPa) with a hydrogen flow rate of 30 mL min^{-1} and DDGS corn oil flow rate of 0.08 mL min^{-1}. The catalysts showed significant differences in activity and selectivity, with the catalyst having a Ni−W ratio of 9:1 achieving 100% conversion of corn oil and 100% selectivity to diesel for 2 days. Results indicate that by minimizing metal alloy formation and enhancement of the metal dispersion leads to higher activity, selectivity, and durability of the catalysts. A dendrimer-encapsulated nanoparticle (DENP) method was employed to minimize alloy formation and increase the metal dispersion on the support. The catalysts prepared by the DENP method showed activity greater than that of the catalyst prepared by the impregnation method for the hydrocracking of DDGS corn oil.

Second, Nickel-based carbide catalysts combined with four different metals (Mo, Nb, W, and Zr) and supported on Al-SBA-15 were investigated for the hydrocracking of DDGS corn oil to produce biofuels under mild reaction conditions. The effects of the fractional sums of the electronegativities of the transition metals on the catalyst activities, selectivities, and stabilities were investigated. The closer the fractional sum of the transition metal electronegativities was to the electronegativity range of the noble catalysts (2.0–2.2), the better was the catalyst performance. The highest diesel selectivity was obtained from NiWC/Al-SBA-15, with a fractional sum of electronegativity of 2.06. The effects of doping a promoter (Ce) on the catalyst electronegativity and activity were studied. Adding Ce generally improved the catalyst performance, by adjusting the combined electronegativities nearer to 2.0–2.2. However, other parameters affected by Ce addition, such as textural properties, or the performance of individual metals could also

impact catalyst performance. The NiNbC/Al-SBA-15 catalyst promoted with 5% Ce maintained stable activity for 168 h at 400 ° C and 4.48 MPa H_2 .

Third, several Ni-based transition metal carbide catalysts supported on Al-SBA-15 were studied for the hydrothermal decarboxylation of oleic acid and soybean oil to produce diesel range hydrocarbons with no added H_2. The effect of pre-reduction, sub-critical and super-critical water conditions on the catalyst activity and selectivity was investigated. Both the conversion of oleic acid and selectivity of decarboxylation products under super-critical conditions for each catalyst were about 2-times greater than at sub-critical conditions. In addition, the potential of these catalysts for utilizing aqueous phase reforming (APR) of glycerol for *in situ* H_2 production to meet process demands was demonstrated. The performance of the catalysts increases with the addition of glycerol, especially for the NiWC/Al-SBA-15 catalyst. With the addition of glycerol, the NiWC/Al-SBA-15 catalyst showed greater conversion of oleic acid and selectivity to heptadecane; however, most of the oleic acid was hydrogenated to produce stearic acid. The highest conversion of oleic acid and selectivity for heptadecane was 97.3% and 5.2%, respectively. Furthermore, the NiWC/Al-SBA-15 catalyst exhibited good potential for hydrolyzing triglycerides (soybean oil) to produce fatty acids and glycerol, and then generating H_2 *in situ* from the APR of the glycerol produced. A complete conversion of soybean oil and hydrogenation of produced oleic acid were obtained over the NiWC/Al-SBA-15 at super-critical conditions.

AUTOBIOGRAPHICAL STATEMENT

BASEM AL ALWAN

ee0274@wayne.edu

Education:

- 2009 - M.S. Chemical Engineering, California State University, Long Beach, CA

- 2003 - B.S. Chemical Engineering, King Saud University, Riyadh, Saudi Arabia

Publications:

1. Al Alwan, B.; Sari, E.; Salley, S.; Ng, K. Effect of Metal Ratio and Preparation Method on Nickel-Tungsten Carbide Catalyst for Hydrocracking of Distillers Dried Grains with Solubles Corn Oil. *Ind. Eng. Chem. Res.* **2014**, 53 (17), 6923-6933.

2. Al Alwan, B.; Salley, S.; Ng, K. Hydrocracking of DDGS Corn Oil over Transition Metal Carbides Supported on Al-SBA-15: Effect of Fractional Sum of Metal Electronegativities. *Applied Catalysis A: General* **2014**, 485, 58-66.

3. Al Alwan, B.; Salley, S.; Ng, K. Biofuels Production from Hydrothermal Decarboxylation of Oleic Acid and Soybean Oil Over Ni-based Transition Metal Carbides Supported on Al-SBA-15. *Applied Catalysis A: General*. Submitted.

Selected Presentations:

- Al Alwan, B.; Sari, E.; Salley, S.; Ng, K. *Hydrocracking of DDGS Corn Oil over Transition Metal Carbides Supported on Al-SBA-15: Effect of Metal Ratio, Preparation Method, and Fractional Sum of Metal Electronegativities*. Michigan Catalysis Society Spring Symposium, Warren, MI, 2014.

- Al Alwan, B.; Sari, E.; Salley, S.; Ng, K. *Biofuels Production via Hydrocracking of DDGS Corn Oil Over Bimetallic Carbides Supported by SBA-15 (Prepared by impregnation method & DENPs method)*. 23rd North American Catalysis Society Meeting, Louisville, KY, 2013.

- Al Alwan, B.; Salley, S.; Ng, K. *Hydrocarbon Fuels Production from Hydrocracking of Corn Oil Over Bimetallic Carbide Catalysts supported by Al-SBA-15*. Michigan Green Chemistry & Green Engineering, Detroit, MI, 2011.